PNL-7600 Pt. 4
UC-408

17

Pacific Northwest Laboratory Annual Report for ~~1989~~ 1990 to the DOE Office of Energy Research

Part 4 Physical Sciences
February 1991

Prepared for the U.S. Department of Energy
under Contract DE-AC06-76RLO 1830

Pacific Northwest Laboratory
Operated for the U.S. Department of Energy
by Battelle Memorial Institute

Battelle

DISCLAIMER

This report was prepared as an account of work sponsored by an agency of the United States Government. Neither the United States Government nor any agency thereof, nor Battelle Memorial Institute, nor any of their employees, makes **any warranty, expressed or implied, or assumes any legal liability or responsibility for the accuracy, completeness, or usefulness of any information, apparatus, product, or process disclosed, or represents that its use would not infringe privately owned rights.** Reference herein to any specific commercial product, process, or service by trade name, trademark, manufacturer, or otherwise does not necessarily constitute or imply its endorsement, recommendation, or favoring by the United States Government or any agency thereof, or Battelle Memorial Institute. The views and opinions of authors expressed herein do not necessarily state or reflect those of the United States Government or any agency thereof.

PACIFIC NORTHWEST LABORATORY
operated by
BATTELLE MEMORIAL INSTITUTE
for the
UNITED STATES DEPARTMENT OF ENERGY
under Contract DE-AC06-76RLO 1830

Printed in the United States of America

Available to DOE and DOE contractors from the Office of Scientific and Technical Information, P.O. Box 62, Oak Ridge, TN 37831; prices available from (615) 576-8401. FTS 626-8401.

Available to the public from the National Technical Information Service, U.S. Department of Commerce, 5285 Port Royal Rd., Springfield, VA 22161.

3 3679 00055 1350

PNL-7600 Pt. 4
UC-408

Pacific Northwest Laboratory Annual Report for 1990 to the DOE Office of Energy Research

Part 4 Physical Sciences

L. H. Toburen, B. R. Stults,
J. A. Mahaffey, and members of
the Physical and Technological
Programs Staff

February 1991

Prepared for
the U.S. Department of Energy
under Contract DE-AC06-76RLO 1830

Pacific Northwest Laboratory
Richland, Washington 99352

Preface

This 1990 Annual Report from Pacific Northwest Laboratory (PNL) to the U.S. Department of Energy (DOE) describes research in environment, safety, and health conducted during fiscal year 1990. The report again consists of five parts, each in a separate volume.

The five parts of the report are oriented to particular segments of the PNL program. Parts 1 to 4 report on research performed for the DOE Office of Health and Environmental Research in the Office of Energy Research. Part 5 reports progress on all research performed for the Assistant Secretary for Environment, Safety, and Health. In some instances, the volumes report on research funded by other DOE components or by other governmental entities under interagency agreements. Each part consists of project reports authored by scientists from several PNL research departments, reflecting the multidisciplinary nature of the research effort.

The parts of the 1990 Annual Report are:

Part 1: Biomedical Sciences			
	Program Manager:	J. F. Park	J. F. Park, Report Coordinator S. A. Kreml, Editor
Part 2: Environmental Sciences			
	Program Manager:	R. E. Wildung	M. G. Hefty, Report Coordinator D. A. Perez, Editor K. K. Chase, Text Processor
Part 3: Atmospheric Sciences			
	Program Manager:	C. E. Elderkin	C. E. Elderkin, Report Coordinator E. L. Owczarski, Editor
Part 4: Physical Sciences			
	Program Manager:	L. H. Toburen	L. H. Toburen, Report Coordinator K. A. Parnell, Editor
Part 5: Environment, Safety, Health, and Quality Assurance			
	Program Managers:	L. G. Faust R. V. Moraski J. M. Selby	D. K. Hilliard, Report Coordinator and Editor

Activities of the scientists whose work is described in this annual report are broader in scope than the articles indicate. PNL staff have responded to numerous requests from DOE during the year for planning, for service on various task groups, and for special assistance.

Credit for this annual report goes to the many scientists who performed the research and wrote the individual project reports, to the program managers who directed the research and coordinated the technical progress reports, to the editors who edited the individual project reports and assembled the five parts, and to Ray Baalman, editor in chief, who directed the total effort.

T. S. Tenforde
Health and Environmental
Research Program Office

Previous reports in this series:

Annual Report for:

1951	HW-25021, HW-25709
1952	HW-27814, HW-28636
1953	HW-30437, HW-30464
1954	HW-30306, HW-33128, HW-35905, HW-35917
1955	HW-39558, HW-41315, HW-41500
1956	HW-47500
1957	HW-53500
1958	HW-59500
1959	HW-63824, HW-65500
1960	HW-69500, HW-70050
1961	HW-72500, HW-73337
1962	HW-76000, HW-77609
1963	HW-80500, HW-81746
1964	BNWL-122
1965	BNWL-280, BNWL 235, Vol. 1-4; BNWL-361
1966	BNWL-480, Vol. 1; BNWL-481, Vol. 2, Pt. 1-4
1967	BNWL-714, Vol. 1; BNWL-715, Vol. 2, Pt. 1-4
1968	BNWL-1050, Vol. 1;, Pt. 1-2; BNWL-1051, Vol. 2, Pt. 1-3
1969	BNWL-1306, Vol. 1;, Pt. 1-2; BNWL-1307, Vol. 2, Pt. 1-3
1970	BNWL-1550, Vol, 1;, Pt. 1-2; BNWL-1551, Vol. 2, Pt. 1-2
1971	BNWL-1650, Vol. 1;, Pt. 1-2; BNWL-1651, Vol. 2, Pt. 1-2
1972	BNWL-1750, Vol. 1;, Pt. 1-2; BNWL-1751, Vol. 2, Pt. 1-2
1973	BNWL-1850, Pt. 1-4
1974	BNWL-1950, Pt. 1-4
1975	BNWL-2000, Pt. 1-4
1976	BNWL-2100, Pt. 1-5
1977	PNL-2500, Pt. 1-5
1978	PNL-2850, Pt. 1-5
1979	PNL-3300, Pt. 1-5
1980	PNL-3700, Pt. 1-5
1981	PNL-4100, Pt. 1-5
1982	PNL-4600, Pt. 1-5
1983	PNL-5000, Pt. 1-5
1984	PNL-5500, Pt. 1-5
1985	PNL-5750, Pt. 1-5
1986	PNL-6100, Pt. 1-5
1987	PNL-6500, Pt. 1-5
1988	PNL-6800, Pt. 1-5
1989	PNL-7200, Pt. 1-5

Foreword

Part 4 of the Pacific Northwest Laboratory Annual Report for 1990 to the DOE Office of Energy Research includes those programs funded under the title "Physical and Technological Research." The Field Task Program Studies reported in this document are grouped by budget category and each Field Task proposal/agreement is introduced by an abstract that describes the projects reported in that section. These reports only briefly indicate progress made during 1990. The reader should contact the principal investigators named or examine the publications cited for more details.

Contents

Dosimetry
Research

Chernobyl Database Management

The purpose of this project is to create and maintain an information system to collect, manage, and distribute data that can be used for research studies relating to the Chernobyl nuclear power plant accident in 1986. The system contains a collection of Chernobyl-related documents, a computerized bibliography with abstracts, and computerized radiological measurements with supporting information about how and where the measurements were collected and analyzed.

Project staff continue to enhance and maintain this information system. Activities performed during FY 1990 and planned for subsequent years include 1) collecting data and documents related to the Chernobyl accident; 2) analyzing the types and uses of information collected and developing methods for its storage and retrieval; 3) processing the information for loading into the library, bibliography, and measurements databases; and 4) facilitating the distribution of data and documents to researchers in response to their requests.

Chernobyl Database

J. A. Mahaffey and F. Carr, Jr.

Developing the Chernobyl Database has been challenging for at least four reasons. First, no formal agreements exist to provide data from the accident to our information system. Organizations must be identified, contacted, and asked to share their data. Second, there is no standardized approach to measurement recording; information is reported with varying levels of detail and summarization. Often, reports from a given agency have varying content and format. Third, supporting information required for long-term research needs were not (and possibly could not be) collected during the emergency-response period. These items include precise measurement locations, data quality information, background levels, equipment used for collection and analysis, etc. Fourth, specific uses and users for the system were not identified. Requests for data vary tremendously.

To meet these challenges, project staff have adopted an iterative approach to system development, making use of new software tools to facilitate response to user needs. Each year work is performed in the areas of data collection, system analysis and design, data processing and loading, and answering data requests. The work performed last year and how it relates to planned work is described below.

Collection of Information

Contact was initiated or continued with staff of the following organizations:

- Haut Commissariate à la Recherche in Algeria
- Umweltbundesamt, Bundesamt für Umwelt, and University of Salzburg in Austria
- Institut National des Radioèlèments and l'Institut d'Hygiene et d'Epidemiologie in Belgium
- FURNAS Centrais Elèctricas S.A. in Brazil
- Sofia University in Bulgaria
- Bureau of Radiation and Medical Devices, and Ontario Hydro in Canada
- Nuclear Research Institute, and the Institute of Hygiene and Epidemiology in Czechoslovakia
- Imatran Power Company in Finland
- Commissariat à l'Energie Atomique in France

- Institut für Medizin; and Referat Rückstände von Pflanzenschutzmitteln in Lebensmitteln Bundesministerium f. Jugend, Familie in the Federal Republic of Germany
- Direccion General de Energia Nuclear in Guatemala
- University of Veterinary Science in Hungary
- Instituto Superiore Di Sanita, Food and Agriculture Division, and ENEA in Italy
- National Institute of Radiological Sciences and Radiation Protection Board in Japan
- Service de Radiologie et de Mèdecine Nuclèaire in Mali
- Ministry of Housing, Physical Planning, and Environment; National Institute of Public Health and Environmental Protection; and Ministry of Welfare, Health, and Cultural Affairs in the Netherlands
- Institutt for Energiteknikk in Norway
- Instituto de Investigacion Agropecuaria in Panama
- Ministry of Public Health in the People's Republic of China
- Bucharest Polytechnical Institute in Romania
- Ministerio de Sanidad y Consumo in Spain
- National Defence Research Institute and Statens Stralskyddsinstitut in Sweden
- Atomic Energy Commission in Syria
- H.M. Inspectorate of Pollution, Institute of Naval Medicine, Institute of Terrestrial Ecology, and Ministry of Defense in the United Kingdom
- Ukraine Foreign Economic Export/Import Association for Medical Service, Technique, and Equipment in the USSR
- Facultad de Quimica in Uruguay
- Institute for Medical Research and Occupational Health; Institute of Occupational and Radiological Health; and Josef Stefan Institute in Yugoslavia.

Approximately 100 reports and reprints were received including materials from Austria, Belgium, Bulgaria, Canada, Czechoslovakia, Finland, France, Federal Republic of Germany, Guatemala, Hungary, Italy, Japan, Netherlands, Panama, People's Republic of China, Sweden, Syria, United Kingdom, United States, USSR, and Yugoslavia. Paper copies of radiological measurements were received from Algeria, Canada, Czechoslovakia, Kenya (students returning from the USSR), Sweden, and Yugoslavia. Copies of radiological measurements on diskette were received from the l'Institut d' Hygiene et d'Epidemiologie in Brussels, Belgium, and the FURNAS Centrais Elèctricas S.A. in Rio de Janeiro, Brazil.

System Analysis and Design

To take advantage of recent software technology, a new method for the computerized collection, processing, standardization, and storage of the Chernobyl radiological measurements has been implemented. This method, which has evolved over the previous three years, involves a "database of databases" approach. The approach has been developed to provide a central repository containing standardized information representing all measurements incorporated into the database. Standard information currently includes country, media, isotope, and collection date. In the future, standard values will include measurement value notation and the unit of measure. The approach also has the following features:

- a common interface for viewing and managing the original data provided to project staff
- access to the original measurement data while browsing or reporting from the central repository
- a reproducible and auditable path of the data transformations performed during

processing from the original data to the standardized data

- the ability to reprocess the data transformations based on new or different assumptions.

The database has been transferred from the mainframe/mini VAX computers to a personal computer environment. This will provide better support for measurement processing and will provide better tools for interactive data reviewing, searching, sorting, and summarization.

Data Processing/Loading

The bibliographic attributes of the 310 references collected by project staff have been entered into the computerized bibliography. There are now 2364 references in the bibliography.

All of the radiological measurement data on the VAX have been transferred to the PC. Approximately half of these data have been incorporated into the new measurement database structure and central repository.

Menu-driven software has been developed that allows browsing of the bibliography and radiological measurements. There are two particular features that facilitate use of the information. First, users may view the bibliography and perform searches to locate key words in any of the displayed data fields. For entries with abstracts available, the user may optionally view the abstract. Second, for radiological measurements, users have the option of viewing the original databases, the central repository, or summary statistics on the database content. While viewing the central repository, users may switch between viewing the standard information and the original data. The summary statistics include tables of counts for the country, media, and isotope values in the database. Bar charts and pie charts are also available to show the relative distribution of these items.

Data Requests/Interactions with Others

Thirteen users from nine countries requested information about or from the Chernobyl Database.

Copies of the bibliography produced during FY 1989 were distributed to 19 people in addition to those who received a copy in the initial distribution. Among the recipients were scientists from Austria, Belgium, Canada, Czechoslovakia, Italy, Japan, Kenya, the Netherlands, United Kingdom, and Yugoslavia.

Contact was further established with Dr. Alicia Bauman of Yugoslavia. She visited PNL to learn more about the Chernobyl Database and to assist in providing data from Yugoslavia.

Finally, an abstract has been accepted to present the Chernobyl Database at the Winter Technical Conference of the American Statistical Association.

Determination of Radon Exposure

The goal of this project is to determine the correlation between radon exposure and the ratio of ^{210}Pb to ^{208}Pb in the body. This requires development of a sensitive analytical procedure capable of measuring extremely small quantities of ^{210}Pb in the presence of about 10^{10} greater amounts of stable Pb isotopes. The method being developed uses high-resolution continuous wave (cw) laser ionization techniques coupled with mass spectrometry to provide selectivity and a sensitivity sufficient for dealing with small samples. These analytical capabilities have been established using prepared reference samples, as described in this report. The emphasis of the research will now be directed toward determining the correlation between radon exposure and the ^{210}Pb levels and isotopic ratios in various tissues and how specific factors such as diet influence that correlation. These measurements will not only contribute to quantifying the lung cancer risk associated with radon exposure, but also to understanding the recently postulated correlation of radon absorption in fatty tissues with Alzheimer's disease and leukemia. The method will also be used for determining long-term integrated radon levels in homes and the environment.

MEASUREMENT OF ^{210}Pb AT THE SUBFEMTOGRAM LEVEL WITH RELATIVE ISOTOPIC CONCENTRATIONS OF 10^{-10}

B. A. Bushaw and J. T. Munley

In our approach to ^{210}Pb detection, the analyte atoms are generated with a vacuum-compatible graphite furnace and detected using the scheme depicted in Figure 1: a single-frequency cw dye laser is tuned to a resonance of the Pb atoms originating in the ground state, which raises it to a low-lying excited state. A second single-frequency cw dye laser is tuned to promote the initially excited atom into a high-lying Rydberg state, and the Rydberg state atom is ionized by a cw CO_2 laser. The ions produced are then analyzed with a quadrupole mass spectrometer. The merits of this approach for low-level isotopic measurements have been discussed in a review article (Bushaw 1989), and, in previous studies on Ba (Bushaw and Gerke 1988), we have shown that this approach is capable of yielding detection limits near 10^{-17} g. Pb has much larger isotope shifts than Ba and thus provides greater optical selectivity (Bushaw et al. 1990)--as much as 10^9 in the double-resonance excitation to the Rydberg state. However, efficient ionization is more difficult to achieve. In Ba, the first excitation is of a two-level system and any atoms not promoted to the Rydberg state will return to the ground state where reexcitation can occur. In contrast, the first excitation in Pb is very susceptible to optical pumping: approximately 85% of the atoms excited to the 6p7s $^3P_1$ state decay into the metastable $^3P_1$ and $^3P_2$ fine structure components of the ground state, where they are not accessible for further excitation and ionization. We have applied density matrix calculations to develop a theoretical understanding of how metastable trapping can be decreased. The results of this theoretical work have been implemented experimentally to yield subfemtogram detection limits.

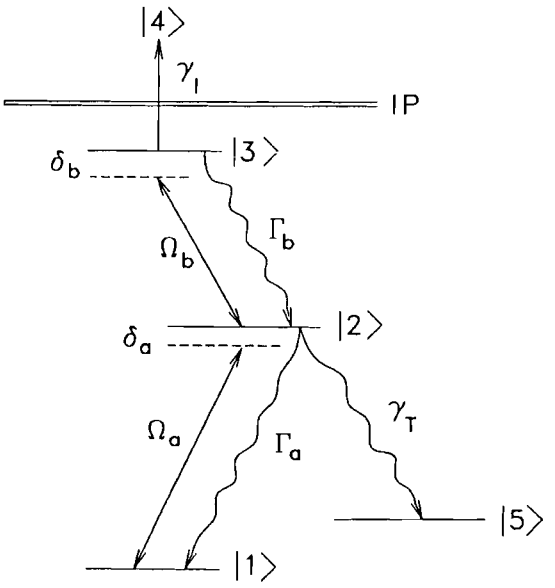

Figure 1. Energy Level for Pb Atoms. The excitation pathway for double-resonance excitation to Rydberg states followed by photoionization with a CO_2 laser is shown. The parameters used in calculation of time evolution of the density matrix are also given.

Density Matrix Calculations

Figure 1 shows the parameters necessary for calculating the time evolution of the five-level system density matrix, which is appropriate to the excitation of Pb atoms with two monochromatic lasers. Equations that describe this system have been derived by extending the development for a three-level atom (Whitley and Stroud 1976) to include terms for ionization and the trapping states. The result is a set of 11 coupled differential equations that describe the evolution of atomic state populations and coherences in the presence of the laser fields. Computer codes have been developed to solve these differential equations numerically. For the ideal three-level system ($\Gamma_I = \Gamma_T = 0$), optimum conditions are found when $\Omega_a = \Gamma_a/2$ (Rabi frequency for the first laser set to 1/2 the spontaneous decay rate of the intermediate state) and $\Omega_a/\Omega_b = (\Gamma_a/2\Gamma_b)^{1/4}$. Under these conditions, the steady-state population of the upper (Rydberg) state approaches 60%. However, when these same conditions are applied to the five-level system representing Pb, we find that approximately 93% of the atoms are transferred into the metastable trapping states and the remaining 7% are ionized. Furthermore, this is achieved only with ideal conditions of a perfectly collimated atomic beam. Under real conditions, with residual Doppler broadening, we expect ionization efficiencies of less than a few tenths of a percent using the three-level optimal conditions.

To reduce this strong metastable state trapping, we have carried out five-level calculations for a number of different (experimentally practical) laser intensities and geometries. The conditions we find that produce the best ion yields involve detuning the two lasers by offsetting amounts from the intermediate state and focusing the laser beams into thin "sheets" of light with cylindrical lenses to minimize the atom's exposure time as it traverses the laser beams. With this geometry and laser detuning, we predicted an increase in the ion yield of about a factor of ten; this has been demonstrated experimentally.

Analytical Measurements of ^{210}Pb

Test analytical measurements on prepared samples containing traces of ^{210}Pb were performed using the new cylindrical focusing geometry as follows: both dye lasers were set at the appropriate frequencies for excitation of ^{210}Pb to the 6p16p $(1/2,3/2)_2$ Rydberg state with 60% MHz offsetting detunings in the intermediate state, the mass spectrometer was set at mass 210, and ion counts were integrated as the graphite furnace temperature was ramped to evolve the sample. Figure 2A shows the result for a sample containing 18.4 fg of ^{210}Pb in the presence of 2.95 μg of the stable Pb isotopes. This was compared to a "blank" containing only the 2.95 μg of the stable isotopes. The ^{210}Pb signal is clearly observed, producing an average of about 15 counts per second at the peak of the temperature profile, while the blank produces no observable increase in the count rate above the constant background of approximately 0.3 counts per second. The rapid increase in signal above 1400°C is present without laser excitation and is attributed to the onset of blackbody ultraviolet photons generated by the furnace, which can be detected with the channeltron detector. Figure 2B shows the result for a sample having an even lower ^{210}Pb content of 1.6 fg, but still containing 2.95 μg of the stable isotopes: a relative ^{210}Pb concentration of 5.6×10^{-10} with respect to the stable isotopes. Because the expected count rate at the peak of the temperature profile is less than 2 per second, the signal has been summed over 1-min intervals. The signal from the 1.6 fg of ^{210}Pb is still clearly observed, and, with the blank sample, there is still no apparent increase in signal due to the stable isotopes, above the constant background. The results appear to be statistically limited: over the period including the fourth through seventh minutes, 200 total ion counts were recorded for the sample containing ^{210}Pb, while 64 counts were recorded for the sample without ^{210}Pb. This corresponds to a net signal of 136 ion counts from the 1.6 fg of ^{210}Pb and a signal-to-background noise ratio $[(S-B)/\sqrt{B}]$ of 17. Thus, the 3σ detection limit is slightly less than 3×10^{-16} g. This is sufficient sensitivity for making ^{210}Pb measurements on a variety of biological and environmental samples at near background levels.

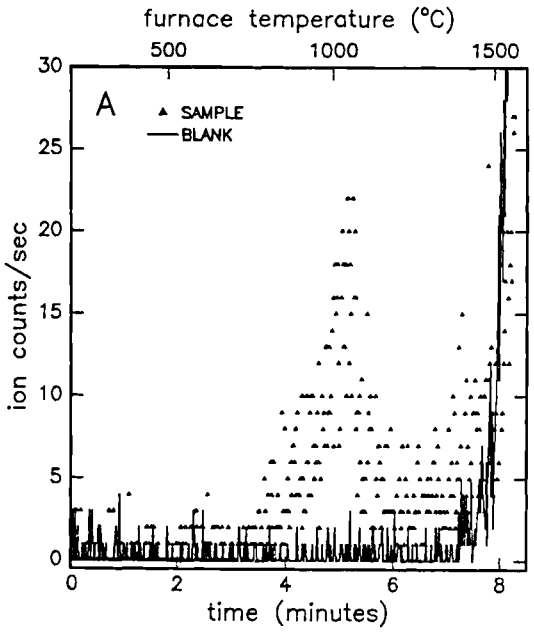

(A)

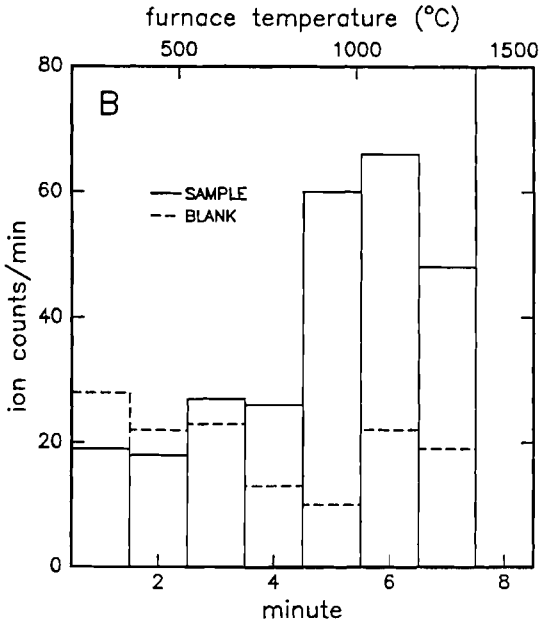

(B)

Figure 2. Analytical Measurements on Prepared Samples Containing Traces of ^{210}Pb. The sample in (A) contained 18.4 fg of ^{210}Pb while (B) contained 1.6 fg. Both samples and the blanks contained 2.95 μg of the stable isotopes. The relative isotopic concentration of ^{210}Pb in (B) is 5.6×10^{-10}.

References

Bushaw, B. A. 1989. "High-Resolution Laser-Induced Ionization Spectroscopy." *Prog. Analyt. Spectrosc.* 12:247-276.

Bushaw, B. A., and G. K. Gerke. 1988. "Trace Isotopic Analysis by Double Resonance Ionization with cw-Lasers and Graphite Furnace Atomization." *Inst. Phys. Conf. Ser.* 94:277-280.

Bushaw, B. A., W. L. Glab, G. K. Gerke, and J. T. Munley. 1990. "Selectivity and Sensitivity in the Detection of ^{210}Pb." In *Physical Sciences, Part 4 of Pacific Northwest Laboratory Annual Report for 1989 to the DOE Office of Energy Research,* PNL-7200 Pt. 4. Pacific Northwest Laboratory, Richland, Washington.

Whitley, R. M., and C. R. Stroud. 1976. "Double Optical Resonance." *Phys. Rev. A.* 14:1498-1513.

DNA Adducts as Indicators of Health Risks

The objective of this program is to develop specific analytical methods for the determination of adducts formed in mammals by the reaction of carcinogenic compounds with cellular DNA. DNA adducts are closely associated with the formation of cancerous cells, and their concentrations are thought to be related to the amount of exposure to carcinogenic chemicals. This program is developing mass spectrometric methods for analysis of adducts that may be applied toward health studies of human exposure to carcinogens.

Determination of Adducts of Polycyclic Aromatic Hydrocarbons to DNA

R. M. Bean, S. D. Harvey, H. R. Udseth, and D. L. Springer

Metabolites of carcinogenic organic compounds have the ability to bond with deoxyribonucleic acids (DNA) to form DNA adducts. These species are retained for relatively long periods of time in the body and are thought to be associated with the formation of cancer. Analysis of DNA for adducts may therefore provide an estimate of individual exposure to carcinogens. The currently available methods suffer either from a lack of sufficient sensitivity for environmental screening or from a lack of qualitative specificity. Although data on humans are sparse, we may expect, allowing for initial rapid decay after environmental exposure, adduct levels of 0.1 to 0.01 ng/mg of DNA. The objective of this project is to develop methods for the analysis of DNA adducts that will permit identification and quantitation of adducted polycyclic aromatic hydrocarbon metabolites at environmental levels.

Analysis of DNA Adducts as the Nucleotide: Benzo[a]pyrene-Adducted Deoxyguanosine-5'-Monophosphate

A major effort was initiated this past year to establish the necessary groundwork for application of powerful microcolumn liquid chromatography/mass spectrometry (LC/MS) capabilities for the specific analysis of adducted nucleotides. Two LC/MS interface techniques have promise for the analysis of DNA adducts: electrospray ionization and continuous flow fast-atom bombardment (FAB). Both approaches are being pursued through collaborative efforts with D. F. Barofsky's group at Oregon State University (FAB) and R. D. Smith's group at Pacific Northwest Laboratory (electrospray ionization). Microgram quantities of purified benzo[a]pyrene (BaP)- adducted 5'-monophosphate nucleotides were a necessity for initiation of these studies. Adducted nucleotides were specifically targeted because the electrospray approach requires charged analytes for successful analysis. In addition, charged compounds are also more efficiently volatilized under FAB conditions than are neutral molecules.

BaP-adducted calf thymus DNA was hydrolyzed to the 5'-monophosphates by incubation with DNAase-I and snake venom phosphodiesterase. Purification of the BaP-adducted nucleotides was based on the procedure described by Blobstein et al. (1975) for the isolation of 7,12-dimethylbenz[a]anthracene-adducted nucleotides from DNA hydrolysis mixtures. An aliquot of the enzymatic hydrolysis mixture was applied to a Sephadex LH-20 column that was previously equilibrated with ammonium bicarbonate buffer (20 mM, pH = 8.4). This buffer was used to rinse the enzymes and the unadducted nucleotides from the column. Elution of the BaP-adducted nucleotides was accomplished with 40:60 methanol:ammonium bicarbonate buffer and detected by absorbance at 344 nm. The purified adducted nucleotide fraction was characterized by conventional high-performance liquid chromatography (HPLC) with sequential fluorescence and photodiode array detection. The adducted nucleotide eluted more rapidly from the reversed-phase column than the corresponding adducted nucleoside due to the presence of the polar phosphate group. The ultraviolet spectrum of BaP nucleotide matched that of the adducted nucleoside; both adducted compounds had spectra characteristic of a pyrene moiety. Comparison of the relative detector responses indicated that the fluorescence of

the adducted nucleotide was severely quenched. This expected result is attributed to the proximity of the covalently bound DNA base. The nucleotide fraction contained only a small amount of BaP tetrahydrotetrol (BaP tetrol) contaminant. A chromatogram of the adducted nucleotide fraction separated under high-resolution microcolumn conditions is shown in Figure 1.

Because electrospray ionization often yields erratic results in the presence of salts, the buffer was first removed from the adducted nucleotide fraction by a C-18 Sep-Pak prior to analysis by this technique. The desalted solution was prepared in 50:50 methanol:water at a concentration of 32 μM and examined by direct infusion electrospray mass spectrometry. A full-scan negative ion mass spectrum (50 to 700 amu) resulting from the introduction of approximately 3 ng of BaP-adducted nucleotide is shown in Figure 2. The prominent ions in the mass range of 150 to 300 amu are characteristic of the methanol-water solvent. A detail of the region between 600 and 700 amu is shown in Figure 3. The $(M-1)^{-1}$ ion at m/e of 348 corresponds to the BaP-adducted deoxyguanosine-5'-phosphate and appears at a signal intensity of approximately 13 times background. Experiments planned for the near future will examine near future will examine the detection limit for BaP-adducted deoxyguanosine-5'-phosphate under

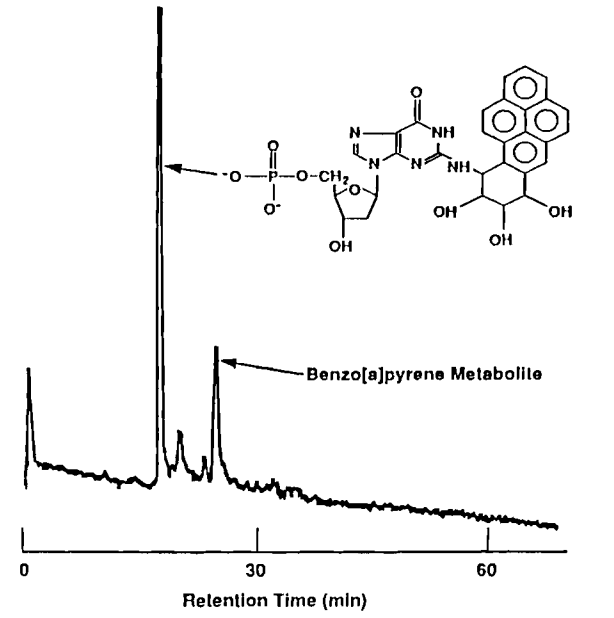

Figure 1. Microcolumn HPLC Chromatogram of the BaP-Adducted Nucleotide Fraction

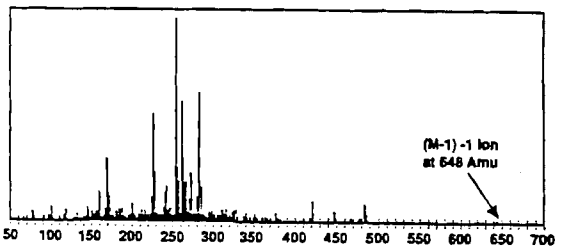

Figure 2. Full-Scan Negative Ion Electrospray Mass Spectra of BaP-Adducted Deoxyguanosine-5'-monophosphate

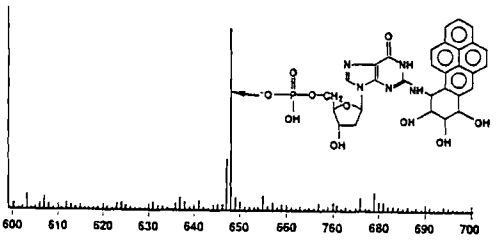

Figure 3. Detail of the Region Between 600 to 700 amu in Figure 2

single ion monitoring conditions. An increase in sensitivity of approximately three orders of magnitude can be expected by use of this acquisition mode. Further experiments will demonstrate the powerful combination of microcolumn HPLC with electrospray-mass spectrometric detection.

In a collaborative effort with Dr. Barofsky, a continuous flow/FAB interface is presently under construction for evaluation of FAB mass spectrometry of adducted nucleotides. Flexibility will be retained in the interface design and construction to allow for substitution of a liquid metal ion gun and the associated ion optics. The substitution of a liquid metal ion source will allow for more flexibility in source configuration than possible with argon atom bombardment. Experiments examining direct infusion of BaP-adducted deoxyguanosine-5'-monophosphate into a FAB source are presently in progress. As with the electrospray interface, we plan on interfacing the FAB mass spectrometry with microcolumn HPLC separations during the next fiscal year.

Analysis of Benzo[a]pyrene Tetrahydrotetrols

Many organic chemical metabolite species that are adducted to DNA can be released from the DNA biopolymer by treatment with acid. For example, BaP adducts release BaP tetrol when treated with 0.1 N HCl. While some of the chemical characteristics of the adduct are lost during this process, a species that is smaller, less polar, and more amenable to a variety of analytical procedures is produced. The following sections describe procedures investigated to analyze BaP tetrol at the required levels of sensitivity. One approach has been to improve existing detection technology with the novel ultrasensitive separation and detection techniques available with microcolumn chromatography; the other has been to enhance detectability through derivatization.

Microcolumn HPLC of BaP Tetrols with Fluorescence Detection

A microcolumn HPLC system was constructed for the direct determination of BaP tetrols. Direct analysis offers the distinct advantage of avoiding problems associated with derivatization such as incomplete reaction and sample losses. The microcolumn system is based on a 1-m x 250-μm inside diameter (ID) column packed with 5-μm reverse-phase adsorbent. When operated at optimal flow rates (1 to 2 μL/min), these columns typically provide separation efficiencies in excess of 75,000 theoretical plates (Novotny 1988). A conventional fluorescence detector was modified to be compatible with the low dead-volume requirements of the technique. The ultra-high sensitivities available from microcolumn chromatographic systems are due largely to the high concentration of analyte present in the small volume of mobile phase eluant. This system is ideally suited for laser-induced fluorescence (Diebold and Zare 1977; Gluckman et al. 1984). Although studies involving laser-induced fluorescence have not yet been conducted, an increase in sensitivity of at least two orders of magnitude over conventional fluorescence detection can be expected. Figure 4 illustrates a separation of approximately 15 pg of each BaP tetrol. Since the detection limit of the modified conventional detector is roughly 1 pg, laser-induced fluorescence can be expected to give detection limits well below the 10-fg level. At sample capacities of about 0.2 μL,

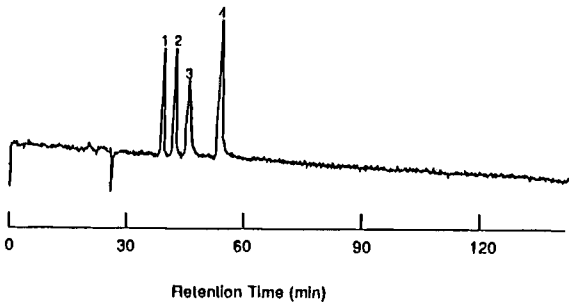

Figure 4. Microcolumn HPLC Separation of 1) Benzo[a]pyrene-r-7, +-8, 9, c-10-tetrahydrotetrol; 2) Benzo[a]pyrene-r-7, +-8, c-9, +-10-tetrahydrotetrol; 3) Benzo[a]pyrene-r-7, +-8, 9, 10-tetrahydrotetrol; and 4) Benzo[a]pyrene-r-7, +-8, c-9, 10-tetrahydrotetrol.

detection concentrations for BaP tetrol approach 0.1 nmole/μL (10^{-10} mole/L). The uncompromised sensitivity of laser-induced fluorescence in combination with the high-resolution profiling capabilities of microcolumn HPLC may prove to be the method of choice for analyzing fluorescent tetrols liberated from DNA adducts at the levels expected to occur from environmental exposure to polycyclic aromatic hydrocarbons.

Electrophoric Derivatization

One of the possible ways to increase the sensitivity of BaP tetrol in analytical instrumentation is to react it with species that enhance its detection in specific detectors. Attachment of derivatives that are electrophores has the effect of rendering an analyte detectable by electron-capture detector or by negative ion mass spectrometry at extremely low levels.

Considerable effort was spent this past year attempting formation of the tetra-substituted bromomethyldimethylchlorosilane derivative of BaP tetrol. The required reaction is shown below:

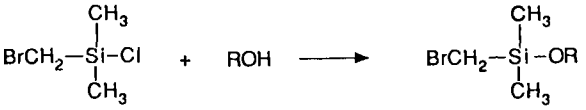

By virtue of the four bromine atoms contained in the product, this derivative would allow highly sensitive detection by either electron-capture detection or negative ion chemical ionization

mass spectrometry (Zlatkis and Poole 1980; Thomas 1971; Brooks et al. 1975). Additionally, by further reaction it is possible to replace the bromine atom with iodine allowing for even more sensitive detection; however, substitution of iodine would result in a nonvolatile compound that would not be suitable for gas chromatographic analysis. A variety of reaction conditions were tested using model alcohols (1-hexanol, 2-decanol, and 1,2,6-hexanetriol). It was found that room-temperature reaction of alcohol with 5-μL bromomethyldimethylchlorosilane in 100-μL pyridine resulted in complete derivatization of even the stearically hindered triol. These conditions were next applied to BaP tetrols. Reaction resulted in a mixture of brominated derivatives, some of which were sufficiently volatile to be eluted from a short gas capillary column near the stationary phase temperature limit of 325°C. The derivatized mixture contained at least two fluorescent products as evidenced by HPLC analysis. The fact that these compounds eluted at 100% acetonitrile indicated that reaction products were hydrophobic and probably not completely derivatized. The products from the derivatization reaction were collected by repetitive HPLC and examined by particle beam mass spectrometry. The mass spectra obtained did not correspond to the expected bromomethyldimethylchlorosilyl ether derivative. It was additionally found that extended reaction times resulted in the destruction of the pyrene ring as indicated by loss of fluorescence. The bromine formed from decomposition of the derivatizing reagent evidently attacks the starting material resulting in additional products of BaP tetrol. We have concluded that this derivative will not be effective for tetrol analysis.

Formation of the pertrifluoroacetyl derivative of BaP tetrol utilized trifluoroacetic anhydride (TFAA) or N-methylbis(trifluoroacetamide) (MBTFA) (Sullivan and Schewe 1973; Chess et al. 1988). BaP tetrol was dissolved in pyridine solvent and 50 to 100 μL of derivatizing reagent was added. The mixture was heated at 65°C for periods ranging from 2 to 12 h. All reactions were performed in a dry nitrogen atmosphere with freshly distilled anhydrous solvent. After reaction, solvent and excess reagent were removed under vacuum by use of a Speed-Vac concentrator. The pertrifluoroacyl derivative was sporadically formed by use of both reagents; however, reaction yield was very low. Increased reaction times did not increase the yield of perfluoroacyl product.

Derivatization for Chemiluminescence Detection

This reaction scheme involves the oxidation of BaP tetrol to diformyl pyrene and subsequent reaction of the dialdehyde with glycine and cyanide to form a highly fluorescent cyanoisoindole derivative (Matuszewski et al. 1987; Lunte and Wong 1989), as shown in the general reaction below:

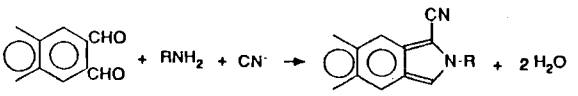

These types of derivatives are capable of being detected at extremely low levels through the use of chemiluminescence techniques. Oxidation of the tetrol to the required dialdehyde was accomplished with periodic acid (1 mg/mL) in 0.01 M acetate buffer (pH = 4.95). Gas chromatography/MS and HPLC studies revealed that the periodic acid oxidation proceeded with good yields to the diformyl pyrene product. Diformyl pyrene product was next reacted with 20 μL to 10-mM glycine in 500 μL of 50:50 methanol: 0.1 M borate buffer (pH = 8.05), in the presence of 20 μL of 10-mM sodium cyanide. The persistence of diformyl pyrene starting material 8 h after initiation of the reaction gave evidence that the reaction did not proceed to the expected cyanoisoindole product. It is known that larger homologues of o-phthalaldehyde such as 3-benzoyl-2-quinolinecarboxaldehyde react at a slower rate with primary amines to form cyanoisoindole derivatives (Beal et al. 1988). It is possible that the reaction kinetics governing the formation of the cyanoisoindole derivative of diformyl pyrene are prohibitively slow. An additional possibility is that diformyl pyrene may not possess sufficient solubility in the methanol/buffer solution to facilitate reaction. To exclude this possibility, systems utilizing various solvents need to be investigated.

References

Beal, S. C., J. C. Savage, D. Wiesler, S. M. Wietstock, and M. Novotny. 1988. "Fluorescence Reagents for High-Sensitivity Chromatographic Measurements of Primary Amines." *Anal. Chem.* 60:1765-1769.

Blobstein, S. H., I. B. Weinstein, D. Grunberger, J. Weisgras, and R. G. Harvey. 1975. "Products Obtained After In Vitro Reaction of 7,12-Dimethylbenz[a]anthracene 5,6-Oxide with Nucleic Acids." *Biochemistry* 14:3451-3458.

Brooks, J. B., J. A. Liddle, and C. C. Alley. 1975. "Electron Capture Gas Chromatography and Mass Spectral Studies of Iodomethyltetramethylmethyl-disiloxane Esters and Iodomethyldimethylsilyl Ethers of Some Short-Chain Acids, Hydroxy Acids and Alcohols." *Anal. Chem.* 47:1960-1965.

Chess, E. K., B. L. Thomas, D. J. Hendren, and R. M. Bean. 1988. "Mass Spectral Characteristics of Derivatized Metabolites of Benzo[a]pyrene." *Biomed. Environ. Mass Spectrom.* 15:485-493.

Diebold, G. J., and R. N. Zare. 1977. "Laser Fluorimetry: Subpicogram Detection of Aflatoxins Using High-Pressure Liquid Chromatography." *Science* 196:1439-1441.

Gluckman, J., D. Shelly, and M. Novotny. 1984. "Laser Fluorimetry for Capillary Liquid Chromatography: High-Sensitivity Detection of Derivatized Biological Compounds." *J. Chromatogr.* 317:443-453.

Lunte, S. M., and O. S. Wong. 1989. "Naphthalenedialdehyde-Cyanide: A Versatile Fluorogenic Reagent for the LC Analysis of Peptides and Other Primary Amines." *LC-GC* 7:908-916.

Matuszewski, B. K., R. S. Givens, K. Srinivasachar, R. G. Carlson, and T. Higuchi. 1987. "N-Substituted 1-Cyanobenz[f]isoindol: Evaluation of Fluorescence Efficiencies of a New Fluorogenic Label for Primary Amines and Amino Acids." *Anal. Chem.* 59:1102-1105.

Novotny, M. V. 1988. "Recent Advances in Microcolumn Liquid Chromatography." *Anal. Chem.* 60:500A-509A.

Sullivan, J. E., and L. R. Schewe. 1977. "Preparation and Gas Chromatography of Highly Volatile Trifluoroacylated Carbohydrates Using N-Methyl Bis[trifluoroacetamide]." *J. Chromatogr. Sci.* 15:196-197.

Thomas, B. S. 1971. "Measurement of Plasma Testosterone as the Iodomethylsilyl Ether by Gas-Liquid Chromatography." *J. Chromatogr.* 56:37-50.

Zlatkis, A., and C. F. Poole. 1980. "Derivatization Techniques for the Electron-Capture Detector." *Anal. Chem.* 161:111-117.

Biological Effectiveness of Radon Alpha Particles

Environmentally relevant exposures to alpha particles from radon decay products amount to only one or two particle tracks per cell. The consequences of these exposures, relative to the effects of the large numbers of electron tracks required to produce the same dose, is a major concern in establishing exposure limits for radon. The length of time between the alpha particle events also seems to influence the probability of the cell being transformed, just as the dose rate influences the extent of life shortening in animals exposed to radon. In order to study the effects of low doses of radiation and to test alternative biophysical models of the dose-rate effect, an irradiation system that will produce single-charged particle tracks through specific subcellular structures has been developed.

Single-Particle Irradiation System

L. A. Braby

Present estimates of risk associated with environmental radiation exposures such as those from radon decay products are based on extrapolation from epidemiological data and experimental observations at much higher doses. These estimates rely on models of the dose-response relationship to provide extrapolation from the effects at high doses and high dose rates, where individual cells are exposed to relatively large numbers of charged particle events, to the low doses, where the average number of energy deposition events per cell may be less than one. The response of cells and organisms to irradiation is complex; involved are different chemical products, different spatial distributions of the products, different repair systems with the possibility of erroneous repair, differences in response as a function of the position of the cell in the mitotic cycle, and other factors that affect the configuration of the DNA within the nucleus. Unfortunately, the nature of these effects is not yet understood, and even if they were it would probably not be practical to include them in the model of cellular response since such a complex model could not be verified experimentally. Instead, the models that are used to extrapolate to the effects of low dose are relatively simple, largely phenomenological expressions that are believed to be consistent with mechanisms that may represent the rate-limiting steps in the response of the cell. However, the experimental data still do not yield precise and unequivocal tests of the models, and there is considerable controversy over the best model to use to extrapolate to the effects of low doses and low dose rates. Determining the validity of the model is particularly difficult for high linear energy transfer (LET) radiations because at the relevant doses the mean number of energy deposition events per cell is quite low. Although a few cells have two or more energy deposition events, many have none.

In order to establish the response of cells to low doses of high-LET radiation, we have assembled an irradiation system designed to irradiate individual cells with specific numbers of charged particle tracks passing through specified cellular structures at specified times. This apparatus, which was described by Braby and Reece (1990), utilizes a charged particle beam collimated to irradiate a limited area and a particle detection system that allows a shutter to limit the exposure to a specified number of charged particle tracks.

During preliminary testing, several problems were found with the original design of the single-particle irradiation system. The most troublesome problem has been the low light output of the thin scintillator, combined with higher than expected light loss in the microscope. The photomultiplier was originally mounted on the main camera port of the microscope, the port with the smallest number of intermediate optical elements. However, tests indicated that only a small fraction of the light collected by the objective lens was reaching the photomultiplier. In retrospect, this should not be surprising--the microscope optics are optimized for resolution and for contrast, but not for total transmission. In order to get a more reliable measure of the light-collecting efficiency required and to test the effectiveness of other aspects of the microbeam system, the entire microscope was removed and replaced by a 2-in. photomultiplier tube that could be placed at different distances above the thin

scintillator. By adjusting this distance, detection systems with different numerical apertures could be approximated.

Experiments with proton and alpha particle beams have indicated that for the thin scintillator, the light output is significantly less than expected, and that reliable detection of single-particle events above the single-photon noise required a numerical aperture of approximately 2 (a 2-in.-diameter detector 1 in. above the source). A much larger numerical aperture would be required for a microscope objective in order to compensate for light loss in the correcting optics, or the microscope would have to be modified to remove most of those correcting elements. Neither of these alternatives seemed practical, so we explored other systems for detecting the passage of a single particle and other ways of detecting the light from a scintillator flash. Unfortunately, alternative physical processes such as secondary electron emission and the electromagnetic pulse produced by the passage of the particle give very small signals. Detection of these signals would have the same problems. Thin proportional counters or ion chambers could be built to detect the particles reliably, but the additional foils and the distance required by the detector would increase the scatter of the primary particles and produce some of the scatter farther from the target, reducing the spatial resolution.

The scintillator still seems to be the most efficient detector, but an improved light-gathering system is required. Condensing lenses with large numerical apertures were considered, but they could not be arranged with sufficiently large apertures and working distances to keep the first element of the lens out of the tissue culture medium. Mirror systems that direct the light out to the side and to a photomultiplier mounted under the microscope were also studied. Parabaloidal and elliptical reflectors were considered, but again the geometry of the situation was difficult. Attempts to place reflectors around the objective lens (which was required to position the cell relative to the collimator) failed due to the lens body blocking much of the light. Reflectors mounted in the place of another objective on the lens turret could be rotated into place for each irradiation, but had to be very large due to the fact that they collect light efficiently from only one half of the available solid angle.

Given these constraints, the best solution was to mount a compact photomultiplier (PMT) directly on the lens turret. This would require rotating the PMT into position for each exposure, as would the other possible detection systems. Problems of aligning the collection system and the detector would be eliminated, as would the light losses associated with reflectors and lenses. However, to be practical this approach required a very compact PMT with sufficient gain for single photon counting. The recently introduced Hamamatsu R1924-10 (1 in. diameter, 2 in. long) is satisfactory. Mounting this tube on the lens turret requires raising the microscope 2 in. and installing a 2-in. extension tube on the lens used to position the cells. However, the Zeiss Axiomat is designed for an infinite tube length so this does not affect magnification or resolution. The necessary changes have been made, and a prototype system for rotating the lens turret has been installed; this compact PMT seems to work well.

While the microscope had been replaced by a large PMT, we were able to test several other aspects of the microbeam system. The collimator was aligned and a small piece of radiachromic dosimetry film was placed at the position where the cells will be irradiated. The collimator was adjusted to produce a 5-μm square beam based on changes in the particle count rate, and the film was exposed to about 5×10^5 protons. A clearly visible blue dye spot was produced, which was found by comparison with an optical stage micrometer to be in good agreement with the predicted size. The transition from unexposed dye to exposed dye seemed to be quite sharp, suggesting that even smaller collimator sizes may be practical. The radiachromic dye film will also provide a convenient way to accurately locate the pixel address of the beam in future experiments. Although the film is relatively insensitive, it has no grain and the exposed area can be located in the video image using the same system that will be used to locate the cells.

The track etch film for detecting single-charged particle interactions was also tested. The track etch film, mounted on the petri dish positioning arm, was moved in 50-μm increments, and the shutter was opened until a single alpha particle

track was detected at each point. This test revealed a problem with the positioning system. The arm and mechanism designed to grip the petri dish was apparently too heavy and caused the servo motor system to be unstable and oscillate around the new setpoint. Furthermore, the weight of the track etch plastic distorted the thin mylar and caused it to hang up on the beam exit window. As a result, the track etch pits were not always uniformly spaced, but there was no evidence of two tracks at a single position. The dish-holding mechanism has been made much lighter, and recent tests of the positioning of single cells indicate that dishes can be positioned with the 0.1-μm precision specified for the motors.

During the tests with the microscope removed, there was very little trouble with accelerator beam alignment. Once the collimator was aligned and set for a specific spot size, the system needed very little additional adjustment for tests on several days over a period of a few weeks. This was very encouraging since beam alignment through a tandem accelerator can vary significantly from one day to the next. The results seemed to suggest that, as expected, the relatively large diameter of the beam before the collimator avoided the need for precise alignment. However, after the microscope was reinstalled and the miniature PMT was installed on the lens turret, the alignment was completely lost. The problem was traced to a defective clamp that had allowed the vertical bending magnet to rotate. The clamp problem was easily corrected, but realigning the beam has proved to be difficult due to detection of scattered beam. We are now exploring alternative methods for getting the system aligned well enough to be able to detect the primary beam through the 300-μm exit window. Once that has been achieved, past experience has indicated that it is relatively easy to complete the alignment.

Reference

Braby, L. A., and W. D. Reece. 1990. "Alpha Particle Microbeam Irradiation System." In *Physical Sciences, Part 4 of Pacific Northwest Laboratory Annual Report for 1989 to the DOE Office of Energy Research*, PNL-7200, Pt. 4, pp. 15-17. Pacific Northwest Laboratory, Richland, Washington.

Measurement
Science

Capillary Electrophoresis-Mass Spectrometry

The analysis of environmental, hazardous mixed waste or biological mixtures is best addressed by combined separation-mass spectrometry techniques. The development of these improved analytical methods rests upon the speed, selectivity, and efficiency of the separation combined with the sensitivity and flexibility of mass spectrometric analysis methods. This program is developing methods that are widely applicable to nonvolatile or highly polar compounds, intractable by more conventional methods such as gas chromatography-mass spectrometry. Currently, new methods based upon capillary electrophoresis-mass spectrometry (CE-MS) are being investigated. The goal of this research is to develop ultrasensitive CE-MS methods applicable at the attomole level for environmental and health-related problems.

Development of Capillary Electrophoresis-Mass Spectrometry

R. D. Smith, H. R. Udseth, J. A. Loo, and C. G. Edmonds

The history of analytical advances in MS has highlighted the special importance of the combination of separation methods having high selectivity and resolving power in conjunction with the high sensitivity and specificity of mass spectrometric detection. "Real-world" samples are invariably mixtures, and often very complex mixtures. Any useful analytical method must accommodate contributions from the sample matrix, interfering substances, etc. The dynamic combination of CE, a separation method of high efficiency and flexibility, with electrospray ionization (ESI)-MS is thus particularly advantageous.

Electrophoresis consists of a family of related techniques, including polyacrylamide gel electrophoresis, isotachophoresis, isoelectric focusing, gel electrofocusing, and two-dimensional electrophoresis, for very complex mixtures (i.e., extraordinarily high peak capacity). These methods are of fundamental importance in biochemical analysis where different techniques are applied according to the type of sample and the information required. Electrophoresis can be conducted in narrow tubes [10- to 250-μm inside diameter (ID)] with important advantages in efficiency and speed of analysis and unique benefits when the manipulation of very small samples is mandatory. A suite of operational modes that are highly complementary to conventional electrophoretic methods is available in the capillary format including capillary zone electrophoresis (CZE), capillary gel electrophoresis (CGE), capillary isoelectric focusing (CIEF), and capillary isotachophoresis (CITP).

The on-line combination of CZE with ESI-MS (Olivares et al. 1987; Smith et al. 1988b) was developed at PNL. Subsequently, a liquid sheath-electrode interface was developed from which the solvent composition and flow rate of the electrosprayed liquid could be controlled independent of the CZE buffer (which is desirable since high-percentage aqueous and high-ionic-strength buffers that are useful in CZE are not well tolerated by ESI) (Smith et al. 1988a). The interface provides greatly improved performance and is adaptable to other forms of CE. Because CE relies on analyte charge in solution and the ESI process appears to function most effectively for ionic species, the CE/ESI-MS combination is highly complementary. It has been reported that the analysis by CZE/MS of a mixture of quaternary ammonium compounds (Olivares et al. 1987) obtains over 600,000 plates with detection limits of $\leq$10 attomoles achievable using single ion detection. Thus, the CZE/MS approach offers previously unobtainable separation efficiencies (for the combination with MS) as well as detection limits that can greatly surpass existing methods (Edmonds et al. 1989; Loo et al. 1989a; Loo et al. 1989b; Smith et al. 1989b; Smith et al. 1990d; Smith et al. 1990a).

One reason for the current interest in CE-MS techniques is for identification and analysis of DNA adducts. This is an important but formidable analytical challenge due to the "difficult" nature of the compounds and their extremely low concentrations. Ideally, we desire not only the ability to detect "known" compounds, but to determine the structure of unknown DNA adducts with sample sizes far too small to be addressed by other analytical methods. These desires lead to our interest in CE, ESI-MS, and

ESI-MS/MS. In fact, it can be argued that the CE-MS/MS combination obtained using the ESI interface should provide a near-ideal analytical approach for DNA adducts.

To realize the full potential of this new analytical marriage, several problems remain to be addressed:

- The ESI ionization must be better understood and controlled to ensure effective analyte ionization (Smith et al. 1990c).
- The utilization and transmission of ESI-produced ions must be increased. Currently, ESI losses in the interface and during transmission reduce potential sensitivity by 10^4 (Smith et al. 1990c).
- High-resolution separations utilizing an analyte enrichment scheme are required to both deal with the complexity of "real" samples and to obtain sufficient sensitivity with the small volumes utilized in CE.
- MS/MS methods are needed that provide efficient utilization of analyte signal in order to obtain both more selective detection as well as qualitative information on structure.

We have begun research activities addressing all four of these problems. We are conducting studies that are increasing our understanding of ESI phenomena and have improved our ability to detect desired compound classes (Edmonds and Smith 1990; Loo et al. 1990b).[(a)] As an example, Figure 1 shows an ESI spectrum produced for an oligonucleotide for which sodium attachment has been greatly reduced compared to earlier efforts. In the second problem area, several new interface arrangements are being investigated that offer the potential for a substantial increase in ESI ion transmission efficiency. In the third area, we have begun collaborative efforts with several academic groups aimed at improving CE separations in conjunction with ESI-MS. We also plan to investigate multidimensional CITP, CZE, and microbore liquid chromatography-CITP multidimensional enrichment-separation schemes for obtaining increases in both sensitivity and selectivity. Finally, we are making substantial progress in the

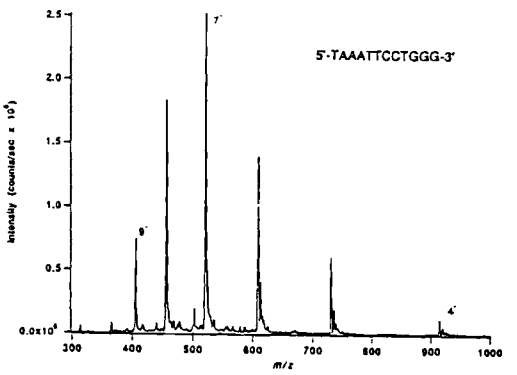

Figure 1. An Electrospray Ionization Mass Spectrum for a Synthetic Deoxyoligonucleotide (12 mer). The spectrum shows the typical distribution of anion charge states (due to protonation) and reduced complexity due to sodium.

understanding of dissociation processes for the large multiply charged ions often produced by ESI (Loo et al. 1990a; Loo et al. 1990c; Smith et al. 1989a; Smith and Barinaga 1990; Smith et al. 1990b).[(b)] We have also recently demonstrated the ability for MS/MS collisional dissociation for large multiply charged ions (up to 66 kdalton at present). In order to conduct more effective dissociation studies, we plan to begin development of an ESI interface to a fourier transform ion cyclotron resonance (FT-ICR) mass spectrometer in FY 1991. A fascinating new concept for the structural analysis of *single* large multiply charged ions in the ICR ion trap has been proposed based on sequential photodissociation processes (i.e., MS^n). This new approach would offer the ability to examine long DNA segments to determine both the site and the identity of DNA adducts. This capability, if we succeed, would literally lead to a renaissance for analytical biochemical research.

References

Edmonds, C. G., J. A. Loo, C. J. Barinaga, H. R. Udseth, and R. D. Smith. 1989. "Capillary Electrophoresis-Electrospray Ionization-Mass Spectrometry." *J. Chromatogr.* 474:21-37.

(a) Edmonds, C. G., and R. D. Smith. In press. "Electrospray Ionization Mass Spectrometry." *Methods in Enzymology: Mass Spectrometry.*

(b) Loo, J. A., C. G. Edmonds, H. R. Udseth, and R. D. Smith. In press. "Collisional Activation and Dissociation of Large Multiply Charged Proteins Produced by Electrospray Ionization." *Anal. Chim. Acta.*

Edmonds, C. G., and R. D. Smith. 1990. "Mass Spectrometry, DNA Sequencing and the Human Genome Initiative." *Division of Anal. Chem. Newsletter* Fall:27-34.

Loo, J. A., C. G. Edmonds, and R. D. Smith. 1990a. "Comparison of Electrospray Ionization and Plasma Desorption Mass Spectra of Peptides and Proteins." *Biomed. Environ. Mass Spectrom.* 19:286-295.

Loo, J. A., C. G. Edmonds, and R. D. Smith. 1990b. "Primary Sequence Information from Electrospray Ionization Tandem Mass Spectrometry of Intact Proteins." *Science* 248:201-204.

Loo, J. A., C. G. Edmonds, H. R. Udseth, and R. D. Smith. 1990c. "Effect of Reducing Disulfide-Containing Proteins on Electrospray Ionization Mass Spectra." *Anal. Chem.* 62:693-698.

Loo, J. A., H. K. Jones, H. R. Udseth, and R. D. Smith. 1989a. "Capillary Zone Electrophoresis-Mass Spectrometry with Electrospray Ionization of Peptides and Proteins." *J. Microcolumn Sep.* 1:223-229.

Loo, J. A., H. R. Udseth, and R. D. Smith. 1989b. "Peptide and Protein Analysis by Electrospray Ionization Mass Spectrometry and Capillary Zone Electrophoresis-Mass Spectrometry." *Anal. Biochem.* 179:404-412.

Olivares, J. A., N. T. Nguyen, C. R. Yonker, and R. D. Smith. 1987. "On-Line Mass Spectrometric Detection for Capillary Zone Electrophoresis." *Anal. Chem.* 59:1230-1232.

Smith, R. D., and C. J. Barinaga. 1990. "Internal Energy Effects in the Collision Induced Dissociation of Large Biopolymer Molecular Ions Produced by Electrospray Ionization: Tandem Mass Spectrometry of Cytochrome c." *Rapid Comm. Mass Spectrom.* 4:54-57.

Smith, R. D., C. J. Barinaga, and H. R. Udseth. 1988a. "Improved Electrospray Ionization Interface for Capillary Zone Electrophoresis-Mass Spectrometry." *Anal. Chem.* 60:1948-1952.

Smith, R. D., C. J. Barinaga, and H. R. Udseth. 1989a. "Tandem Mass Spectrometry of Highly Charged Cytochrome c Molecular Ions Produced by Electrospray Ionization." *J. Phys. Chem.* 93:5019-5022.

Smith, R. D., S. M. Fields, J. A. Loo, C. J. Barinaga, and H. R. Udseth. 1990a. "Capillary Isotachophoresis with UV and Tandem Mass Spectrometric Detection for Peptides and Proteins." *Electrophoresis* 11:709-717.

Smith, R. D., J. A. Loo, C. J. Barinaga, C. G. Edmonds, and H. R. Udseth. 1989b. "Capillary Zone Electrophoresis and Isotachophoresis-Mass Spectrometry of Polypeptides and Proteins Based Upon an Electrospray Ionization Interface." *J. Chromatogr.* 480:211-232.

Smith, R. D., J. A. Loo, C. J. Barinaga, C. G. Edmonds, and H. R. Udseth. 1990b. "Collisional Activation and Collision-Activated Dissociation of Large Multiply Charged Polypeptides and Proteins Produced by Electrospray Ionization." *J. Am. Soc. Mass Spectrom.* 1:53-65.

Smith, R. D., J. A. Loo, C. G. Edmonds, C. J. Barinaga, and H. R. Udseth. 1990c. "New Developments in Biochemical Mass Spectrometry: Electrospray Ionization." *Anal. Chem.* 62:882-899.

Smith, R. D., J. A. Loo, C. G. Edmonds, C. J. Barinaga, and H. R. Udseth. 1990d. "Sensitivity Considerations for Large Molecule Detection by Capillary Electrophoresis-Electrospray Ionization Mass Spectrometry." *J. Chromatogr.* 516:157-165.

Smith, R. D., J. A. Olivares, N. T. Nguyen, and H. R. Udseth. 1988b. "Capillary Zone Electrophoresis-Mass Spectrometry Using an Electrospray Ionization Interface." *Anal. Chem.* 60:436-441.

Lasers in Environmental Research

This program has historically investigated the use of high-resolution continuous-wave (cw) lasers for atomic spectroscopy measurements of extremely rare isotopes. In FY 1989, high-resolution multiphoton spectroscopic techniques were extended to the investigation of molecular species. The extremely high resolution available under cw excitation conditions is yielding unprecedented information on the structural and dynamical properties of excited electronic states of molecules. In addition to exploring analytical applications, this work will yield a basic understanding of both the detailed structure of small molecules and their complex decay dynamics through processes such as autoionization and predissociation. Studies of nitric oxide (NO), an important atmospheric pollutant generated in energy production, have continued with comprehensive measurements of rotational structure in the two-photon laser-induced fluorescence (LIF) of the $A^2\Sigma^+$ ($\upsilon = 1$) $\leftarrow X^2\Pi$ ($\upsilon = 0$) transition. These measurements have resulted in new, high-precision structural constants that allow an accurate description of the molecule in high rotational states. The new cw-cw double-resonance spectroscopic technique, used for the measurement of term energies and predissociation rates in higher lying Rydberg states that was initially demonstrated last year, has been extended to a comprehensive set of measurements examining the multistate perturbations and predissociation dynamics in the region of the $K^2\Pi$ ($\upsilon = 2$) and $F^2\Delta$ ($\upsilon = 3$) Rydberg states.

Two-Photon LIF Spectroscopy of Nitric Oxide: $A^2\Sigma^+$ ($\upsilon = 1$) $\leftarrow X^2\Pi$ ($\upsilon = 0$)

B. A. Bushaw

These experiments involved counterpropagating the focused laser beam through a static cell containing (typically) 50 millitorr of NO, inducing the two-photon excitation to the *A* state. The *A* state population produced was then monitored by observing the resulting one-photon fluorescence decay back to the ground state. Initial measurements (Miller et al. 1989) on this transition covered a very limited frequency range and were directed toward demonstrating the ability to fully resolve hyperfine structure. Since then, a complete spectrum from 46,330 cm^{-1} to 46,650 cm^{-1}, encompassing the $A \leftarrow X(1,0)$ vibronic band, has been acquired and all of the 357 observed rotational lines have been assigned. The energies of the individual rotational transitions can be described by

$$E_A = E_{ev} + B'[N(N+1)] - D'[N(N+1)]^2 + H'[N(N+1)]^3 + \ldots + Q$$

$$E_X(\Omega = 1/2) = B''_1 J(J+1)] - D''_1[J(J+1)]^2 + H''_1[J(J+1)]^3 + \ldots \pm \tfrac{1}{2} g_1 (J + \tfrac{1}{2})$$

$$E_X(\Omega = 3/2) = A_\Omega + B'_3[J(J+1)] - D'_3 [J(J+1)]^2 + H'_3[J(J+1)]^3 + \ldots \pm \tfrac{1}{2} g_3 (J + \tfrac{1}{2})^3$$

$$E_T = E_A - E_X$$

where $Q = \gamma N/2$ or $-\gamma(N+1)/2$, respectively, for the F_1 and F_2 components of the excited state fine structure doublet and γ is the fine structure splitting parameter. E_{ev} is the total electronic and vibrational energy of the transition; for each state, B is the rotational constant, and D and H are corrections for centrifugal distortion. The two ground state spin-orbit components are treated as distinct potential surfaces separated by A_Ω, the term splitting due to the spin-orbit interaction in the absence of nuclear rotation. Lambda doubling in the ground state rotational levels is described by the constants g_1 and g_3, respectively, for the $\Omega = 1/2$ and $\Omega = 3/2$ spin-orbit components. *N* is the rotational total angular momentum excluding spin in the excited state, the quantum number appropriate to Hund's case (b) coupling for a Σ state; *J* is the total angular momentum excluding nuclear spin in the ground state, the quantum number appropriate to case (a) coupling. The values of these constants, given in Table 1, were found by least-squares fitting to the measured energies for all the observed lines. Using these constants gives an accurate

Table 1. Constants Derived from Analysis of the $(3s\sigma)\ A^2\Sigma^+(v = 1) \leftarrow X_2\Pi(v = 0)$ Doppler-Free LIF Spectrum of $^{14}N^{16}O$. All values are in cm^{-1} and the uncertainties given in parentheses are in units of the last reported digit.

	State		
Constant	$X^2\Pi(\Omega = 1/2, v = 0)$	$X^2\Pi\ (\Omega = 3/2, v = 0)$	$A^2\Sigma^+\ (v = 1)$
B	1.67204(2)	1.72005(2)	1.96732(2)
D	9.5(6) x 10^{-7}	1.003(6) x 10^{-5}	5.46(7) x 10^{-6}
H	-8.1(4) x 10^{-10}	9.5(4) x 10^{-10}	1.2(5) x 10^{-10}
g, γ	1.008(6) x 10^{-2}	4.32(8) x 10^{-6}	-2.67 x 10^{-3}
A_Ω		119.718(1)	
E_{ev}			46542.1856(7)

description of the transition energies (root-mean-square deviation of 0.005 cm^{-1}) for rotational levels up J" = 30.5. Figure 1 compares the observed transition energies with calculated values using the constants given in Table 1 and with previously available literature constants (Huber and Herzberg 1979; Amoit and Verges 1982). It can be seen that while both produce accurate descriptions at lower (N < 20) rotational levels, the existing literature values fail for the higher rotation states that are important in high-energy processes.

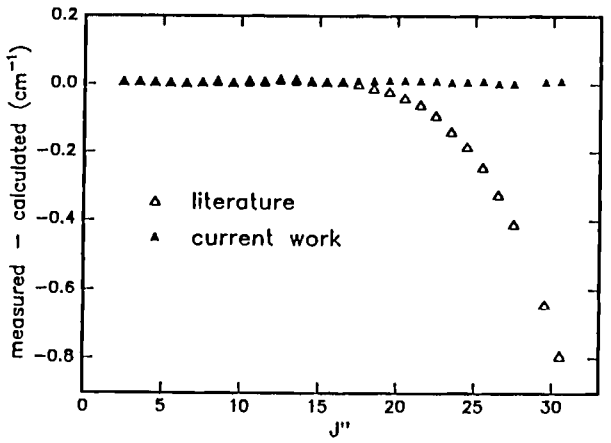

Figure 1. Differences Between Measured and Calculated Energies for the O_{12} Branch of the $(3s\sigma)A^2\Sigma^+(v = 1) \leftarrow X^2\Pi(v = 0)$ Transition of $^{14}N^{16}O$ Using Best Available Structural Constants from the Literature and Constants Derived from the Current Doppler-Free LIF Spectrum

References

Amoit, C., and J. Verges. 1982. "Fourier Transform Spectrometry of the $D^2\Sigma^+$-$A^2\Sigma^+$, E^2R^+-D^2R^+, and E^2R^+-$A^2\Sigma^+$ Systems of Nitric Oxide." *Phys. Scr.* 26:422-438.

Huber, K. P., and G. Herzberg. 1979. *Molecular Spectra and Molecular Structure IV. Constants of Diatomic Molecules.* Van Nostrand, New York.

Miller, R. J., W. L. Glab, and B. A. Bushaw. 1989. "Two-photon Spectroscopy at Ultrahigh Resolution: Fine Structure and Hyperfine Structure of the $(3s\sigma)A^2\Sigma^+(v = 1, N = 3)$ Rydberg State of NO." *J. Chem. Phys.* 91:3277-3279.

2 + 1' LIF Dip Spectroscopy of the $K^2\Pi(v = 2)$ and $F^2\Delta(v = 3)$ States of NO

R. J. Miller and B. A. Bushaw

The excitation scheme used in these experiments begins with a two-photon excitation to a selected level of the $A^2\Sigma^+(v = 1)$ state, similar to that described above for the Doppler-free excitation. However, the laser beam is not counterpropagated and thus, when the laser is tuned to the center of the Doppler profile, only those molecules with zero longitudinal velocity are excited to the A state. Then, subsequent one-photon excitation to higher lying states can be performed in a Doppler-free manner on the velocity-selected population. For the second step in the current measurements, another cw single-frequency dye laser was used to promote the initially excited molecules to a higher lying Rydberg state, which can then decay by a variety of channels. As long as this decay differs from the excitation (predissociation or radiative cascade through other states), there is a concomitant reduction in the one-photon fluorescence intensity from the A state, and

hence a "dip" in the signal. A preliminary report of this technique discussed the use of a single $A \leftarrow X$ pump transition and the six K state levels that could then be populated from this selected pump level (Miller and Bushaw 1990). These measurements have now been extended to all of the rotational levels, and the individual spin and lambda doubling components thereof, of the K state up through rotational level $N = 15$. The spectral resolution obtained in these experiments has provided measurements of the frequencies (Figure 1A), to an absolute accuracy of better than 0.002 cm^{-1}, and of the widths (Figure 1B), to an average precision of 3%, of the $K \leftarrow A(2,1)$ rotational transitions of interest. The lifetimes of these levels range from 100 to 600 ps and show substantial structure. Some levels of the F state have also been observed in cases wheremixing by accidental energy degeneracy with the K state gives sufficient oscillator strength to these normally forbidden $\Delta \leftarrow \Sigma$ transitions. These results are currently being interpreted in terms of the structural and dynamical ramifications of the weak $(4p\pi)K^2\Pi(v = 2) \sim (3d\delta)F^2\Delta(v = 3)$ perturbation occurring in this energy region as well as other perturbations coupling the $(4p\pi)K^2\Pi(v = 2)$ state to the dissociative continua.

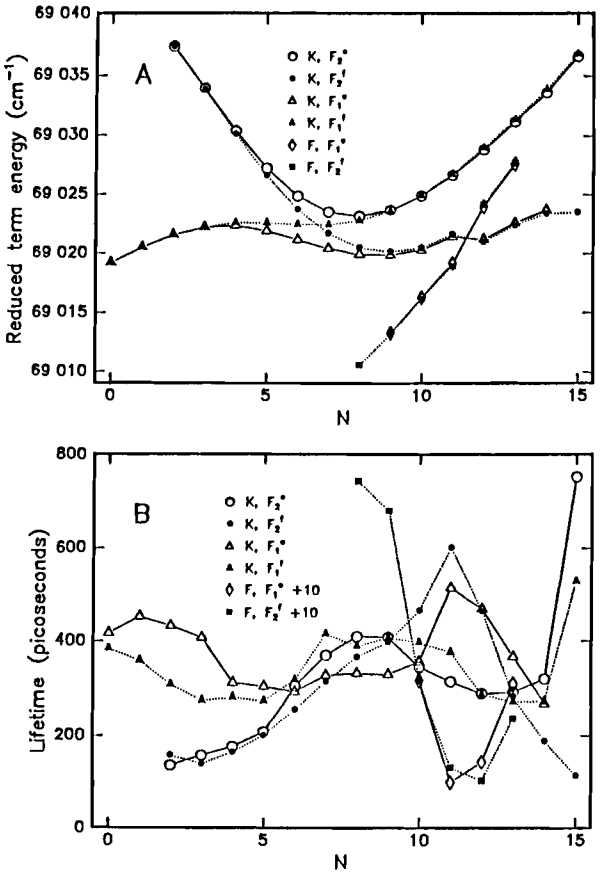

Figure 1. A) Reduced Term Energies [actual transition energy minus approximate rotational energy of 1.75 x N(N + 1)] and B) Predissociation Lifetimes, Deducted from Lineshape Analysis, for Individual Rotational, Spin, and Parity Components of the $K^2\Pi(v = 2)$ and $F^2\Delta(v = 3)$ States of $^{14}N^{16}O$.

Reference

Miller, R. J., and B. A. Bushaw. 1990. "Continuous Wave-Continuous Wave Molecular Double Resonance Spectroscopy: Lifetimes and Term Energies of Individual Rovibronic Levels of the $(4p\pi)K^2\Pi(v = 2)$ Rydberg State of Nitric Oxide." *J. Chem. Phys.* 92:3245-3247.

Radiological and Chemical Physics

Radiation Physics

The spatial and temporal patterns of energy deposition play a dominant role in determining the subsequent chemical and biological processes leading to radiation damage in biological systems. For high linear energy transfer (high-LET) radiation, these patterns of energy deposition are determined by the production and slowing down of secondary electrons that define the structure of charged particle tracks. Our studies focus on investigation of the absolute cross sections for interactions involving charged particles and electrons with atomic and molecular targets that contribute to the structure of charged particle tracks in tissue-like material. Emphasis is on the study of differential ionization cross sections, charge-transfer processes, and on the fate of the target atom/molecule that has undergone an ionizing event. The information from these studies is then incorporated in Monte Carlo models developed to provide detailed descriptions of charged particle track structure and the influence of that structure on subsequent chemical and biological processes.

During the past year, our studies have focused on efforts to understand the effects of projectile structure on interaction cross sections and to implement new target structures into the Monte Carlo transport codes. A combined experimental and theoretical study of the doubly differential cross sections for electron emission in C^+-He collisions was completed. Collaborative studies were also undertaken to investigate the role of projectile structure in simpler systems such as H°- He in order to test the adequacy of Born theory and available wave functions. Progress has also been made in the development of techniques to extend measurements to condensed phase targets. Such measurements will serve to test evolving models of energy transport in liquid and solid targets. A new effort was also initiated to incorporate more realistic biological target material into the Monte Carlo transport codes. This makes use of recent studies of the detailed electronic structure of chromatin.

Doubly Differential Cross Sections in Electron Emission for H°-He, Ar Collisions

R. D. DuBois

Numerous experimental and theoretical studies have demonstrated that ionization of atoms by fast, fully stripped ion impact can be adequately calculated using the first Born approximation. The next step is to extend this level of understanding to collisions involving partially stripped projectile ions. For these collisions, however, the picture is complicated due to screening of the nuclear charge by the bound projectile electrons and the possibility of ionizing either, or both, the target and the projectile. Therefore, several years ago we introduced an emitted electron-ionized projectile coincidence technique to provide details about electron emission occurring as the result of partially stripped ion impact (DuBois and Manson 1986). Using this technique, combined with noncoincidence differential electron emission data, we were able to identify electron emission attributable to target, projectile, and simultaneous (meaning in a single collision) target-projectile ionization.

Initially we studied fast He^+-He collisions. A comparison with calculations performed using the first Born theory indicated that when the theory was modified to account for screening of the nuclear charge and simultaneous ionization of both collision partners, reasonable agreement with the experimental data for target and for projectile ionization was achieved. Simultaneous target-projectile ionization probabilities were severely underestimated.

In a followup, more extensive study of He^+-Ar collisions (DuBois and Manson 1990), poor agreement between experiment and theory was found. This opened the following questions: was the good agreement for the He target merely fortuitous, was the poor agreement for Ar simply a consequence of using inadequate wave functions, or is there an unknown inadequacy in the theoretical treatment?

To answer these questions and to extend our basic understanding of collisions involving partially stripped ion impact, we have conducted a study of fast (0.5 and 1 MeV) H° impact on He and Ar targets (Heil et al. 1990). This study was made in collaboration with the Institut für Kernphysik at the J. W. Goethe Universität, Frankfurt/M, FRG. Data from these measurements again demonstrated the importance of simultaneous target-projectile ionization. The data for ionization of He when compared to Plane Wave Born Approximation (PWBA) calculations using hydrogenic wave functions yielded good agreement with theory for projectile ionization and, indirectly, reasonably good agreement for target ionization; simultaneous target-projectile ionization events were not included in the model. Thus we conclude that the discrepancies noted in our earlier study of He^+-Ar collisions, as discussed above, resulted from inadequate wave functions used in the theoretical treatment. In our recent study of H°-Ar collisions, electron emission in angles between and including 0° and 180° was investigated. These data were compared with more sophisticated calculations for electron loss. This comparison indicated that second-order effects play a dominant role in electron emission at large observation angles.

References

DuBois, R. D., and S. T. Manson. 1986. "Coincidence Study of Doubly Differential Cross Sections: Projectile Ionization in He^+-He Collisions." *Phys. Rev. Lett.* 57:1130-1132.

DuBois, R. D., and S. T. Manson. 1990. "Electron Emission in He^+-Atom and He^+-Molecule Collisions: A Combined Experimental and Theoretical Study." *Phys. Rev. A* 42:1222-1230.

Heil, O., R. D. DuBois, R. Maier, M. Kuzel, and K.-O. Groeneveld. 1990. "Electron Emission in H°-Atom Collisions: A Coincidence Study of the Angular Dependence." Presented at the Eleventh International Conference on the Application of Accelerators in Research and Industry, Novmeber 5-8, Denton, Texas.

Differential Cross Sections for Electron Emission in Heavy Ion Collisions

L. H. Toburen and R. D. DuBois

Cross sections for the production of secondary electrons by low- and intermediate-energy carbon, oxygen, and nitrogen ions are of interest for analysis of the track structure features relevant to the interaction of fission spectrum neutrons with biological tissue. A microdosimetric description of the energy deposition resulting from such neutron exposures must include the track structure contributions of these "heavy" ion recoils. A major obstacle to the understanding of energy loss in heavy ion collisions has been the lack of adequate theory. During the past 2 years we have collaborated with Drs. Reinhold, Shultz, and Olson of the University of Missouri-Rolla, who have applied their Classical Trajectory Monte Carlo (CTMC) techniques to calculate the singly and doubly differential cross sections for electron emission in C^+-He collisions. These calculations have focused on the ion energy range from 66.7 to 350 keV/u, for which we have experimental data. These are the first CTMC calculations of the electronic spectra arising from both target and projectile ionization. A comparison of experiment and theory was shown in last year's report. During the past year additional experimental studies were undertaken to improve the basis for the absolute magnitude of the measured cross sections, and additional calculations were completed with improved model potentials.

The experimental system for differential electron emission uses a defuse gas beam target. This technique precludes a direct determination of the absolute cross sections owing to inadequate information on the density profiles within the interaction region. To obtain absolute calibration of the relative cross sections, data were accumulated for C^+ and H^+ ions under identical target conditions. The proton data were

then compared to previously measured absolute cross sections to obtain the system calibration. This calibration was then applied to the C^+ data to place them on an absolute scale. Figure 1 provides an illustration of the doubly differential cross sections obtained for 3.6-MeV (300 keV/u) C^+ ionization of He.

A test of the accuracy of the absolute magnitude of the cross sections derived using this calibration technique can be made based on the total electron yields. The total electron emission cross sections obtained from integration of the doubly differential cross sections over emission energy and ejection angle can be compared to total yields derived from measurement of target charge states measured using coincidence techniques. Such measurements, described by DuBois in another section of this report, provide an independent measure of the total cross section. The integrated yields are compared to measure total yields for C^+ and N^+ ions in Figure 2. The excellent agreement lends confidence to our calibration technique.

A second method to test the internal consistency of the measured yields compares the cross sections for K-shell ionization of the carbon projectile with measurements in which the collision is reversed, i.e., carbon atoms are ionized by He ion beams. The cross sections for ionization of the projectile K-shell are obtained from the yield of Auger electrons emitted when the K-shell vacancy is filled; the fluorescence yield for this low Z element is negligible. In practice, the area under the Auger spectra, observed as small peaks on the continuum spectra of electrons emitted into the forward direction in Figure 1, is determined, translated into the projectile-centered reference frame, and converted to cross sections. These cross sections can then be compared to independent measurements based on either Auger or x-ray detection; such a comparison is shown in Figure 3. Excellent agreement is again seen between the cross sections derived from the present data and independent measurements (Watson and Toburen 1973; Stolterfoht et al. 1973; Stolterfoht and Schneider 1975; Kobayashi et al. 1976; Langenberg and Van Eck 1976; Harrison et al. 1973) using different techniques. These tests provide confidence in the measured differential cross sections and enable reliable evaluation of collision theory.

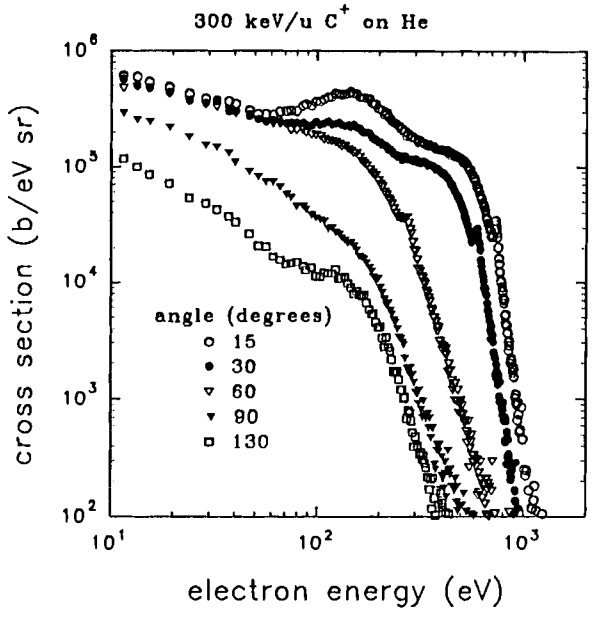

Figure 1. Doubly Differential Cross Sections for Electron Emission into 15, 30, 60, 90, and 130° by 300=keV/u C^+ Ions

An example of the ability of CTMC theory to describe these intermediate energy collisions is shown in Figure 4. The degree of agreement seen here is comparable to that found throughout the energy range from 66- to 350-keV/u where measurements were made. In general, excellent agreement between theory and experiment is found for ejected electron energies greater than 100 eV with measured values being larger than calculated values for the lower energy electrons. The reason for the discrepancies between theory and experiment for low-energy ejected electrons is not clear. This may be a result of inadequate treatment of multiple ionization processes or electron-electron correlation. Further study will be required to try to understand these features.

The results presented in this section have been discussed in two publications during the past year (Reinhold et al. 1990; Toburen et al. 1990). The interested reader is directed to those publications for the details of the measurement and computational techniques.

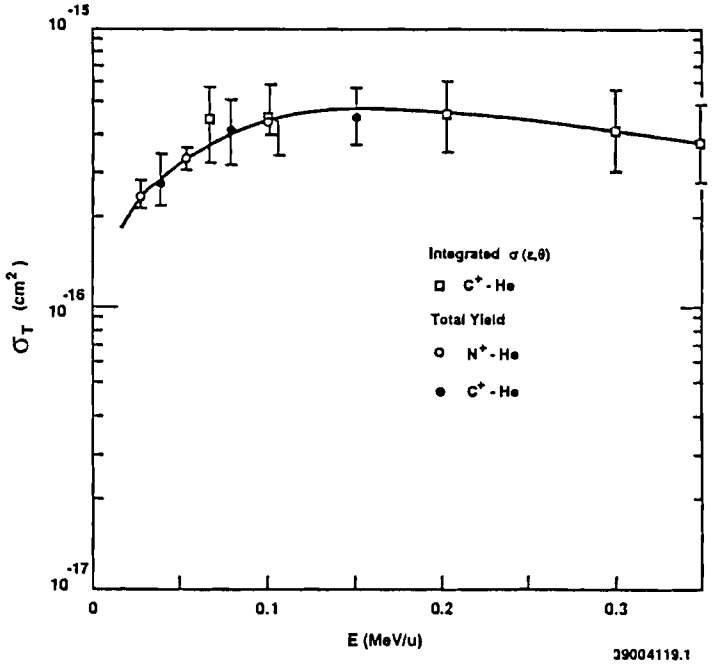

Figure 2. Total Cross Sections for the Production of Electrons in Collisions of C^+ - N^+ Ion with Helium. Cross sections obtained by integration of measured doubly differential cross sections are compared to those obtained from coincidence measurements of total ion yields.

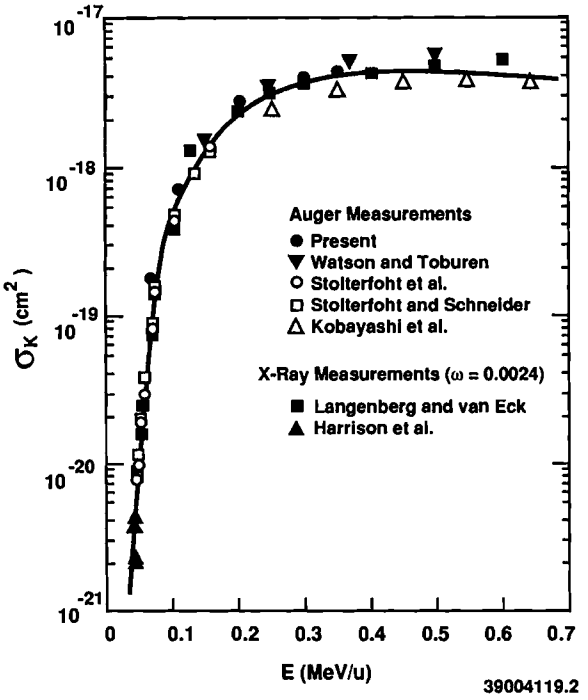

Figure 3. Carbon K-Shell Ionization Cross Sections from C^+-He Collisions Compared with Previous Measurements for He^+ and He^{2+} Collisions with Carbon Targets. The previously published data are from Watson and Toburen (1973), Stolterfoht et al. (1973), Stolterfoht and Schneider (1975), Kobayashi et al. (1976), Langenberg and Van Eck (1976), and Harrison et al. (1973).

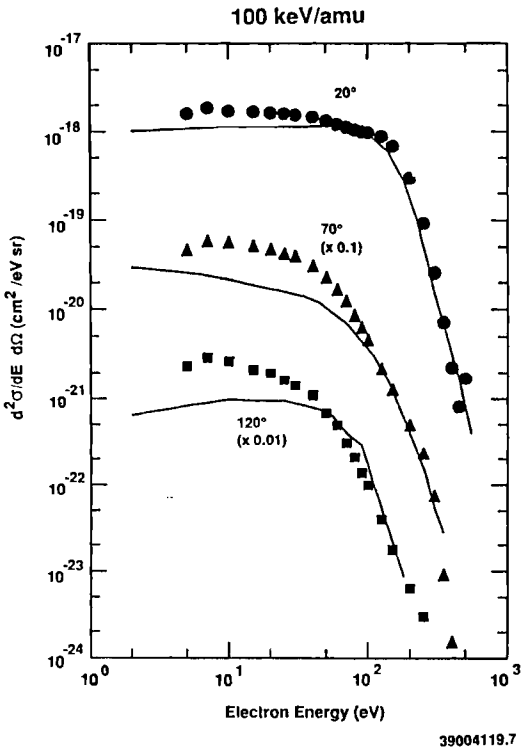

Figure 4. Comparison of Calculated CTMC Cross Sections (solid lines) with Measured Doubly Differential Electron Emission Cross Sections for 100-keV/u C^+ Collisions with Helium Atoms

References

Harrison, K. G., H. Tawara, and F. J. de Heer. 1973. "K-Shell X-Ray Emission Cross Sections and Ionization Cross Sections for Light Ions and Molecules by H^+, H_2^+, and He^+ Impact at 30-145 keV." *Physica* 66:16-32.

Kobayashi, N., N. Maeda, H. Hari, and M. Sakisaka. 1976. "K-Shell Ionization of Carbon, Nitrogen, Fluorine and Neon by Proton and Alpha Particle Bombardment." *J. Phys. Soc. Japan* 40:1421-1429.

Langenberg, A., and J. Van Eck. 1976. "Carbon, Nitrogen, Neon, and Argon K-Shell Ionization by Proportional Helium Ion Impact: X-Ray Emission Cross Sections and Fluorescence Yields." *J. Phys. B* 9:2421-2433.

Reinhold, C. O., D. R. Schultz, R. E. Olson, L. H. Toburen, and R. D. DuBois. 1990. "Electron Emission from Both Target and Projectile in C^+ + He Collisions." *J. Phys. B* 23:L297-L302.

Stolterfoht, N., and D. Schneider. 1975. "Cross Sections for K-Shell Ionization of CH_4, Ne by 50- to 600-keV H^+ and He^+ Impact." *Phys. Rev. A* 11:721-723.

Stolterfoht, N., D. Schneider, and K. G. Harrison. 1973. "K-Shell Ionization of N_2 and CH_4 by 50- to 600-keV H^+, D^+, H_2^+ and He^+ Impact." *Phys. Rev. A* 8:2363-2371.

Toburen, L. H., R. D. DuBois, C. O. Reinhold, D. R. Schultz, and R. E. Olson. 1990. "Experimental and Theoretical Study of the Electron Spectra in 66.7 to 350 keV/u C^+ + He Collisions." *Phys. Rev. A* 42:5338-5347.

Watson, R. L., and L. H. Toburen. 1973. "Auger Spectra of Carbon and Argon Following Ionization by Equal Velocity α Particles and Deuterons." *Phys. Rev. A* 7:1853-1863.

Electron Emission from Condensed Targets

Ling-Jun Wang,[a] L. H. Toburen, and R. D. DuBois

An understanding of energy transport by secondary electrons in condensed phase material is a critical ingredient in the modeling of chemical and biological damage from interactions of high-LET radiation in biological systems. Our present models are based on measurements made in gas phase and/or theoretical models of energy transport in model liquids. The objective of this work is to obtain experimental results that can test our knowledge of condensed phase energy transport.

We have designed and assembled an ultrahigh vacuum chamber for use in the study of electron emission from condensed phase targets bombarded by fast protons and alpha particles. Preliminary measurements will focus on electron emission from thin carbon films where considerable data exist for testing the reliability of our analysis system. We have installed a time-of-flight analyzer for the study of doubly differential cross sections for electron emission. Both gas and foil targets are incorporated to provide accurate comparison of spectra as a function of target phase.

During the past year the vacuum system was assembled and tested on the 2-MV Van de Graaff beam line of the PNL charged particle irradiation facility. Alignment of the system was accomplished, and proton beams were detected through the system. In addition, software was developed for data analysis and plotting using model time-of-flight spectra. Actual tests of the time-of-flight system had to be delayed because of a malfunction of the ion beam pulsing system. The required upgrade of the ion beam pulsing system is now under way and we expect to begin operation in the near future.

(a) Visiting professor, Department of Physics, University of Tennessee-Chattanooga, Chattanooga, TN.

Multiple Ionization of Helium by Carbon, Nitrogen, and Oxygen Ions

R. D. DuBois

Using our recoil ion-projectile ion coincidence technique, we investigated ionization occurring in C^{q+}-, N^{q+}-, and O^{q+}-He collisions ($1 \leq q \leq 3$). Absolute cross sections for single- and double-target ionization were measured for direct target ionization (where the projectile charge q is unchanged in the collision), for single-electron capture by the projectile, and

for single and double electron loss by the projectile. The impact energy range investigated was from 25 to 150 keV/amu, although only the most intense processes (those accounting for >1% of the total cross section) were investigated at each energy.

Several different aspects of these collisions can be investigated using these data. For example, information about the effective projectile charge during the collision can be extracted (DuBois and Toburen 1988). The relative importance of various ionization channels (direct target, electron capture, or single/double electron loss) can also be investigated. For example, in Figure 1, data for 100-keV/amu N^{q+}-He collisions (q = 0, 1, 2, 3) are shown. The percentage of the total electron production arising from direct target ionization is seen to increase from roughly 30% to nearly 80% as the projectile charge increases. Collisions where single loss from the projectile occurs account for 50% of the electron production for neutral nitrogen impact. This decreases to approximately 10% as q increases; double loss contributions are roughly a factor of 3 to 5 smaller. On the other hand, electron capture contributions increase as q increases.

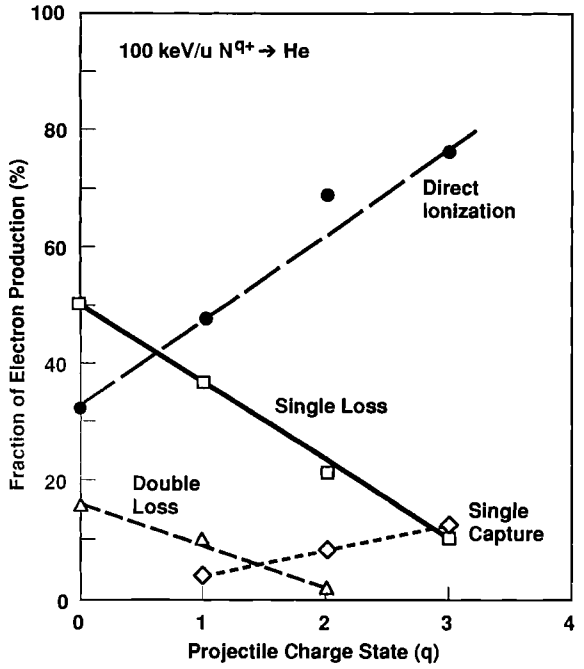

Figure 1. Fraction of Total Electron Production Due to Direct Ionization, Electron Capture, and Electron Loss Channels in N^{q+}-He Collisions

Another utility of these data is for normalization purposes, e.g., these data have been used to place our relative measurements for differential electron production on an absolute scale (see previous section for details).

Reference

DuBois, R. D., and L. H. Toburen. 1988. "Single and Double Ionization of Helium by Neutral-Particle to Fully Stripped Ion Impact." *Phys. Rev. A* 38:3960-3968.

Molecular Dissociation

R. D. DuBois

For the past several years we have been using a recoil ion-projectile ion coincidence technique to provide information about the various electron production channels active in ion-atom collisions. A year ago we extended these studies to simple molecular targets. In these collisions, the ionized molecule often dissociates into charged and uncharged fragments. The charged fragments are detected and their intensities converted into absolute cross sections. As an example of such data, absolute cross sections for target ion production in He^+-N_2 collisions are shown in Figure 1.

These data are obtained by using an electric field to extract the fragment from the interaction region. This method, however, suffers from the fact that dissociation into two identically charged fragment ions, e.g., dissociation into two N^+ ions, cannot be measured since both ions arrive at the detector at the same, or nearly the same, time. It is possible to obtain an estimate of the importance of such events by summing the present cross sections to obtain the total free electron production cross section (▼ in Figure 1A). This sum can then be compared to results obtained previously using a total yield technique (Rudd et al. 1985) (— in Figure 1A). If the sum is smaller than the total yield result, the difference may be attributable to N^+-N^+ dissociation events. For He^+-N_2 collisions, the data shown in Figure 1 imply that approximately half of the recorded N^+ intensity comes from N^+-N° events and half comes from N^+-N^+ events.

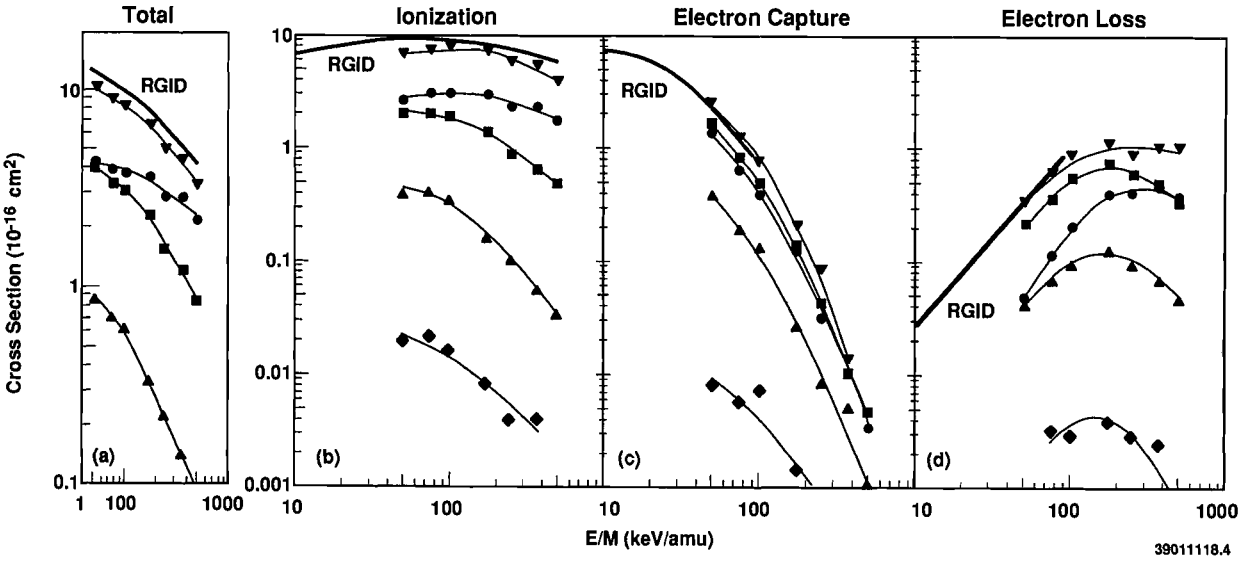

Figure 1. Absolute Cross Sections for Target Ion Production in He^+-N_2 Collisions. ■, ▲, ♦ = N^+, N^{2+}, N^{3+}, respectively. ▽ are total cross sections obtained by summing the individual cross sections, e.g., total ion production (A), total electron production (B), electron capture (C), electron loss (D). The lines through the data serve only to guide the eye. The bold lines (RGID) are total cross sections for ion production, electron production, electron capture and loss (A-D) taken from Rudd et al. (1985).

To test this and to provide additional information about ionization of molecules, an experimental apparatus was constructed in collaboration with the atomic collision group of H. Schmidt-Böcking at the Institut für Kernphysik, J. W. Goethe Universität, Frankfurt/M, FRG. The apparatus consisted of two channelplate detectors located at ±90° with respect to the beam direction. Centered in the field-free region between the detectors was a point target, simulated by a gas jet. Low-energy molecular ions, as well as energetic atomic ions resulting from dissociation, could be identified via their flight times from the source to the detector (see Figure 2). Ions could be detected in the Θ and ϕ directions between approximately 15° and 165°.

Signal intensities for atomic ions detected in *either* detector are proportional to dissociation into one charged and one uncharged fragment, whereas intensities recorded in *both* detectors simultaneously indicate dissociation into two charged fragments. This is demonstrated in the lower portion of Figure 2. Data obtained for He^+ impact on molecular nitrogen are currently being evaluated to determine whether our estimates of the amount of dissociation into two charged fragments are correct.

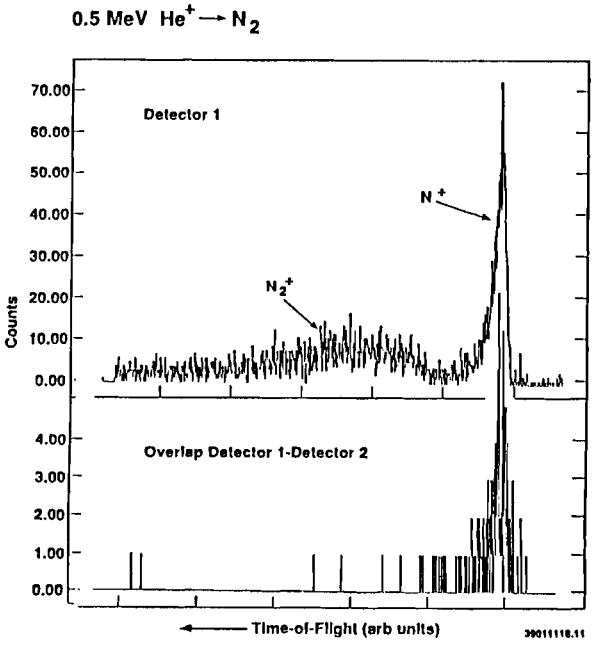

Figure 2. Time-of-Flight Spectra for Target Ions Created in 0.5 MeV $He^+ + N_2 \rightarrow He^+ +$ Dissociation Fragments Collisions. Upper portion of figure shows molecular and atomic ions as detected by a single detector. Lower portion shows ions detected by second detector associated with atomic ions detected by first detector, i.e., $N^+ + N^+$ dissociation fragments.

Reference

Rudd, M. E., T. V. Goffe, A. Itoh, and R. D. DuBois. 1985. "Cross Sections for Ionization of Gases by 10-2000 keV He^+ Ions and for Electron Capture and Loss by 5-350 keV He^+ Ions." *Phys. Rev. A* 32:829-835.

A Relativistic Model for Calculating Secondary-Electron Energy Spectra from Optical Oscillator Strengths and Total Ionization Cross Sections

J. H. Miller and S. T. Manson[(a)]

The energy spectrum of secondary electrons plays a central role in our understanding of the effects on the stopping medium of energy absorbed from ionizing radiation. Therefore, ionization cross sections that are differential in the energy of secondary electrons contribute to several areas of applied science including plasma physics, atmospheric studies, and radiation therapy. In many of these applications it is important to have cross section data over a broad range of projectile velocities and secondary-electron energies for several target species. These needs are rarely satisfied completely by experimental data. Furthermore, even though supercomputers have become more accessible in recent years, *ab initio* calculations are still too costly, time consuming, and unreliable to fill all the gaps in the experimental data. For these reasons, semiempirical methods continue to be an important source of cross section data.

Since experimental single differential cross sections (SDCS) are obtained by integrating doubly differential measurements over the full range of emission angles of secondary electrons, it is not surprising that total ionization cross sections (TICS), which can be measured directly, are more readily available. Therefore, we are interested in developing semiempirical methods that do not require any differential ionization data to predict the energy spectrum of secondary energies with an accuracy that is comparable to current experimental techniques. This objective seems reasonable for primary electrons and bare ions with velocities that exceed the average velocity of valance electrons in the target because 1) optical oscillator strengths determine the shape of the spectrum at low secondary-electron energies, 2) the shape of the spectrum at high secondary-electron energy is reasonably well approximated by binary-encounter models, and 3) total cross sections provide the normalization of the spectrum. When the projectile's velocity is comparable to or less than the average velocity of valance electrons in the target, the first Born approximation, which is the theoretical basis of our model, is no longer a valid description of the ionization process. Extension of our semiempirical methods into the low-velocity region requires a better understanding of the effects of electron exchange, quasi-molecular states, and charge transfer processes on the energy spectrum of secondary electrons. Nevertheless, at high and intermediate projectile velocities, our model is well suited for application to complex target species such as macromolecules and condensed matter since for these systems experimental differential ionization data are very limited.

Calculations of SDCS must include relativistic effects if they are to be applicable to primary and secondary electrons with very high energy. This intensifies the difficulty of the *ab initio* approach since the relativistic form factor must be evaluated with relativistic wave functions for the initial and final states; however, our semiempirical model that combines the theories of glancing and close collisions is well suited to approximate these effects. In the limit of small momentum transfer (i.e., glancing collisions), the relativistic form factor is well approximated by the nonrelativistic form factor plus a term that is proportional to the nonrelativistic dipole matrix element. Relativistic effects in close collisions can be approximated without introducing parameters, other than kinematic factors, that are not already present in the nonrelativistic binary-encounter approximation. In addition, the simple analytic form of the model facilitates investigation of the regions of primary- and secondary-electron energies where relativistic effects are important. Figure 1 shows that relativistic corrections to SDCS for ionization of He by electron impact are larger at low and high secondary-electron

(a) Department of Physics and Astronomy, Georgia State University, Atlanta, Georgia.

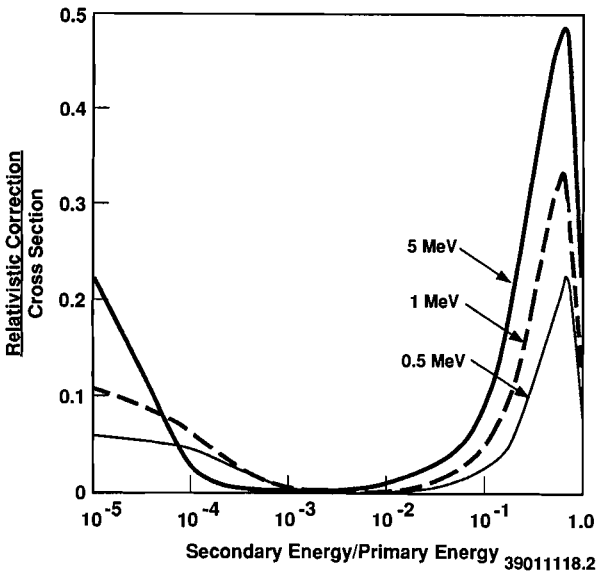

Figure 1. Relativistic Corrections to the Energy Spectrum of Secondary Electrons Ejected from Helium by 0.5-, 1.0-, and 5.0-MeV Primary Electrons

energies than they are at intermediate energies. We believe that similar effects will be found for more complex target species.

Modeling Chromatin Fibers

W. E. Wilson and J. H. Miller

It is generally believed that damage to critical subcellular targets of nanometer dimension is responsible for lethal and mutagenic effects of ionizing radiation (Goodhead and Nikjoo 1986). Most efforts at cellular and subcellular stochastic dosimetry calculations have used a homogeneous model for the target media, and generally that media has been water in either liquid or vapor phase. To provide a more realistic and detailed target for radiation effects, we are collaborating with Professor John P. Langmore at the University of Michigan to investigate the role of chromatin structure in radiation damage to the cell's genetic material.

Structural biology studies (Williams et al. 1986) have suggested several possible configurations for in vivo thick fibers of chromatin. A consensus believes that the fundamental repeating subunit of chromatin is the nucleosome; DNA wraps around the nucleosomes and links them as "beads-on-a-string." How the beads-on-a-string are then compacted to form fibers is not yet completely understood. A common feature of the different description of DNA structure is that the nucleosomes form a solenoid-like structure of closely packed spheres, but just how the linker-DNA is involved with the solenoid is uncertain. Two classes of structure seem to prevail; one has the solenoid essentially empty and the tissue-specific linker somehow wrapped among and between the nucleosome spheres comprising the bulk of the solenoid. The other class, preferred by Langmore and coworkers, has the linker-DNA crossing and more or less filling the solenoid core.

The two classes of models for the thick chromatin fibers may predict distinctly different radiation sensitivities for the genetic material. For example, in the crossed-linker models, linker-DNA may be protected from indirect radical attack by limited water access and shielded from the direct ionization by the surrounding nucleosomes. To explore these possibilities, we are using the space-filled computer models of the thick fiber developed by Williams et al. (1986) to extend our track simulation techniques to heterogeneous materials of biological significance.

References

Goodhead, D. T., and H. Nikjoo. 1986. "Track Structure Analysis of Ultra-Soft X-Rays Compared to High- and Low-LET Radiations." *Int. J. Radiat. Bio.* 55: 513-529.

Williams, S. P., B. D. Athey, L. J. Muglia, R. S. Schappe, A. H. Gough, and J. P. Langmore. 1986. "Chromatin Fibers Are Left-Handed Double-Helices with Diameter and Mass Per Unit Length That Depend on Linker Length." *Biophys. J.* 49:233-248.

Radiation Dosimetry

The primary goal underlying the Radiation Dosimetry task is to understand the connections between the physical events produced by the interaction of ionizing radiation with matter and their biological consequences. These consequences result from complex combinations of events involving a variety of initial radiochemical products as well as the products of later chemical reactions and biological responses. However, the probability of specific products being formed must depend initially on the spatial distribution of the ionizations produced by the radiation. The dosimetry task attempts to test alternative models that can be used to organize the available data on these physical, chemical, and biological processes into a self-consistent system. These models begin with descriptions of the physical aspects of the problem in terms of the energy deposited by individual charged particle tracks in small volumes such as cell components or macromolecules. The results of these calculations are compared with experimental measurements such as those of the radial distribution of energy deposition around charged particle tracks. They are also utilized in the Modeling Cellular Response program to develop mechanistic models for the production of specific biochemical changes and to estimate the frequency of relevant damage as a function of the charge and velocity of the incident particle. The characteristics of plausible mechanistic models are utilized in phenomenological models of the response of cellular systems, and the resulting models are compared to experimental data from the literature and from the Radiation Biophysics program in order to determine which mechanisms are consistent with the response of typical biological systems.

Models of the response of cells have evolved to where we now have a sufficient understanding of the kinetics of repair, to allow us to relate these kinetics to specific types of damage and to specific repair mechanisms. New models that relate initial damage to mutation frequency and possibly to malignant transformation are being considered. The models for energy deposition along charged particle tracks have been developed to the point that the events due to delta rays as well as primary ions can be evaluated, and it may be possible to use the results predicted by these models to estimate the frequency of specific combinations of radiation-induced changes in DNA. The experimental techniques used in testing the track structure models are also being utilized in practical dosimetry situations in order to improve the quality of the data available for future studies of dose effect relationships.

Applications of Microdosimetry

L. A. Braby

The Radiological Physics task has included basic research on the measurement of energy deposition in small volumes, typically about 1 μm in diameter, since the technique was first suggested by Rossi as a possible way to measure the linear energy transfer (LET) spectrum of unknown radiation fields (Rossi and Rosenzweig 1955). The applicability of this approach for evaluating the dose and the quality of radiations has been well established. Not only can the quality factor be determined by unfolding the LET distribution from the measured lineal energy distribution for most radiations, but other quantities such as the hit size effectiveness factor developed by Bond and Varma (1982) have been shown to relate the biological effectiveness of radiations to energy deposition in small sites. Laboratory-style microdosimetry instrumentation has been used to characterize radiation fields in a variety of special situations (Menzel et al. 1975; Brackenbush et al. 1979). However, little practical use of this technique has been made in routine health physics applications. This seems surprising since instruments based on microdosimetry measure dose with relatively uniform response over a wide range of particles and energies, and the instruments can be made significantly smaller and lighter than neutron area monitors currently in use. The Commission of the European Communities (CEC) has funded development of several prototype instruments and a comparison of the results for specific radiation fields (Alberts et al. 1989). This comparison clearly shows the

superiority of the response of these instruments relative to thermal neutron detectors embedded in a moderator.

Although it is not possible to point to a single factor that has prevented widespread application of microdosimetry, several technical problems as well as the general reluctance of operational health physicists to convert to an "unproven technology" may be involved. The signals produced by low-LET radiations are small, and microdosimetric measurements can be improved by reducing the noise level of the electronics used to process the signal. Although portable electronics that would serve the purpose have been available for several years, there has been a rapid evolution in the available components so that by the time one system is assembled, it becomes evident that newly introduced components would make a significantly better device possible. Thus it has been impossible to settle on a single design and work with it long enough for it to acquire the attributes of a "proven technology." Furthermore, the sensitivity of the instrumentation to small signals has also led to a problem with noise signals introduced by vibration and rough handling. This microphonic response has probably led to the impression that the instruments are still too delicate for routine field use.

While maintaining research on the basic properties of the interaction of radiation with small tissue volumes,[(a)] we have also watched for opportunities to demonstrate the practical application of microdosimetry. National Aeronautics and Space Administration (NASA) has funded development of a miniaturized data acquisition system for microdosimetry that utilizes two analog-to-digital converters to record the total energy deposited by events with lineal energy less than 10 keV/μm, the number of such events, and the number of events occurring in each of 14 logarithmically spaced bins between 10 and 200 keV/μm. The resulting 16-channel spectrum is recorded periodically, typically each minute, so that the dose rate and radiation quality can be evaluated as a function of time or location. Most of the problems of reliability and microphonics have been solved for these instruments.

Recently there has been increasing concern among commercial airline crew members and frequent flyers about the cosmic ray dose rate on aircraft flying at high altitudes. Calculations of the expected dose on specific flights, based on models of the cosmic ray fluence as a function of the solar cycle time and the geomagnetic latitude, have shown that in some cases crew members could exceed the maximum permissible dose for nonradiation workers (FAA 1990). Approximately half of the dose equivalent on aircraft is due to neutrons and the other half is due to low-LET radiation. Although this mixed radiation field can be evaluated with a variety of different combinations of detectors, the tissue equivalent proportional counter (TEPC) system is a single detector that can measure the dose due to all components of the field and can evaluate the dose equivalent without requiring calibration for the specific neutron spectrum.

A special instrument based on the circuitry developed for the NASA project has been constructed and operated on several commercial airline flights out of Salt Lake City. The data accumulated on one of these flights is plotted in Figure 1. The results clearly show the change in dose rate with altitude. A very small detector (a cylinder 0.5 in. in diameter and 3 in. long) was used, so only a few neutron events were detected each minute, resulting in the relatively large variation in dose from minute to minute. Data could be averaged over longer intervals, or a larger detector could be used to

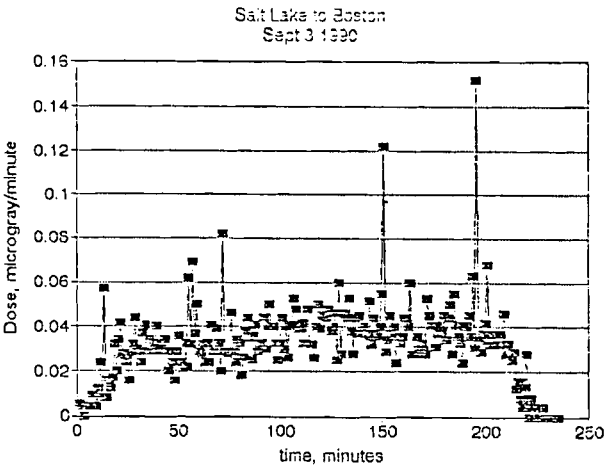

Figure 1. Dose Rate Measured at 1-min Intervals on a Typical Airline Flight

(a) Braby, L. A. In Press. "Microdosimetric Measurements of Heavy Ion Tracks." *Advances in Space Research.*

increase the counting rate. In this type of system, the count rate detected increases with the cross sectional area of the detector, but the response as a function of neutron energy is not affected. Another advantage of this approach to dosimetry is that the dose equivalent can easily be reevaluated if the definition of the quality factor is changed. For this flight the total dose was 7.7 μGy. Using the definition of quality factor given in ICRP 26 (ICRP 1977), the dose equivalent was 17 μSv, but using the definition used in the FAA circular (increasing the quality factor for neutrons by a factor of two), the dose equivalent was 27 μSv.

This approach to dosimetry and the results of these measurements were discussed at the FAA workshop held in September 1990 on cosmic-ray radiation in aircraft. We expect that this type of demonstration will increase the acceptance of microdosimetric techniques, and that they will eventually become a standard part of health physics practice. When this is accomplished, the data of occupational exposure will improve significantly, and future evaluation of the effects of occupational exposure will be made more reliable.

References

Alberts, W. G., G. Dietze, S. Guldbakke, H. Kluge, and H. Schumacher. 1989. "International Intercomparison of TEPC Systems Used for Radiation." *Radiat. Prot. Dosim.* 29:47-53.

Bond, V. P., and M. N. Varma. 1982. "Low Level Radiation Response Explained in Terms of Fluence and Cell Critical Volume Dose." In *Radiation Protection*, eds. J. Booz and H. G. Bert, pp. 423-437. Harwood Academic, London.

Brackenbush, L. W., G.W.R. Endres, and L. G. Faust. 1979. "Measuring Neutron Dose and Quality Factors with Tissue Equivalent Proportional Counters." In *Advances in Radiation Protection Monitoring*, ST1/PUB/494; ISBN 92-0-020279-9, pp. 231-239. International Atomic Energy Agency, Vienna, Austria.

Friedberg, W., D. N. Faulkner, L. Snyder, E. B. Darden, and K. O'Brien. 1989. "Galactic Cosmic Radiation Exposure and Associated Health Risks for Air Carrier Crewmembers." *Aviation Space and Environmental Medicine* 60:1104-1108.

ICRP. 1977. *Recommendations of the International Commission on Radiation Protection*. Pergamon Press, Oxford.

Menzel, H. G., A. J. Waker, and G. Hartman. 1975. "Radiation Quality Studies of a Fast Neutron Therapy Beam." In *Proceedings of the Fifth Symposium on Microdosimetry*, pp. 591-608, EUR 5452 d-e-f. Commission of the European Communities, Luxembourg.

Rossi, H. H., and W. Rosenzweig. 1955. "Measurements of Neutron Dose as a Function of Linear Energy Transfer." *Radiat. Res.* 2:417-427.

Modeling Survival and Mutation

L. A. Braby

Extensive tests comparing existing mathematical models to the response of plateau-phase Chinese hamster ovary (CHO) cells (Nelson et al. 1989; Nelson et al. 1988; Nelson et al. 1990) have been carried out. These tests show that the response of CHO cells is consistent with the assumption that the shoulder of the survival curve is due to the interaction of damage produced by separate charged particle tracks and that the majority of the interaction involves fixation of repairable damage. In this respect the experimental data are consistent with the lethal-potentially lethal (LPL) model (Curtis 1986), but the biology seems to be considerably more complex than that model envisions. In order to be testable with relatively simple experiments, the LPL model, like most others, assumes a single type of damage. However, the experimental data clearly show that the plateau-phase cells repair two independent types of damage. When a second type of damage, with its independent repair and fixation rates, is added, the model can no longer be tested by comparison with data on survival as a function of a single experimental variable such as dose rate, and testing the additional parameters in the model requires data on response as a function of additional variables. On the other hand, such a model can be expected to be consistent with a wider range of experimental observations.

The response of CHO cells relevant to the mechanisms of damage and repair appears to be consistent with the response of other cell types. Observations of such responses include:

- Two repair processes that can be separated as separate exponential repair rates.
- Only a portion of the radiation damage is oxygen dependent.
- Repair rates evaluated from dose rate and split dose measurements are equal.
- Cell cycle age affects probability of mutation and lethality, but maximum mutation frequency is in G_1 and maximum lethality is in S.
- Lethality is a linear/quadratic function of dose, but mutation frequency is a linear function.

A new model is being developed that is qualitatively consistent with the above observations and that is applicable to both lethality and specific locus mutation. It is hoped that, when complete, this model will provide predictions of gene deletions and modifications that can be used as input to a two-step model of malignant transformation. The underlying assumption of this model is that radiation produces DNA damage, which leads to deletion of segments of the genome. If a deletion includes a portion of an essential gene, it will cause reproductive death of the cell; otherwise it will produce a mutation. Many of these mutations will be detectable because they convey detrimental (malignancy, dysfunction, etc.) characteristics to future cell progeny.

If we assume that lethality comes only from the deletion of essential genes, there must be two components to the model. The first component gives the frequency of DNA deletions of different lengths as a function of dose, radiation quality, and repair time for cells at a specific point in the cell cycle. The second component deals with the change in the distribution of deletion sizes, and therefore the probability of affecting an essential gene, as a function of time in the cell cycle. The first component can be developed and tested using data on synchronous or stationary phase cells and can be treated as a refinement of existing models for cell survival. The second component requires data on mutation frequency and deletion spectra as a function of cell cycle age (data that are not yet available) and thus must be more speculative in nature.

The assumptions used in modeling the response of cells at a fixed point in the cell cycle are the following:

- There are two biochemically distinct types of damage, both potentially lethal in nature, and both subject to radiation-induced fixation as described by the LPL model (Curtis 1986).
- Both types of damage are repairable but by different enzyme systems and with different rates.
- Trypsinization or refeeding plateau-phase cells initiates growth and fixation of damage, but repair continues for a period, T_m, that depends on the cell type but may be as long as several hours.
- One type of damage is the result of the reaction of oxygen with radiation-induced DNA free radicals and is repaired rapidly relative to T_m.
- The second type of damage is oxygen independent but requires a "locally multiply damaged site" (Ward 1985) and is repaired relatively slowly.
- Unrepaired damage and damage that is fixed by interaction leads to large deletions that are generally lethal.
- Repair (split dose, delayed plating, or dose rate) has a significant error rate that results in a spectrum of deletion lengths, some of which are mutagenic.

Several consequences of this model can be determined directly. Two independent repair processes operating on independent types of damage will result in the two components of split-dose repair observed in the plateau-phase CHO cells (Nelson et al. 1990). In plateau-phase CHO cells, the rapid process has a characteristic time (mean time to repair a lesion) of about 1 h, and the slower process

has a characteristic time of about 18 h. Each type of damage and its associated repair is assumed to be described by the LPL model, so each can be detected in either a split-dose experiment or a delayed-plating experiment. However, the rapidly repaired damage is nearly completely repaired during T_m (Figure 1) and cannot normally be detected in a delayed-plating experiment unless a repair inhibitor is used. This is also consistent with the observations for CHO cells. Since we have assumed that the rapidly repaired damage is oxygen dependent and the slowly repaired damage is not, we expect that cells irradiated in the absence of oxygen would show less damage at a specified dose (the OER) and that this damage would be removed only by the slow repair process. This is consistent with the experimental observations (Nelson et al. 1986) considering that the slow repair would have been very difficult to detect in the short split-dose intervals that could be used in those experiments.

This model assumes that lethality results only from the deletion of an essential gene. This generally results from a large deletion caused by progression of the cell through the cycle with continued DNA replication, in the presence of unrepaired damage or damage fixed by interaction with additional damage. These large deletions lead to the production of visible micronuclei, as observed experimentally by Joshi et al. (1982). Enzymatic processes repair potentially lethal damage but result in a spectrum of smaller deletions as well as accurately repaired sites. The initial damage is proportional to the dose, and under conditions of constant repair, the resulting mutation frequency will be linear. However, the mutation frequency is predicted to increase with increasing repair opportunity (split dose, delayed plating, or reduced dose rate). This effect may be small because most rapidly repaired damage will be repaired independent of the experimental conditions due to the inherent repair time, T_m. The experimental evidence is not clear; mutation frequency is often independent of repair time, but occasionally decreases with additional repair (Evans et al. 1990).

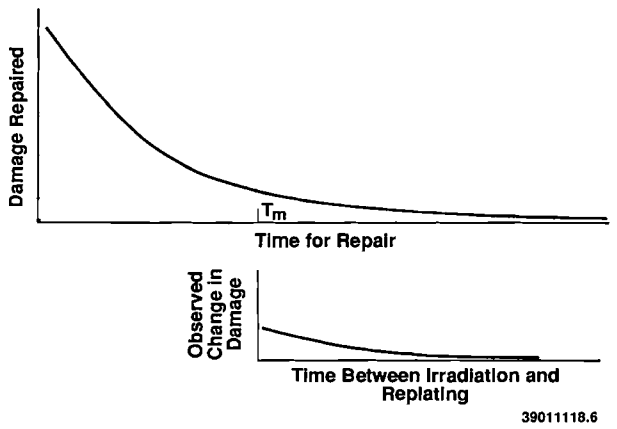

Figure 1. Cells Repair Damage for a Time, T_m, After Replating in a Delayed-Plating Experiment so the Amount of Damage Repaired is Greater Than Indicated by the Observed Change in Survival

Increasing LET results in increased probability that damage will be produced and fixed by separate reactions along a single track. Since the resulting very large deletions do not contribute significantly to the production of measurable mutations, the RBE for lethality appears independent of the RBE for mutation frequency. The frequency of multiply locally damaged sites (oxygen-independent damage) also increases with increasing LET. If repair of this type of damage results in more deletions or larger deletions than repair of oxygen-dependent damage, the model predicts that the mutation frequency and the frequency of "large" deletions detected in mutant cells will also increase with increasing LET. This is observed in some experiments (Evans et al. 1990), but not for all mutations.

As mentioned previously, there is relatively little data on which to base a model for the variation in deletion size as a function of cell age, i.e., position in the cell cycle. However, the fact that the mutation frequency is highest in G_1 and lethality is highest in S suggests that the deletions resulting from repair of a specific type of damage are relatively small in G_1 and become larger in S phase.

References

Curtis, S. B. 1986. "Lethal and Potentially Lethal Lesions Induced by Radiation--A Unified Repair Model." *Radiat. Res.* 106:252-270.

Evans, H. H., M. Nielsen, J. Mencl, M-F. Horng, and M. Ricanati. 1990. "The Effect of Dose Rate on X-Radiation-Induced Mutation Frequency and the Nature of DNA Lesions in Mouse Lymphoma L51784 Cells." *Radiat. Res.* 122:316-325.

Joshi, G. P., W. J. Nelson, S. H. Revell, and C. A. Shaw. 1982. "X-Ray-Induced Chromosome Damage in Live Mammalian Cells and Improved Measurements of Its Effects on Their Colony-Forming Ability." *Int. J. Radiat. Biol.* 41:161-181.

Nelson, J. M., L. A. Braby, and N. F. Metting. 1989. "Relative Split-Dose and Delayed-Plating Effects Following Low Doses of X-Radiation." *Physical Sciences, Part 4 of Pacific Northwest Laboratory Annual Report for 1988 to the DOE Office of Energy Research*, PNL-6800 Pt. 4, p. 44. Pacific Northwest Laboratory, Richland, Washington.

Nelson, J. M., L. A. Braby, N. F. Metting, and W. C. Roesch. 1988. "Interpreting Survival Observations Using Phenomenological Models." In *Quantitative Mathematical Models in Radiation Biology*. Springer-Verlag, pp. 125-134.

Nelson, J. M., L. A. Braby, N. F. Metting, and W. C. Roesch. 1990. "Multiple Components of Split-Dose Repair in Plateau-Phase Mammalian Cells: A New Challenge for Phenomenological Modelers." *Radiat. Res.* 121:154-160.

Nelson, J. M., L. A. Braby, W. C. Roesch, and N. F. Metting. 1986. "Effect of Oxygen on Damage Production and Repair." In *Physical Sciences, Part 4 of Pacific Northwest Laboratory Annual Report for 1985 to the DOE Office of Energy Research*, PNL-5500 Pt. 4, pp. 36-37. Pacific Northwest Laboratory, Richland, Washington.

Ward, J. F. 1985. "Biochemistry of DNA Lesions." *Radiat. Res.* 104:S103-S111.

Modeling the Stochastic Track Structure of High-LET Radiations

W. E. Wilson

In our effort to develop an analytic model for the stochastics of the penumbra around an ion track, extensive simulation and analysis of touchers (ions that pass outside an absorber region of interest but deposit energy inside via delta rays) were carried out. Frequency distributions for ionization and energy deposition for 0.3- to 20-MeV protons and for simulated spherical sites of 2 to 100 nm in diameter were obtained.

Our analysis indicates that the description of the stochastics of the penumbra naturally divides into two related concepts: the probability that a distant site will experience an energy deposition of any magnitude, and the frequency distribution in ionization or energy deposition, conditional on the site being hit.

Frequency Distributions

Our computations indicate that the normalized frequency distributions in ionization are relatively simple, approximately exponential in shape, and do not vary significantly with radial distance away from the ions' path. These features are illustrated by the data in Figures 1 and 2 for a 5-MeV proton indirectly depositing energy in a 50-nm site. Figure 1 shows, in histogram form, the dependence on radial distance of the probability density that a site will experience a number of ionizations, k, given that it is hit at least once. The set of histograms extending out to 10-site radii show little variation in shape; furthermore, since the logarithm of the frequency is plotted, the linearity of the histograms as a function of ionization number, k, indicates that the distributions are essentially exponential in shape. Figure 2 further illustrates the exponential nature of the distributions by projecting all onto one plane.

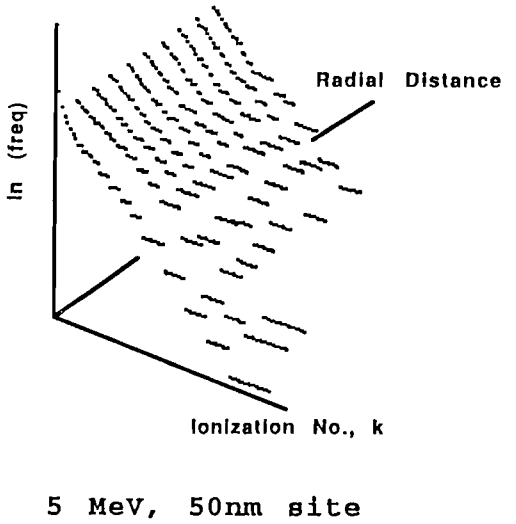

Figure 1. Frequency-Density Distributions in Ionization Number, k, as a Function of Radial Distance. The semilog histograms indicate that the distributions are approximately exponential in shape and do not vary significantly with radial distance.

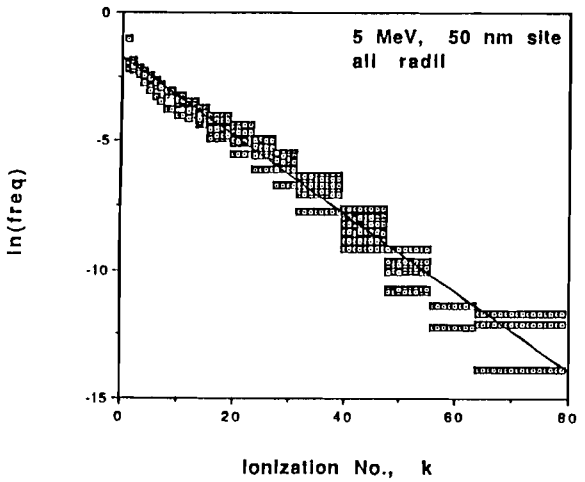

Figure 2. Frequency-Density Distributions in Ionization Number, k, for 5-MeV Protons Passing a 50-nm Site. The data of Figure 1 are projected onto the ln(freq)-k plane. The solid line is a least-squares fit to the data.

The solid line is a least-squares fit to the natural logarithm of the data. Quantitatively, the results indicate that an energy deposition event that produces approximately 70 ionizations in a 50-nm site is about one million times less frequent than an event that produces one or two ionizations.

Figure 3 illustrates the degree to which the shape of the distributions is constant for other ion energies. Invariance in shape implies invariant moments. The ratio of the second moment to the first, the so-called

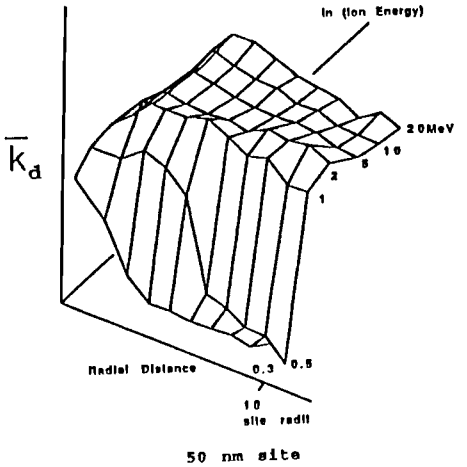

Figure 3. Dose-Mean Ionization Number as a Function of Radial Distance and Ion Energy. The dose-mean is the ratio of the second moment to the first of the ionization distributions. This example is for a 50-nm site and ion energies of 0.3 to 20 MeV. Results are shown out to ten times the site radius.

dose-mean, of the ionization distributions for the 50-nm site and for ion energies 0.3 to 20 MeV is plotted as a function of radial distance. Above an energy of about 1 MeV and at distances beyond a few site radii, a plateau prevails in which the dose-mean ionization is relatively constant. Our interpretation is that in this plateau region of ion energy and radial distance, the delta rays are primarily crossers; at lower energies or closer distances, low-energy delta-ray stoppers make a significant contribution that reduces the mean.

Only one site size is presented in Figure 3 for the several ion energies. The variation in the dose-mean ionization number as a function of site size is shown in Figures 4 and 5 for an ion energy of 5 MeV. To cover wide ranges of parameters, log scales are used. The line in Figure 4 (5 MeV) for 50-nm sites is the same data as the 5-MeV line in Figure 3 (50 nm). The data of Figure 4 further support the observation that the shape, i.e., the moments of the ionization distributions, do not vary significantly with radial distance from the path of the ion. There is a strong dependence on site size, as one would expect. Fortunately, that dependence is very simple, as can be seen in Figure 5 where all the data points making up Figure 4 are projected onto the mean-ionization versus

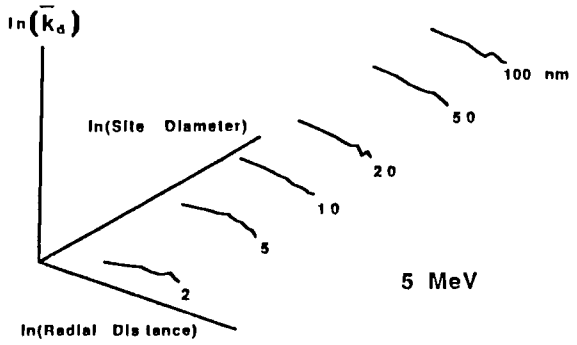

Figure 4. The Dose-Mean Ionization Number as a Function of Site Size and Radial Distance for 5-MeV Protons. The data indicate that the shape of the ionization distributions, i.e., the moments, do not vary significantly with radial distance from the path of the ion, but there is a strong dependence on site size.

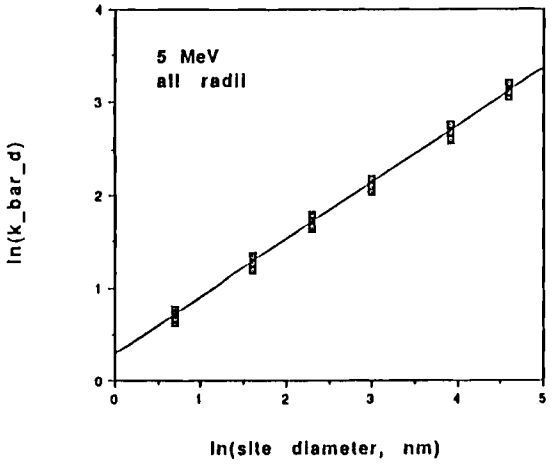

Figure 5. The Dose-Mean Ionization Number as a Function of Site Size. The data of Figure 4 are projected onto the ionization number-site size plane. The solid line is a least-squares fit of a linear function to the log-log data; the results indicate that the mean dose is well represented by a power-law dependence on site diameter.

site-diameter plane. The solid line is a least-squares fit of a linear function to the log-log data; the empirical evidence strongly indicates that the mean dose is well represented by a power-law dependence on site diameter.

Hit Probability

We define the hit probability, P_b, as the cumulative probability that a site will experience any number of ionizations (greater than zero). That is,

$$P_b = \sum_{k=1}^{\infty} f_k \qquad (1)$$

where f_k is the probability that the site will experience k ionizations. The simulations indicate that we can represent P_b by the product of three terms; the first, R_b, is a geometric term, proportional to the square of the site diameter and to the inverse square of the radial distance, i.e., to the solid angle of the site viewed from the ion path.

$$R_b \approx \frac{d^2}{X_b^2} \approx \Omega \qquad (2)$$

The second term is a source-strength term but also includes a provision for absorption of the delta rays. This term is approximated by a partial integral over the single differential cross section (SDCS), for electron ejection,

$$S_\Delta \approx \int_\Delta^\infty \sigma(w,E)dw \qquad (3)$$

where $\sigma(w,E)$ is the SDCS for ejection of a secondary electron of energy, w, and Δ is a cut-off energy parameter that allows for source electrons with insufficient energy to reach the site, i.e., short-range delta-rays.

The third term is the subject of current inquiry. After the first two terms are factored out, what remains exhibits an approximately exponential increase with radial distance and is suggestive of a "build-up" factor, well known in beta-ray dosimetry.

We expect to be able to complete an analytical expression for hit probability and combine it with one to be developed for the frequency distributions. This will make it possible to easily determine the complete energy deposition distribution for any combination of ion, energy, and target site size.

Radiation Biophysics

The Radiation Biophysics project conducts specific radiobiological studies to test various aspects of the mathematical models developed in the Radiation Dosimetry and Modeling Cellular Response programs. These studies are designed to determine whether specific mathematical expressions, intended to characterize the expected effects of biochemical mechanisms on cellular response, are consistent with the behavior of selected biological systems. Cultured mammalian cells are used for many of these experiments. Since stringent requirements are usually placed on the cellular system, special techniques and culture conditions are used to minimize biological variability. Cells that have ceased progression through the cell cycle are used to study the effects of dose protraction during long-interval split-dose or dose-rate studies. These carefully characterized cell populations are providing data on the extent of repair following low doses of radiation and on changes in the types of damage that can be repaired as the cells progress toward mitosis.

Other experiments attempt to identify the mechanisms of physical and chemical damage to deoxyribonucleic acid (DNA) and determine the spatial distribution of DNA single-strand breaks. Particular attention is given to investigating the influence of higher order structure, such as supercoiling of plasmid DNA and scaffold attachment, on the probability of strand scission. It appears that these structures and the resulting molecular strain lead to local areas of increased susceptibility to chemical and physical attack.

Another significant consequence of radiation damage to DNA is the mutation of mammalian cells. While it is well established that most radiation-induced mutations result from the deletion of a portion of the genome, there are not enough data available to characterize the processes leading from the initial DNA damage to these deletions. The initial damage probably involves only a few base pairs, at most, but this ultimately results in deletions of a few hundreds or even thousands of base pairs. Experiments exploring the characteristics of deleted regions are in progress to evaluate the role of higher order chromatin structure and the repair of base damage on the production of large deletions.

Testing Biophysical Models at Very Low Doses

J. M. Nelson and L. A. Braby

Our previous studies (Nelson et al. 1990) of plateau-phase Chinese hamster ovary (CHO) cells exposed to x-rays in split-dose and delayed-plating protocols have shown that the response of these cells is consistent with cell-response models that assume that interaction of sublethal damage or potentially lethal damage is responsible for the curvature of the dose-response relationship, but not with models that assume that repair saturation is responsible for this curvature. This, combined with previous findings that the probability of damage interaction increases with the concentration of damage in the cell and that the rates of damage removal determined from split-dose experiments and dose-rate experiments are equal (Metting et al. 1985), has greatly reduced the number and variety of possible mechanisms that must be considered when devising a model of cell response. However, one fundamental question remained to be answered. Of those radiochemical changes that can ultimately lead to cell inactivation, will they inevitably result in cell death if they remain unrepaired (potentially lethal damage), or must they interact with additional damage in order to become lethal (sublethal damage)?

These two alternative responses of cells to unrepaired damage remaining in the cell are the basis for the difference in damage accumulation models such as dual radiation action (Kellerer and Rossi 1978) and the lethal-potentially lethal (LPL) model (Curtis 1986). In order to distinguish between the mechanisms that form the basis of these two types of models, we have designed an experiment for which the models predict different and mutually exclusive results. At very low doses, lesion interaction is highly improbable. If the lesions are sublethal, as assumed by the accumulation models, repair will have little effect on measured survival

because unrepaired damage would not be detected unless it had interacted and produced a lethal lesion. However, unrepaired potentially lethal damage is assumed to be lethal in the LPL model, and repair would become more effective with decreasing dose because the opportunity for binary misrepair or damage fixation would be decreased.

Since the chemical identity of the lethal damage is unknown, we cannot measure its repair directly. However, we can deduce the amount of repair by measuring the survival when maximum repair has been allowed to occur and relating this to survival at the same dose when repair has been blocked. We found that repair can be effectively prevented by subculturing the irradiated cells in the presence of the repair inhibitor β-ara-A, a nucleic acid analogue that interferes with polymerase activity.

We measured survival of irradiated cells subcultured in the presence and absence of β-ara-A, given immediately after exposure, and compared these measurements with the survival of cells given sufficient time for maximum repair. Using x-ray doses of 0.5 to 2.5 Gy, we found that when repair was not allowed to occur, the survival curve became considerably steeper, and appeared to be a simple exponential. As shown in Figure 1, the initial slope of the line fitted to these data is significantly greater than that obtained for cells plated immediately after irradiation, when no postirradiation delay time was provided. These data are consistent with the assumptions that most of the damage is potentially lethal and that most of the damage is removed even when no postirradiation delay interval is given to allow for repair.

The data have been replotted to illustrate the effect of repair on survival as a function of dose in Figure 2. The difference between the maximum survival (resulting from a 24-h plating delay) and the minimum survival (when repair is blocked by β-ara-A) divided by one minus the minimum survival is plotted for each dose. Although some scatter in the data is unavoidable in experiments that involve low doses and relatively small effects, the trend in these results clearly indicates an increase in the effectiveness of repair with decreasing dose.

These results seem incompatible with models that assume that sublethal damage interaction is a major contributor to radiation cell killing. This

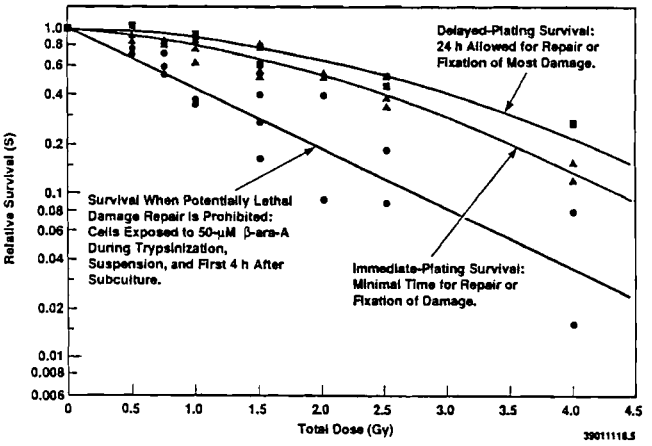

Figure 1. The Shape of the Survival Curve Changes When Cells Are Irradiated Under Conditions Designed to Maximize or Minimize the Effects of Repair. Trypsinization and subculture in the presence of the repair inhibitor β-ara-A reveals the large amount of damage that is repaired when cells are plated immediately after irradiation in drug-free medium.

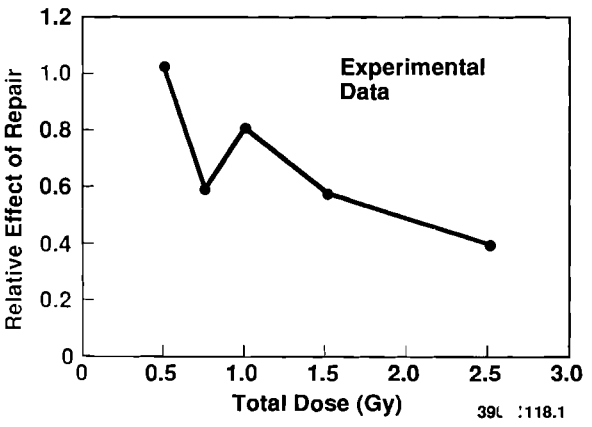

Figure 2. In the Shoulder Region of the Survival Curve, the Relative Effect of Repair Decreases with Increasing Dose. Survival observed in a delayed-plating experiment, when normalized to the survival when repair is inhibited by β-ara-A, shows that repair of radiation damage becomes relatively more effective as the total dose decreases. This finding is consistent with the lethal-potentially lethal models, but not with accumulation models.

This interpretation does not rule out sublethal damage interaction, but simply implies that such interaction does not play a significant role in survival at low doses. The results are consistent with the mechanisms upon which the LPL model is based, specifically, some sort of interaction of potentially lethal rather than

sublethal damage occurs, which blocks the repair of that damage. Since this interaction occurs at relatively low doses of low linear energy transfer (LET) radiation, the interaction must occur over distances on the order of micrometers.

References

Curtis, S. B. 1986. "Lethal and Potentially Lethal Lesions Induced by Radiation--A Unified Repair Model." *Radiat. Res.* 106:252-270.

Kellerer, A. M., and H. H. Rossi. 1978. "A Generalized Formulation of Dual Radiation Action." *Radiat. Res.* 75:471-488.

Metting, N. F., L. A. Braby, W. C. Roesch, and J. M. Nelson. 1985. "Dose-Rate Evidence for Two Kinds of Radiation Damage in Stationary Phase Mammalian Cells." *Radiat. Res.* 103:204-218.

Nelson, J. M., L. A. Braby, N. F. Metting, and W. C. Roesch. 1990. "Multiple Components of Split-Dose Repair in Plateau-Phase Mammalian Cells: A New Challenge for Phenomenological Modelers." *Radiat. Res.* 121:154-160.

Effect of Excess Iron on Survival of Irradiated Plateau-Phase CHO Cells

J. M. Nelson and R. G. Stevens

Radiation-induced damage and oxidative damage induced by normal metabolic processes in cells have much in common. The background level of metabolically induced oxygen radicals and the products of the interactions of these radicals with chromatin may influence the sensitivity of cells to ionizing radiation damage. This could come about either through chance combinations resulting in a form of multiply, locally damaged sites, by overloading repair systems, or by inducing the production of elevated levels of repair materials. Furthermore, differences in the levels of metabolically produced oxygen radicals may contribute to differences in radiation sensitivity of cells in different tissues and may also contribute to differences observed in the responses of experimental cell cultures in different laboratories and at different times. One way of modifying the level of metabolic oxygen radicals may be to alter the intracellular concentration of iron ions. Iron ions, as well as those of other transition metals, catalyze the Fenton reaction; increased levels of iron also result in increased levels of oxygen radicals (Stevens and Kalkwarf 1990).

The iron content in normal tissue shows considerable variation. Normal liver contains 28 to 162 μg/g, kidney contains 3.3 to 10.1 μg/g, spleen contains 85 to 169 μg/g. The highest levels are found in lung and brain tissue, with iron concentrations of around 200 μg/g and 222 to 510 μg/g, respectively. In experimental cell cultures the iron concentration in the culture medium is not normally monitored and may vary significantly due to differences in the iron content of the serum used to supplement the medium and the amount of that serum used.

It has been shown that the concentration of ferritin in the tissue culture medium affects the actual concentration of iron ions in cells, and that elevated iron increases the frequency of radiation-induced chromosome aberrations (Whiting et al. 1981). We have designed experiments to investigate the influence of variations in available iron on the mechanisms of radiation-induced cell killing. We are comparing the survival of irradiated and unirradiated stationary-phase Chinese hamster ovary (CHO) cells (Nelson et al. 1984), after these cells have been given varying amounts of iron in the form of the iron storage protein ferritin, in addition to the small amount of iron available in the culture medium. The background iron concentration is not known precisely, but is expected to be less than 0.2 μg/mL, with most of it coming from the serum supplement. However, it does not vary throughout the experiment since a single batch of culture medium supplemented with fetal calf serum is used. Both the concentration of iron in the medium and the time the cells are kept in the iron-supplemented medium affect the response of the cells. We prepared the plateau-phase cultures as we have for previous studies (Nelson et al. 1990) and added the ferritin in a minimum volume of phosphate buffered saline (PBS) on the twelfth day of culture, 24 h before irradiation.

The results of the first few experiments are summarized in Table 1. Increased levels of ferritin, up to 16 μg/mL, have negligible effect on

Table 1. Survival of Irradiated and Unirradiated Cells Treated with Varying Doses of Ferritin

Ferritin Dose[(a)] (μg/mL)	Radiation Dose (Gy)	Survival[(b)]	Survival Ratio[(c)]
0.5	0	1.0 ± 8.2%	
	4	0.606 ± 12.5%	0.606
0.5	0	0.983 ± 15.1%	
	4	0.441 ± 18.9%	0.449
2.0	0	1.049 ± 14.2%	
	4	0.498 ± 10.3%	0.475
8.0	0	1.130 ± 23.0%	
	4	0.499 ± 12.1%	0.442
16.0	0	0.954 ±21.9%	
	4	0.592 ± 8.7%	0.621
32.0	0	1.057 ± 12.3%	
	4	0.244 ± 14.0%	0.231
64.0	0	0.609 ± 28.9%	
4	0.085 ± 43.7%	0.140	

(a) Iron delivered to stationary-phase cells via the culture medium, as the ferric form bound to the iron-binding protein ferritin; cultures were exposed to ferritin-containing medium for 24 h prior to harvest and subculture.
(b) Survival of treated cells divided by survival of controls.
(c) Survival of irradiated cells divided by survival of unirradiated cells.

the survival of unirradiated cells. However, there appears to be a ferritin-concentration- dependent decrease in the survival of cells exposed to 4 Gy of x-rays at greater ferritin doses.

Now that the effective range of ferritin concentrations has been determined, we will study the effect of ferritin on survival as a function of dose in single exposure experiments and on the repairability of the damage in split-dose experiments. We expect that if iron-induced damage combines differently with the radiation-induced damage, which leads to increased mutation and survival probabilities, this would suggest that the spectrum of deletions has been changed.

References

Nelson, J. M., P. W. Todd, and N. F. Metting. 1984. "Kinetic Differences Between Fed and Starved Chinese Hamster Ovary Cells." *Cell Tissue Kinet.* 17:411-425.

Nelson, J. M., L. A. Braby, N. F. Metting, and W. C. Roesch. 1990. "Multiple Components of Split-Dose Repair in Plateau-Phase Mammalian Cells: A New Challenge for Phenomenological Modelers." *Radiat. Res.* 121:154-160.

Stevens, R. G., and D. Kalkwarf. 1990. "Iron, Radiation, and Cancer." *Environ. Health Perspec.* 87:291-300.

Whiting, R. F., L. Wei, and F. Stitch. 1981. "Chromosome-Damaging Activity of Ferritin and Its Relation to Chelation and Reduction of Iron." *Cancer Res.* 41:1628-1636.

Influence of Base Composition on Single-Strand Break Induction

J. M. Nelson, M. Ye, and J. H. Miller

Current models of the effects of ionizing radiation on cells suggest a relationship must exist between the structure of DNA and the production of the initial damage that leads to DNA deletions, mutation, and reproductive death. However, the conventional models of cell response and tests of these models using reproductive survival or mutation as the endpoint cannot distinguish between the differences in the probability of producing damage at different points in the genome. It has long been recognized that damage is more likely to occur in regions of the DNA that are under abnormal chemical or physical stress. This has led to the search for "hot spots" where strand breaks are more likely to occur than in the adjacent DNA. Although some "hot spots" have been identified, it has not generally been possible to control the stress on the DNA so that the cause of the increased sensitivity can be isolated.

As mentioned last year, the probability of random coil transitions is considerably higher in AT (adenine-thymine)-rich regions than in other regions of the DNA. In these regions duplex DNA becomes more easily denatured, and it is assumed that radiation-induced single-strand breakage, resulting from both direct and indirect action, is more probable in these denatured regions. The plasmid pIBI 30 is an appropriate system for testing this assumption since it has two regions with high AT content, and in its native form (linking difference -13), it is stressed by being underwound. Craig Benham (Mt. Sanai School of Medicine) has calculated the probability of unwinding as a function of position in the pIBI 30 plasmid, i.e., as a function of the AT:GC (guanine-cytosine) ratio, temperature, and ionic strength. These calculations indicate that under specific conditions of temperature and salt concentration, the probability of random coil transitions can be orders of magnitude higher at AT-rich sites than at other points in the DNA. In pIBI 30 the greatest probability of transition occurs around sequence 2000, with a second sensitive region (about 10% of this transition probability) around sequence 1000.

Using a restriction enzyme to produce a single break at a fixed position in the plasmid and gel electrophoresis to determine the length of the fragments produced by radiation-induced breaks, we have started a series of measurements to determine if the positions of radiation-induced strand breaks correspond to the positions where the probability of random coil transition is highest. We have already determined that at 0°C and under intermediate salt concentrations, TE (10 mM Tris, 1 mM EDTA; pH 7.2) buffer, single-strand breaks are not concentrated near these AT-rich regions. In fact, under these conditions the probability of single-strand break production was found to be considerably less than expected. However, the calculations suggest that irradiation at 40°C and under the same salt conditions should increase the probability of strand breaks considerably at the specified sites. If an increase in strand breakage is detected at the elevated temperature, we will measure the break frequency as a function of temperature to determine if it parallels the calculated probability of random coil transitions at sequence 2000 as a function of temperature.

Genetic Consequences of Radiation Damage to Mammalian Cells

T. L. Morgan, E. W. Fleck, J. Thacker, and J. H. Miller

Our work has focused on determining the nature of mutations induced in mammalian cells by exposure to ionizing radiation. While it is well established that these mutations are typically caused by deletion events, the type, location, and frequency of these events has not been studied in enough detail to be useful for modeling the effects of radiation. We report here the results of our molecular characterization of radiation-induced mutations in the HPRT genes of Chinese hamster cells.

In the first series of experiments, we determined the effects of dose, dose fractionation, and delayed plating on the spectrum of mutations induced in Chinese hamster ovary (CHO) cells. As reported by Morgan et al. (1990), the cellular processes associated with repair to sublethal and potentially lethal damage do not appear to affect the relative frequency of the various types of mutations we encountered: full gene deletions, partial deletions, and small changes. These results suggest that repair acts across all premutagenic lesions equally. However, mutants isolated from cells exposed by 2 Gy of 250-kVp x-rays showed fewer full deletions than those exposed to 4 Gy. This difference was small ($p = 0.06$) and suggests the need for future experiments using a wider dose range (viz., 1 and 5 Gy) to clarify the dose-effect relationship.

In collaboration with Dr. Belinda Rossiter (Institute for Molecular Genetics, Baylor College of Medicine, Houston, Texas), we used a restriction site map of the HPRT locus to localize deletion breakpoints in those mutants containing intragenic lesions (Rossiter 1987; Morgan et al. 1990). In 15 cell lines containing a partial deletion of the HPRT gene, 12 showed evidence of one or more deletion breakpoints in the central region of the gene. In collaboration with Dr. John Thacker (Radiobiology Unit, Medical Research Council, Chilton, Didcot,

Oxon, England), we conducted a similar analysis on mutant cell lines generated by Thacker (1986) using γ-ray or α-particle irradiation of Chinese hamster V79 cells. These cells showed a similar pattern--more deletion breakpoints were observed between exons 4 and 6 than in any other region of the gene (Thacker et al. 1990). Gennett and Thilly (1988) have observed the same distribution in spontaneously arising mutations in the HPRT gene of human B-lymphoblasts. We interpret these data to indicate that this region of the human and hamster HPRT genes contains one or more special DNA sequences or secondary structures that renders it more sensitive to mutagenic effects.

While the underlying mechanism responsible for this effect is unknown, it is tempting to speculate that this region may contain some unique sequence or secondary structure that renders it more sensitive to mutation induction. For example, the organization of chromatin may interfere in some way with the fidelity of DNA repair. Eukaryotic chromatin appears to be organized into looped domains of DNA constrained by sites of interaction with a structure called the nuclear matrix or scaffold (Paulson and Laemmli 1977). Such sites have been observed within active genes. Kas and Chasin (1987) identified a region near the center of the DHFR gene in CHO cells that has affinity for attachment to the nuclear protein scaffold. Two tightly linked sites were localized within this region. Each of these scaffold-associated regions (SARs) is A+T-rich and contains a cleavage consensus sequence for Drosophila topoisomerase II as well as direct and inverted repeated sequences. In the case of the HPRT locus, the region adjacent to exon 5 in RJK159 cells (a derivative of V79) has been sequenced to a limited extent (Rossiter et al. 1990). The region immediately 5' to exon 5 has a very high A+T content (>70%) and contains at least one sequence that shows an 89% (16/18) homology to the cleavage consensus sequence for topoisomerase II purified from both chicken and human cells (Spitzner and Muller 1988). The presence of SARs in the middle of an active zone of chromatin, such as the HPRT gene, might result in steric hindrance of repair enzymes and hence sensitivity to mutagenesis.

We have begun to construct a fine structure map of mutants containing breakpoints in this region of the hamster HPRT gene. Using the polymerase chain reaction (PCR) with primer pairs specific for exons 4, 5, and 6 we have amplified fragments containing each exon. Each primer pair was chosen to include the complete sequence of each exon as well as a limited stretch of adjacent intron sequences. To date, we have tested four mutants and have found no change in the size of any fragment. Since our Southern blot data clearly indicated the presence of a deletion (Morgan et al. 1990), we conclude that the lesions were confined to intron sequences only. Because intron sequences do not code for any portion of the HPRT protein (Rossiter 1987),[(a)] the position of these lesions supports our hypothesis that this region of the gene contains unique DNA sequences that are vital to gene function.

Further characterization of this region is vital to understanding the reason for loss of gene function in these cells. We are continuing our mapping of mutants containing lesions in introns 4 and 5 in an effort to localize the sensitive sequences more precisely. Since two independent radiation-induced mutations have been found adjacent to SARs (Kas and Chasin 1987), we are also exploring the possibility that there is a topoisomerase II binding site in this region of the CHO HPRT gene.

References

Gennett, I. N., and W. G. Thilly. 1988. "Mapping Large Spontaneous Deletion Endpoints in the Human HPRT Gene." *Mutat. Res.* 201:149-160.

Kas, E., and L. A. Chasin. 1987. "Anchorage of the Chinese Hamster Dihydrofolate Reductase Gene to the Nuclear Scaffold Occurs in an Intragenic Region." *J. Mol. Biol.* 198:677-692.

Morgan, T. L., E. W. Fleck, K. A. Poston, B. A. Denovan, C. N. Newman, B.J.F. Rossiter, and J. H. Miller. 1990. "Molecular Characterization of X-Ray-Induced Mutations at the HPRT Locus in Plateau-Phase Chinese Hamster Ovary Cells." *Mutat. Res.* 232:171-182

(a)Rossiter, B.J.F., J. C. Fuscoe, D. M. Muzny, M. Fox, and C. T. Caskey. 1991. "The Chinese Hamster HPRT Gene: Restriction Map, Sequence Analysis, and Multiplex PCR Deletion Screen." *Genomics* (in press).

Paulson, J. R., and U. K. Laemmli. 1977. "The Structure of Histone-Depleted Metaphase Chromosomes." *Cell* 12:817-828.

Rossiter, B.J.F. 1987. "Structure and Mutation of the Chinese Hamster HPRT Gene." Ph.D. Dissertation. University of Manchester, Manchester, England.

Spitzner, J. R., and M. T. Muller. 1988. "A Consensus Sequence for Cleavage by Vertebrate DNA Topoisomerase II." *Nucleic Acids Res.* 16:5533-5556.

Thacker, J. 1986. "The Nature of Mutants Induced by Ionizing Radiation in Cultured Hamster Cells. III. Molecular Characterization of HPRT-Deficient Mutants Induced by γ-Rays or α-Particles Showing that the Majority Have Deletions of All or Part of the HPRT Gene." *Mutat. Res.* 160:267-275.

Thacker, J., E. W. Fleck, B.J.F. Rossiter, and T. L. Morgan. 1990. "Localization of Deletion Breakpoints in Radiation-Induced Mutants of the HPRT Gene in Hamster Cells." *Mutat. Res.* 232:163-170.

Modeling Cellular Response to Genetic Damage

The objective of this research is to understand the biophysical mechanisms that underlie the responses of mammalian cells to energy-related pollutants, with particular emphasis on the role of damage to deoxyribonucleic acids (DNA) in cell killing and mutation induction by ionizing radiation. DNA in cells is associated with proteins and other molecules that contribute to the structural and dynamic properties needed for functional genetic material. The environment and properties of DNA also influence its interaction with radiation and chemicals. Hence, studies of DNA damage as a basis for understanding cellular responses to carcinogenic agents must allow for the role that the cellular environment of DNA plays in damage production and expression. We are using *in vitro* model systems to investigate these phenomena. A plasmid DNA system has been developed to mimic the torsional stress that chromatin structure places on active genes. With this system, we observed that negative supercoiling increases the sensitivity of DNA to radiation-induced strand scission.

DNA Structure and Radiation Sensitivity

J. H. Miller, J. M. Nelson, M. Ye, C. E. Swenberg,[a] C. J. Benham,[b] and E. W. Fleck[c]

Cellular DNA has a rich variety of structural and dynamic properties that are needed for its biological function. The existence of topologically distinct domains of negative supercoiling in the genome of both prokaryotic and eukaryotic organisms is a good example of this phenomenon. These domains are believed to be associated with gene expression since the torsional stress produced by negative supercoiling tends to produce the strand separation that is needed for transcription. In FY 1990 we presented the first observation that negative supercoiling increases the sensitivity of DNA to induction of strand breaks by ionizing radiation. These findings with plasmid DNA in an aqueous buffer are consistent with cellular studies by Chiu and Oleinick (1982) that show that active genes are more sensitive to radiation-induced strand scission than is the bulk of mammalian chromatin.

Double-stranded DNA in a covalently closed plasmid is characterized by a linking number defined as the number of times one strand of the duplex crosses the complementary strand. Plasmids that differ only in their linking number are called topoisomers. It is usually most convenient to specify the linking number of topoisomers relative to that of the fully relaxed topoisomer, which is operationally defined by the invariance of its linking number to the action of nicking and closing enzymes. The linking number of a topoisomer minus the linking number of the fully relaxed conformation is defined as the linking difference of the topoisomer. The ratio of this linking difference to the linking number of the relaxed state is called the specific linking difference or superhelical density. DNA isolated from cells has been found with superhelical densities between -0.03 and -0.09 (Cozzarelli 1980).

Supercoiled plasmids can accommodate the torsional stresses associated with a nonzero linking difference by assuming a variety of conformations that involve both twisting and writhing deformations. The former may involve smooth torsional deformation (i.e., a different helicity than that characterizing the unstressed B-form) and/or abrupt conformational changes that are sequence dependent. Cruciform extrusion at inverted repeats, local denaturation of regions rich in adenine-thymine (AT) base pairs, and B to Z transition are the most widely studied sequence-specific torsional deformations. At thermodynamic equilibrium, the competition among different secondary structures with the same linking number is influenced by base sequence, domain length, and solvent conditions, as well as the linking difference (Benham 1986). The goal of our studies with

(a) Radiation Biochemistry Department, Armed Forces Radiobiology Research Institute, Bethesda, Maryland.
(b) Department of Biomathematical Sciences, Mount Sinai School of Medicine, New York.
(c) Biology Department, Whitman College, Walla Walla, Washington.

supercoiled DNA is to understand the effects of this conformational equilibrium on radiation-induced DNA damage.

Figure 1 shows the combined results of several experiments to measure the sensitivity of topoisomers of the plasmid pIBI 30 to induction of single strand breaks (SSB) by x-rays. Since only one strand scission is needed to convert supercoiled DNA to the fully relaxed nicked-circular form, sensitivity is defined as the reciprocal of the dose required to reduce the population of supercoiled molecules in an irradiated sample to 37% of its value in unirradiated controls. In Figure 1, the sensitivities of five families of topoisomers to the induction of SSB are plotted as a function of their mean linking difference. The bold solid line shows the best estimate of a linear relationship between the sensitivity to strand scission and the mean linking difference of a family of topoisomers. It has a slope of $-8.0 \pm 3.2 \times 10^{-5}$ Gy^{-1} per increment of linking difference and a y-intercept of $2.6 \pm 0.4 \times 10^{-3}$ Gy^{-1}. The latter is an estimate of the sensitivity of fully relaxed pIBI 30 to induction of SSB by x-rays. The lighter curves in Figure 1 denote a region that contains the best linear fit to the data with 95% confidence.

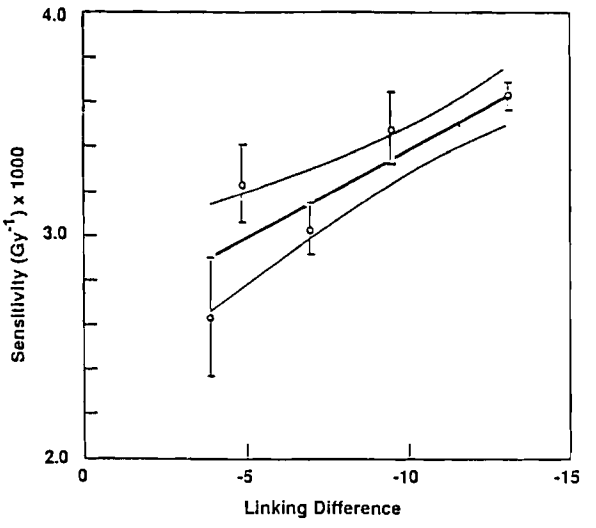

Figure 1. Sensitivity of Families of pIBI 30 Topoisomers to Induction of SSB by X-Rays. The bold line shows the best fit to the data points that were obtained by fitting the exponential dose response for the survival of supercoiled DNA. Lighter curves denote the 95% confidence region for a linear relation between radiation sensitivity and linking difference.

Electron micrographs of relaxed and supercoiled DNA suggest that the latter has a more compact secondary structure. Data obtained by van Rijn et al. (1985) using single-stranded ϕX174 in buffers with different salt concentrations indicated that the more compact conformations were more radioresistant. However, our observation that negative supercoiling increases the sensitivity of double-stranded DNA to radiation-induced strand scission suggests that another mechanism is operating in our experiments. Some insight into this mechanism may come from the biological function of negative supercoiling, which is believed to stimulate the strand separation required for transcription and replication of double-stranded DNA. Ward (1985) has shown that preferred sites of OH radical attack on DNA are more accessible to the aqueous environment in the unwound conformation than they are in the double helix mainly due to the greater exposure of DNA bases. Hence, the increase in sensitivity to strand scission by x-rays that we observe may be correlated with transient strand separation in pIBI 30 as it becomes more negatively supercoiled.

If transient disruptions of base pairing (sometimes called open states) are responsible for the increase in strand scission that we observe with underwound plasmids, then at least a part of that increase should be due to nonrandom breakage in AT-rich regions. To investigate this mechanism in more detail, computational methods developed by Benham (1990) were used to calculate the probability for helix-to-random-coil transitions as a function of sequence location in pIBI 30. Results obtained at a linking difference of -20, physiological ionic strength, and room temperature are shown in Figure 2. Under these conditions, theoretical analysis of the conformational equilibrium predicts that the most probable location for melting of the double helix is near sequence location 2000. Although these preliminary calculations were carried out for higher linking difference and higher temperature than was the case for our present experiments, they indicate the sequence locations where nonrandom breakage due to conformational instability of the double helix is most likely to occur. Therefore, they contribute to the design of

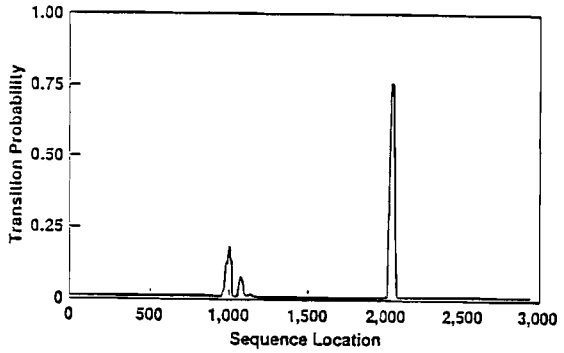

Figure 2. Relative Probability for Helix-to-Random-Coil Transitions as a Function of Base Sequence in Plasmid pIBI 30 Calculated at a Linking Difference of -20, Physiological Ionic Strength, and Room Temperature

experiments that will probe the involvement of open states in radiation-induced strand scission.

References

Benham, C. J. 1986. "Superhelical DNA." *Comments Mole. Cell. Biophys.* 4:35-54.

Benham, C. J. 1990. "Theoretical Analysis of Heteropolymeric Transitions in Superhelical DNA Molecules of Specified Sequence." *J. Chem. Phys.* 92:6294-6305.

Chiu, S-M., and N. L. Oleinick. 1982. "The Sensitivity of Active and Inactive Chromatin to Ionizing Radiation-Induced DNA Strand Breakage." *Int. J. Radiat. Bio.* 41:71-77.

Cozzarelli, N. R. 1980. "DNA Gyrase and the Supercoiling of DNA." *Science* 207:953-960.

van Rijn, K., T. Mayer, J. Blod, J. B. Verberne, and H. Loman. 1985. "Reaction Rate of OH Radicals with ϕX174 DNA: Influence of Salt and Scavenger." *Int. J. Radiat. Bio.* 47:309-317.

Ward, J. F. 1985. "Biochemistry of DNA Lesions." *Radiat. Res.* 104:S103-S111.

Free-Radical Yields in Oriented DNA Exposed to Densely Ionizing Radiation

J. H. Miller and C. E. Swenberg[a]

Loss of reproductive capability, mutation induction, and oncogenic transformation of cells by ionizing radiation is most likely due to lesions in critical subcellular targets of nanometer dimensions. Radiations with high linear energy transfer (LET) have a much greater probability of producing multiple ionizations in targets of this size than is the case for exposure to the same dose of low-LET radiation. This increases the biological effectiveness of high-LET radiation per unit of dose because lesions that develop from a high concentration of energy deposition are more resistant to repair than those produced by isolated ionizations. Therefore, the physical and chemical processes that determine the spatial distribution of damage in critical subcellular targets are central to our understanding of cellular responses to ionizing radiation.

Transport of energy in the form of separated charges, electronic and/or vibrational excitation, or unpaired electron spins (i.e., free-radical character) after it has been transferred from the radiation field to the absorbing material can influence the spatial distribution of damage on the nanometer scale. We are using samples of oriented DNA exposed to protons in the MeV energy range to investigate these phenomena. Since these high-energy protons experience only small deflections as they penetrate the sample, the path of a proton in the sample is, to a first approximation, a line source of low-energy secondary electrons. Thus a proton flux that penetrates a sample of oriented DNA molecules in a direction that is nearly parallel to the helical axis will have a greater probability of producing multiple ionizations in the same DNA chain than is the case for a proton flux that traverses the sample perpendicular to the molecular orientation.

Monte Carlo codes developed by Wilson and Paretzke (1981) can be used to investigate these differences in the patterns of ionization produced by direct proton-beam irradiations of oriented DNA if the molecule is approximated by a 2-nm-diameter cylinder with a specific orientation relative to the proton flux. Results of model calculations of this type are shown in Table 1. A typical interaction in the perpendicular case consists of a pair of ionizations separated by a distance comparable to the diameter of the molecule. This pattern of ionization is not affected by a 10° uncertainty in

(a) Radiation Biochemistry Department, Armed Forces Radiobiology Research Institute, Bethesda, Maryland.

Table 1. Interaction of Oriented DNA with 1-MeV Protons[(a)]

Relative Orientation	Mean Number of Ionizations	Mean Event Size (nm)
0°	10	224
0° ± 10°	5	47
90°	2	2
90° ± 10°	2	2

(a) Modeled by track-structure simulation.

the orientation of DNA fibers relative to the proton flux. The number of ionizations in a typical interaction is five times greater in the parallel case; however, they are distributed over a distance that is 100 times the diameter of the molecule. This pattern of ionization is very sensitive to uncertainty in the alignment between DNA fibers and the proton beam.

If the patterns of multiple energy transfer from a high-energy proton to a DNA chain in the parallel irradiation geometry are as diffuse as our simple model calculations suggest, then only long-range modes of intramolecular energy or charge transfer could cause the large amount of energy deposited in this case to influence free-radical yields. For example, singlet and triplet excitons, which probably migrate only a few nanometers in DNA of heterogeneous base composition, should have an equivalent effect in both irradiation geometries since they can only transfer energy over distances that are much less than the average distance between multiple ionizations in the parallel case. Self-cohering vibrational excitations, sometimes called solitons, are a more speculative mode of energy transfer in DNA that might couple multiple excitations on the same DNA chain. Estimates by Yomosa (1984) of the velocity of solitary waves in DNA suggest that solitons must have lifetimes of the order of 100 ps to be effective in transferring energy between deposition events in the parallel irradiation geometry.

Long-range charge transfer in DNA is more firmly established than long-range excitation transfer. Recently Al-Kazwini et al. (1990) reported evidence for an upper limit of about 100 base pairs (30 to 40 nm) for electron migration in solid DNA samples at room temperature. Above a critical water content, van Lith et al. (1986) deduced electron-migration distances in frozen DNA samples of the order of 100 nm from observations of transient microwave conductivity in pulsed radiolysis. If these experiments are detecting electron transfer through stacked base pairs or in the structured water of hydration, then oriented DNA samples may be analogous in some respects to quasi-one-dimensional semiconductors, and models of photocurrent generation in these materials (Frankevich et al. 1989) may provide insight into mechanisms for the reduced radical yields observed in the parallel irradiation geometry with fission neutrons (Arroyo et al. 1986).

Figure 1, which was adapted from work by Frankevich et al. (1989), illustrates a possible mechanism for this effect. The squares in this figure represent preexisting defects in oriented DNA samples that determine the mean free path for quasi-free electrons in unirradiated samples. The dashed arrows represent trajectories of these electrons that have a high mobility parallel to the fiber orientation and occasionally hop between fibers. In the parallel irradiation geometry, which Figure 1 illustrates, multiple excitations and ionizations on the same DNA fiber provide additional scattering centers in the high mobility path of low-energy secondary electrons ejected in the slowing down of the proton flux. Therefore, electrons that escape geminate recombination may undergo nongeminate recombination with other positive ions as they move predominately parallel to the proton track. A reduction in the

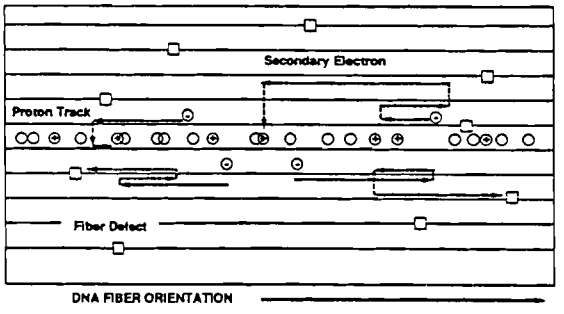

Figure 1. Schematic Diagram of Recombination and Trapping of Secondary Electrons Produced in a Quasi-One-Dimensional Semiconductor by a Proton Flux That Is Parallel to the Direction of High Electron Mobility. Squares and circles denote preexisting and radiation-induced defects, respectively. Broken lines are typical electron trajectories.

free-ion yield will reduce the yield of primary radical anions and cations on stable electron gain and loss centers, respectively. We are currently developing mathematical techniques to model charge recombination in materials with nonisotropic electron mobility following exposure to high-LET radiation.

References

Al-Kazwini, A. T., P. O'Neill, G. E. Adams, and E. M. Fielden. 1990. "Radiation-Induced Energy Migration Within Solid DNA: The Role of Misonidazole as an Electron Trap." *Radiat. Res.* 121:149-153.

Arroyo, C. M., A. J. Carmichael, C. E. Swenberg, and L. S. Myers, Jr. 1986. "Neutron-Induced Free Radicals in Oriented DNA." *Int. J. Radiat. Bio.* 50:789-793.

Frankevich, E. L., I. A. Sokolik, and A. A. Lymarev. 1989. "On the Photogeneration of Charge Carriers in Quasi-One-Dimensional Semiconductors: Polydiacetylene." *Mol. Cryst. Liq. Cryst.* 175:41-56.

van Lith, D., J. M. Warman, M. P. de Hass, and A. Hummel. 1986. "Electron Migration in Hydrated DNA and Collagen at Low Temperature. Part I. Effect of Water Concentration." *J. Chem. Soc., Faraday Trans. 1* 82:2933-2943.

Wilson, W. E., and H. G. Paretzke. 1981. "Calculation of Distributions of Energy Imparted and Ionization by Fast Protons in Nanometer Sites." *Radiat. Res.* 87:521-523.

Yomosa, S. 1984. "Solitary Excitation in Deoxyribonucleic Acid (DNA) Double Helices." *Phys. Rev. A* 30:474-480.

A Radiolytic Study of 5-Bromouracil and Its Derivatives by HPLC and Mass Spectrometry

M. Ye, C. G. Edmonds, and J. D. Zimbrick

The radiation chemistry of 5-halopyrimidines has been examined by a large number of investigators (Zimbrick et al. 1969; Adams 1967; and Edwin and Schuler 1983) due to the interest in using these moieties to localize radiation damage by selective attack of hydrated electrons (e_{aq}^-) on DNA where they have replaced thymine. It is known that the reaction of e_{aq}^- with 5-bromouracil causes elimination of bromide ion and produces uracilyl radicals (Ur·) (Zimbrick et al. 1969; Adams 1967).

$$BrUr + e_{aq}^- \rightarrow Br^- + Ur\cdot \qquad (1)$$

In the presence of a source of abstractable hydrogen, the uracilyl radical is expected to react to produce uracil (UrH) (Bhatia and Schuler 1973).

$$Ur\cdot + RH \rightarrow UrH + R\cdot \qquad (2)$$

Improvements in the separation and sensitivity of high-performance liquid chromatography (HPLC) methods now make it possible to investigate the radiolysis of BrUr, BrdU, and BrdUMP in more detail. We report here the determination of products in radiolysis of BrUr and its derivatives using HPLC and mass spectrometry. The objective of this study is to provide fundamental data that contribute to an understanding of the mechanism involved in radiosensitization of DNA by BrdU.

Bromide ion (Br^-) and 2-deoxyuridine-5'-monophosphate (dUMPH) produced in the x-ray radiolysis of 1-mM BrdUMP solution with 0.4-M 2-propanol at pH ~6.4 were detected by HPLC (Figure 1). The yields of Br^- and dUMPH are given in Table 1. The yields of bromide obtained from the radiolysis of 1-mM BrUr, BrdUR, and BrdUMP solutions N_2-saturated in the presence of the hydroxyl radical scavengers 2-propanol or t-BuOH are about 2.7, showing that the reactions of e_{aq}^- with BrUr, BrdU, and BrdUMP are quantitative and the elimination of bromide ion does not depend on the substituted groups (H, sugar, or sugar-monophosphate). This is not surprising since sugar and sugar-monophosphate have very low reactivity with e_{aq}^- (von Sonntag 1987). In the presence of alcohol, Ur·, dU·, and dUMP· undergo hydrogen abstraction. With 0.4-M 2-propanol in 1-mM solutions of BrUr, BrdU, and BrdUMP, the yields of UrH, dUH, and dUMPH are about 2.15 and the ratio of the yields of bromide and UrH, dUH, or dUMPH is about 0.80. With t-BuOH, the yields of UrH, dUH,

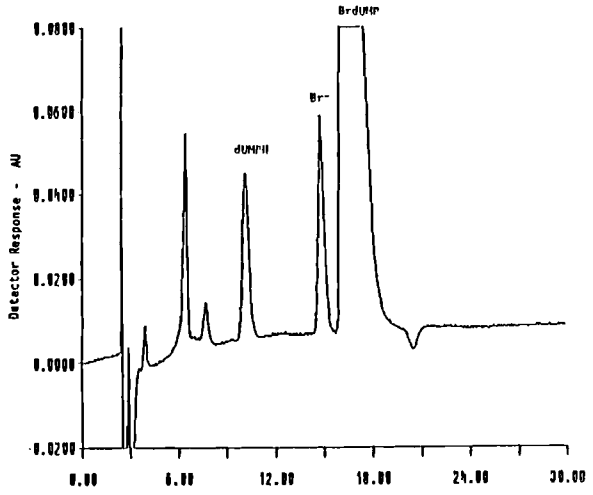

Figure 1. Chromatograms Observed in X-Ray Radiolysis of 1-mM BrdUMP Solution with 0.4-M t-BuOH N_2 Saturated pH 6.5.
Irradiation dose: 120 Gray
Detector: Linear 206 optical detector
Column: VYDAC anion exchange column
Mobil Phase: 0.03 M NaH_2PO_4 and 0.3% acetic acid.

and dUMPH are lower than those with 2-propanol, and the ratio of the yields of bromide and UrH, dUH, or dUMPH is only about 0.65. 2-propanol is about one order of magnitude more reactive as a hydrogen donor than t-BuOH in neutral solution (Ye 1989).

Experiments were also carried out in basic solutions of BrUr, BrdU, and BrdUMP and the results are given in Table 1. The yields of bromide ions were found to be about 2.67, showing that the reaction of e_{aq}^- with BrUr, BrdU, and BrdUMP and the elimination of bromide basically do not depend on the solution pH. This result is similar to the results found in the study of the reaction of e_{aq}^- with halogen-substituted benzene, phenol, and benzoic acid (Ye 1989). In basic solutions (pH ~10.5) with t-BuOH as a hydrogen donor, the yields of bromide ions and complementary UrH, dUH, and dUMPH are similar to those found in neutral solutions (Table 1). With 2-propanol, the yields are significantly higher than with t-BuOH (Table 1). The high yield of bromide must be due to isopropyl radical anion produced in the radiolysis reducing BrUr, BrdU, and BrdUMP to form extra bromide. Chain reactions are involved (Ye 1989).

In the absence of alcohol the yields of dUH and dUMPH are very low ($G < 0.8$, Table 1). These results indicate that hydrogen abstraction from the sugar moiety is not an important process for dU· and dUMP·. This is expected since the unpaired electron of uracilyl radicals is probably localized at C_5 in a σ orbital, which makes these radicals about as reactive as phenyl radicals (Madhavan et al. 1978). As shown in Reaction (3), Ur· can react with the BrUr to form a mixture of radical adducts (Edwin and Schuler 1983).

Table 1. Product Yield[(a)] in the Radiolysis of BrUr, BrdU, and BrdUMP

Solute[(b)]	pH	G(Br⁻)	G[(c)]	pH	G(Br⁻)	G[(c)]
1-mM BrUr, 2-propanol	6.6	2.67	2.14	10.1	5.07	3.95
1-mM BrUr, t-BuOH	6.3	2.65	1.78	10.2	2.69	1.80
1-mM BrdU, 2-propanol	6.2	2.71	2.20	10.2	5.02	4.11
1-mM BrdU, t-BuOH	6.3	2.62	1.70	10.3	2.58	1.55
1-mM BrdU	6.8	5.05	0.77	10.1	5.02	0.71
1-mM BrdUMP, 2-propanol	6.7	2.65	2.15	10.2	4.98	3.95
1-mM BrdUMP, t-BuOH	6.5	2.69	1.61	10.4	2.64	1.85
1-mM BrdUMP	6.5	5.12	0.75	10.4	5.08	0.80

(a) Radiation yields in molecules/100 eV. Yields were averaged from at least three experiments.
(b) The concentration of 2-propanol or t-BuOH is 0.4 M. All solutions were saturated with N_2.
(c) Yield of UrH, dUH, and dUMPH.

$$Ur\cdot + BrUr \rightarrow \text{adducts} \qquad (3)$$

Products formed in the radiolysis of 20-mM BrdU saturated with N_2 were determined by mass spectrometry (Figure 2). The adduct formed in Reaction (3) was found in the irradiated solution (peak C_1 and C_2). Apparently, dU· can also undergo combination reaction to form a dimmer 2 (peak B).

In the absence of alcohol, hydroxyl radicals react with BrUr, BrdU, and BrdUMP. Hydroxyl radical can first add to C_5,

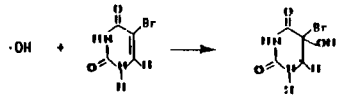

(4)

followed by elimination of hydrogen bromide (Patterson and Bansal 1972).

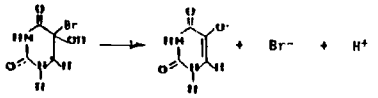

(5)

The radical produced by oxidative dehydrohalogenation of bromouracil [Reaction (5)] has been characterized by electron spin resonance (ESR) experiments (Neta 1972). This radical can react with the starting substrate to form a stable adduct. Our mass spectrometry study shows that the radical adds mainly to C_6 position of the uracil ring. The products are shown in Figure 2 (peak D_1 and D_2).

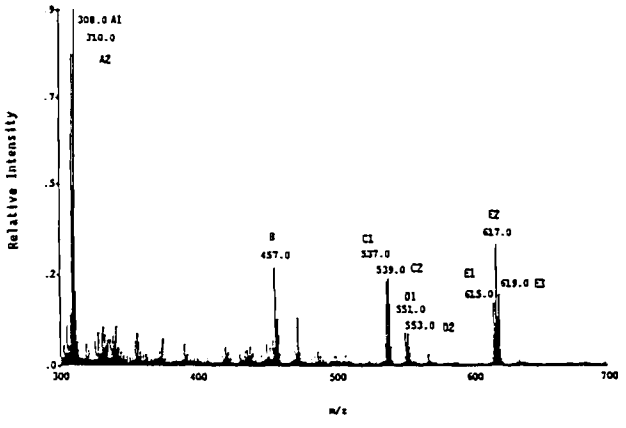

Figure 2. Mass Spectrum of 20-mM 5-Bromo-2'-Deoxyuridine Irradiated with $^{60}C_o$ at Dose 400 Gy.

In summary, this study indicated that hydrogen abstraction from sugar moieties by uracilyl radicals is not an important reaction. Our mass spectrometry experiments provide the first confirmation that uracilyl radicals undergo addition reaction to form adducts as suggested by Edwin and Schuler (1983). Hydroxyl radicals also significantly react with BrUr, BrdU, and BrdUMP to eliminate hydrogen bromide.

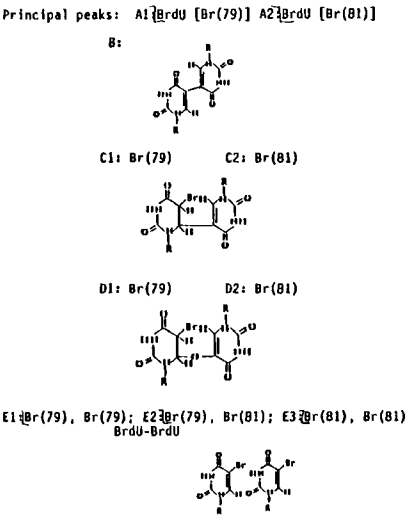

References

Adams, G. E. 1967. *Current Topics in Radiation Research.* Vol. III, eds. M. Ebert and A. Howard, pp. 35-47. Wiley and Sons, New York.

Bhatia, K., and R. H. Schuler. 1973. "Uracilyl Radical Production in the Radiolysis of Aqueous Solutions of the 5-Halouracils." *J. Phys. Chem.* 77:1888-1896.

Edwin, R., and R. H. Schuler. 1983. "Intermediates in the Reduction of 5-Halouracils by e_{aq}^-." *J. Phys. Chem.* 87:3966-3971.

Madhavan, V., R. H. Schuler, and R. W. Fessenden. 1978. "Absolute Rate Constants for Reactions of Phenyl Radicals." *J. Am. Chem. Soc.* 100:888-893.

Neta, P. 1972. "Electron Spin Resonance Study of Radicals Produced in Irradiated Aqueous Solutions of 5-Halouracils." *J. Phys. Chem.* 76:2399-2402.

Patterson, L. K., and K. M. Bansal. 1972. "Pulse Radiolysis Studies of 5-Halouracils in Aqueous Solutions." *J. Phys. Chem.* 76:2392-2399.

von Sonntag, C. 1987. *The Chemical Basis of Radiation Biology*, pp. 167-189. Taylor & Francis Inc., New York.

Ye, M. 1989. "Radiolytic Studies of Reduction and Oxidation of Aromatic Systems." Ph.D. Dissertation, pp. 100-126. Department of Chemistry and Biochemistry, University of Notre Dame.

Zimbrick, J. D., J. F. Ward, and L. S. Myers. 1969. "Studies on the Chemical Basis of Cellular Radiosensitization by 5-Bromouracil Substitution in DNA." *Int. J. Radiat. Biol.* 16:505-523.

Publications and Presentations

Publications

Bernstein, E. M., M. W. Clark, J. A. Tanis, W. T. Woodland, K. H. Berkner, A. S. Schlachter, J. W. Stearns, R. D. DuBois, W. G. Graham, T. J. Morgan, D. W. Mueller, and M. P. Stockli. 1990. "Test of Predicted $\Delta n \geq 1$ L-Shell Dielectronic-Recombination Cross Sections." *Phys. Rev. A* 40:4085-4088.

Braby, L. A. 1990. "Phenomenological Models." In *Proceedings of the Physical and Chemical Mechanisms in Molecular Radiation Biology*. Held September 4-7, 1990, in Woods Hole, Massachusetts (in press).

Braby, L. A., and W. D. Reece. 1990. "Studying Low Dose Effects Using Single Particle Microbeam Irradiation." *Radiat. Protect. Dosim.* 31:311-314.

Braby, L. A., L. H. Toburen, W. E. Wilson, and N. F. Metting. 1990. "Microdosimetric Measurements of Heavy Ion Tracks." *Advances in Space Research* (in press).

Brackenbush, L. W., L. A. Braby, and G. A. Anderson. 1990. "Characterizing the Energy Deposition Events Produced by Trapped Protons in Low Earth Orbit." *Radiat. Protect. Dosim.* 29:119-121.

Clark, M. W., J. A. Tanis, E. M. Berstein, N. R. Badnell, R. D. DuBois, W. G. Graham, T. J. Morgan, V. L. Plano, A. S. Schlachter, and M. P. Stockli. "Cross Sections for Resonant Transfer and Excitation in Fe^{Qt} + He Collisions." Submitted to *Phys. Rev. A.*

DuBois, R. D. 1990. "Coincidence Measurements of Electron Capture and Loss in Ion-Atom Collisions." In *Proceedings of 4th Workshop on High-Energy Ion-Atom Collision Processes*. September 17-19, 1990, Debrecen, Hungary (in press).

DuBois, R. D., and S. T. Manson. 1990. "Electron Emission in He^+ - Atom and He^+ - Molecule Collisions: A Combined Experimental and Theoretical Study." *Phys. Rev. A* 42:1222-1230.

Edmonds, C. G., J. A. Loo, C. J. Barinaga, H. R. Udseth, and R. D. Smith. 1989. "Capillary Electrophoresis-Electrospray Ionization-Mass Spectrometry." *J. Chromatogr.* 474:21-37.

Edmonds, C. G., and R. D. Smith. 1990. "Mass Spectrometry, DNA Sequencing and the Human Genome Initiative." *Division of Anal. Chem. Newsletter* Fall:27-34.

Edmonds, C. G., and R. D. Smith. "Electrospray Ionization Mass Spectrometry." *Methods in Enxymology: Mass Spectrometry* (in press).

Heil, O., R. D. DuBois, R. Maier, M. Kuzel, and K.-O. Groeneveld. 1990. "Electron Emission in H^0- Atom Collisions: A Coincidence Study of the Angular Dependence." Prepared for the XIth International Conference on the Application of Accelerators in Research and Industry. November 5-8, 1990, Denton Texas. *Nuclear Instruments and Methods* (in press).

Jacobson, B. S. 1990. "Indices of Cellular Radiosensitivity and Dose-Survival Curve Shape Based on the Linear Quadratic Survival Model." Submitted to *Radiation Research.*

Loo, J. A., C. G. Edmonds, and R. D. Smith. 1990. "Primary Sequence Information from Electrospray Ionization Tandem Mass Spectrometry of Intact Proteins." *Science* 248:201-204.

Loo, J. A., C. G. Edmonds, R. D. Smith, M. P. Lacey, and T. Keough. 1990. "Comparison of Electrospray Ionization and Plasma Desorption Mass Spectra of Peptides and Proteins." *Biomed. and Environ. Mass Spectrom.* 19:286-295.

Loo, J. A., C. G. Edmonds, H. R. Udseth, R. R. Ogorzalek-Loo, and R. D. Smith. "Electrospray Ionization Mass Spectrometry and Tandem Mass Spectrometry of Large Biomolecules." Submitted to *Experimental Mass Spectrometry.*

Loo, J. A., C. G. Edmonds, H. R. Udseth, and R. D. Smith. 1990. "Effect of Reducing Disulfide-Containing Proteins on Electrospray Ionization Mass Spectra." *Anal. Chem.* 62:693-698.

Loo, J. A., C. G. Edmonds, H. R. Udseth, and R. D. Smith. "Collisional Activation and Dissociation of Large Multiply Charged Proteins Produced by Electrospray Ionization." *Anal. Chim. Acta* (in press).

Loo, J. A., H. K. Jones, H. R. Udseth, and R. D. Smith. 1989. "Capillary Zone Electrophoresis-Mass Spectrometry with Electrospray Ionization of Peptides and Proteins." *J. Microcolumn Sep.* 1:223-229.

Loo, J. A., H. R. Udseth, and R. D. Smith. 1989. "Peptide and Protein Analysis by Electrospray Ionization Mass Spectrometry and Capillary Zone Electrophoresis-Mass Spectrometry." *Anal. Biochem.* 179:404-412.

McCormick, J. J., D. G. Fry, P. J. Herlin, T. L. Morgan, D. M. Wilson, and V. M. Maher. 1989. "Malignant Transformation of Human Fibroblasts by Transfected Oncogenes." In *Cell Transformation and Radiation-Induced Cancer*, eds., K. H. Chadwick, C. Seymour, and B. Barnhart, pp. 75-84. Adam Hilger, Bristol, Great Britain.

Miller, J. H. 1990. "Prediction of Secondary-Electron Energy Spectra." *Nucl. Tracks. Radiat. Meas.* 16:207-211.

Miller, J. H., and C. E. Swenberg. 1990. "Radical Yields in DNA Exposed to Ionizing Radiation: Role of Energy and Charge Transfer." *Can. J. Phys.* (in press).

Miller, J. H., and W. E. Wilson. 1990. "Modeling the Biological Effectiveness of High-LET Radiation." *Health Phys.* 57:363-367.

Miller, J. H., M. Ye, J. M. Nelson, C. E. Swenberg, J. M. Speicher, and C. J. Benham. 1990. "Negative Supercoiling Increases the Sensitivity of Plasmid DNA to Single-Strand-Break Induction by X-Rays." Submitted to *Int. J. of Radiat. Biol.*

Morgan, T. L., E. W. Fleck, K. A. Poston, B. A. Denovan, C. N. Newman, B.J.F. Rossiter, and J. H. Miller. 1990. "Molecular Characterization of X-Ray-Induced Mutations at the HPRT Locus in Plateau-Phase Chinese Hamster Ovary Cells." *Mutat. Res.* 232:171-182.

Morgan, T. L., E. W. Fleck, B.J.F. Rossiter, and J. H. Miller. 1989. "Use of Mammalian Cells to Investigate the Genetic Consequences of DNA Damage Induced by Ionizing Radiation. In *Multilevel Health Effects Research: From Molecules to Man*, eds., J. F. Park and R. A. Pelroy, pp. 305-306. Battelle Press, Columbus, Ohio.

Morgan, T. L., E. W. Fleck, B.J.F. Rossiter, and J. H. Miller. 1989. "Molecular Characterization of X-Ray-Induced Mutations at the HGPRT Locus in Plateau-Phase Chinese Hamster Ovary Cells: Effect of Dose, Dose Fractionation, and Delayed Plating." In *Cell Transformation and Radiation-Induced Cancer*, eds., K. H. Chadwick, C. Seymour, and B. Barnhart, pp. 207-214. Adam Hilger, Bristol, Great Britain.

Morgan, T. L., E. W. Fleck, B.J.F. Rossiter, and J. H. Miller. 1990. "Molecular Characterization of X-Ray-Induced Mutations at the HGPRT Locus in Plateau Phase Chinese Hamster Ovary Cells: The Effect of Dose, Dose Fractionation and Delayed Plating." In *Proceedings of Cell Transformation Systems Relevant of Radiation-Induced Cancer in Man*, pp. 207-214. Held April 4-7, 1989, in Dublin, Ireland.

Nelson, J. M., L. A. Braby, N. F. Metting, and W. C. Roesch. 1990. "Analyzing the Role of Biochemical Processes in Determining Response to Ionizing Radiations." *Health Phys.* 57:369-376.

Nelson, J. M., L. A. Braby, N. F. Metting, and W. C. Roesch. 1990. "Multiple Components of Split-Dose Repair in Plateau-Phase Mammalian Cells: A New Challenge for Phenomenological Modelers." *Radiat. Res.* 121:154-160.

Reinhold, C. O., D. R. Schultz, R. E. Olson, L. H. Toburen, and R. D. DuBois. 1990. "Electron Emission from Both Target and Projectile in C^+ + He Collisions." *J. Phys. B* 23:L297-L302.

Smith, R. D., and C. J. Barinaga. 1990. "Internal Energy Effects in the Collision Induced Dissociation of Large Biopolymer Molecular Ions Produced by Electrospray Ionization: Tandem Mass Spectrometry of Cytochrome c." *Rapid Comm. Mass Spectrom.* 4:54-57.

Smith, R. D., C. J. Barinaga, and H. R. Udseth. 1989. "Tandem Mass Spectrometry of Highly Charged Cytochrome c Molecular Ions Produced by Electrospray Ionization." *J. Phys. Chem.* 93:5019-5022.

Smith, R. D., S. M. Fields, J. A. Loo, C. J. Barinaga, and H. R. Udseth. 1990. "Capillary Isotachophoresis with UV and Tandem Mass Spectrometric Detection for Peptides and Proteins." *Electrophoresis* 11:707-717.

Smith, R. D., J. A. Loo, C. J. Barinaga, C. G. Edmonds, and H. R. Udseth. 1989. "Capillary Zone Electrophoresis and Isotachophoresis-Mass Spectrometry of Polypeptides and Proteins Based Upon an Electrospray Ionization Interface." *J. Chromatogr.* 480:211-232.

Smith, R. D., J. A. Loo, C. J. Barinaga, C. G. Edmonds, and H. R. Udseth. 1990. "Collisional Activation and Collision-Activated Dissociation of Large Multiply Charged Polypeptides and Proteins Produced by Electrospray Ionization." *J. Am. Soc. for Mass Spectrom.* 1:53-65.

Smith, R. D., J. A. Loo, C. G. Edmonds, C. J. Barinaga, and H. R. Udseth. 1990. "New Developments in Biochemical Mass Spectrometry: Electrospray Ionization." *Anal. Chem.* 62:882-899.

Smith, R. D., J. A. Loo, C. G. Edmonds, C. J. Barinaga, and H. R. Udseth. "Sensitivity Considerations for Large Molecule Detection by Capillary Electrophoresis-Electrospray Ionization Mass Spectrometry." *J. Chromatogr.* (in press).

Thacker, J., E. W. Fleck, B.J.F. Rossiter, and T. L. Morgan. 1990. "Localization of Deletion Breakpoints in Radiation-Induced Mutants of the HPRT Gene in Hamster Cells." *Mutat. Res.* 232:163-170.

Toburen, L. H. 1990. "Atomic and Molecular Physics in the Gas Phase." In *Proceedings of Physical and Chemical Mechanisms in Molecular Radiation Biology*. Held September 4-7, 1990, in Woods Hole, Massachusetts (in press).

Toburen, L. H., L. A. Braby, N. F. Metting, G. Kraft, M. Scholz, F. Kraske, H. Schmidt-Böcking, R. Dörner, and R. Seip. 1990. "Radial Distributions of Energy Deposited Along Charged Particle Tracks." *Radiat. Protect. Dosim.* 31:199-203.

Toburen, L. H., R. D. DuBois, C. O. Reinhold, D. R. Schultz, and R. E. Olson. 1990. "Experimental and Theoretical Study of the Electron Spectra in 66.7 to 350 keV/u C^+ + He Collisions." *Phys. Rev. A* 42:5338-5347.

Toburen, L. H., and W. E. Wilson. 1990. "Biological Effects of Inner-Shell Ionization." In *Proceedings of the X-90 15th International Conference on X-Ray and Inner-Shell Processes*. Held July 9-13, 1990, in Knoxville, Tennessee (in press).

Wang, Y. D., J. C. Straton, J. H. McGuire, and R. D. DuBois. 1990. "High-Velocity Limits for the Ratio of Double to Single Ionization of Helium by Projectiles with Electrons." *J. Phys. B: At. Mol. Opt. Phys.* 23:L133-L138.

Ye, M., and R. H. Schuler. 1990. "Determination of Oxidation Products in Radiolysis of Halophenols with Pulse Radiolysis, HPLC and Ion Chromatography." *J. Liq. Chromatog.* (in press).

Presentations

Braby, L. A. 1990. "Dose and Dose Equivalent Measurements with Tissue Equivalent Proportional Counters." (Invited paper.) Presented at the FAA Workshop, Oklahoma City, Oklahoma. PNL-SA-18589A, Pacific Northwest Laboratory, Richland, Washington.

Braby, L. A. 1990. "Interpreting Survival Observations Using Phenomenological Models." (Invited paper.) Presented at the Physical and Chemical Mechanisms in Molecular Radiation Biology Workshop, Woods Hole, Massachusetts. PNL-SA-14960A, Pacific Northwest Laboratory, Richland, Washington.

Braby, L. A., N. F. Metting, W. E. Wilson, and L. H. Toburen. 1990. "Microdosimetric Measurements of Heavy Ion Tracks." (Invited paper.) Presented at the 28th COSPAR Symposium on Heavy Ion Effects in Genetically Important Cellular Structures, The Hague, The Netherlands. PNL-SA-17906A, Pacific Northwest Laboratory, Richland, Washington.

Campbell, J. A., R. B. Lucke, R. M. Bean and S. D. Harvey. 1990. "Application of Particle Beam LC/MS to the Analysis of Derivatized Metabolites of Polynuclear Aromatic Hydrocarbons." Proceedings of the 38th ASMS Conference on Mass Spectrometry and Allied Topics, Tucson, AZ, June 3-8, 1990, pp. 1027-1028.

DuBois, R. D. 1990. "Multiple Ionization Mechanisms in Ion-Atom Collisions." Presented at the University of Innsbruck, Austria.

DuBois, R. D. 1990. "Projectile Ionization in Light Ion-Atom Collisions." Presented at the German Winter Atomic Physics Meeting, Rietzlen, Austria.

DuBois, R. D., R. Herrman, J. Feng, R. Dörner, J. Euler, and K. Ullman. 1990. "Correlations Between Charged Particles Emitted in Ion-Molecule Collisions." Presented at the Vth International Conference on the Physics of Highly-Charged Ions, Giessen, Germany. PNL-SA-18538A, Pacific Northwest Laboratory, Richland, Washington.

Edmonds, C. G. 1989. "New Mass Spectrometric Methods for Biochemical Research." Presented at the American Chemical Society Meeting, Richland, Washington.

Edmonds, C. G. 1989. "Electrospray Ionization Mass Spectrometry and Tandem Mass Spectrometry for Peptide and Protein Analysis." Presented in a seminar at Hoffmann-LaRoche Company, Nutley, New Jersey.

Edmonds, C. G., J. A. Loo, and R. D. Smith. 1990. "Electrospray Ionization Mass Spectrometry and Tandem Mass Spectrometry for the Characterization of Proteins and Proteolytic Digests." Presented at the Fourth Symposium of the Protein Society, San Diego, California.

Edmonds, C. G., R. R. Ogorzalek-Loo, J. A. Loo, H. R. Udseth, and R. D. Smith. 1990. "Application of Electrospray Mass Spectrometry and Mass Spectrometry/Mass Spectrometry to the Analysis of Protein Proteolytic Digests." Presented at the 38th ASMS Conference on Mass Spectrometry and Allied Topics, Tucson, Arizona.

Edmonds, C. G., R. D. Smith, J. A. Loo, H. R. Udseth, and A. L. Rockwood. 1990. "Electrospray Ionization Mass Spectrometry and Tandem Mass Spectrometry for Biochemical Investigations." Presented at FACSS, Cleveland, Ohio.

Heil, O., R. D. DuBois, R. Maier, M. Kuzel, and K. -O. Groeneveld. 1990. "Electron Emission in H°- Atom Collisions: A Coincidence Study of the Angular Dependence." (Invited paper.) Presented at the XIth International Conference on the Application of Accelerators in Research and Industry, Denton, Texas. PNL-SA-18739A, Pacific Northwest Laboratory, Richland, Washington.

Jostes, R. F., E. W. Fleck, R. A. Gies, T. L. Morgan, J. K. Weincke, and F. T. Cross. 1990. "Cytotoxic, Clastogenic, and Mutagenic Response of Mammalian Cells Exposed In Vitro to Radon and Its Progeny." Richland, Washington.

Jostes, R. F., R. A. Gies., T. L. Morgan, E. W. Fleck, K. P. Gasper, and F. T. Cross. 1990. "Molecular Analysis of Radon-Induced Mutants." Presented at Ionizing Radiation Damage to DNA: Molecular Aspects, Lake Tahoe, California.

Loo, J. A., C. G. Edmonds, and R. D. Smith. 1990. "Sequence Information from Electrospray Ionization Tandem Mass Spectrometry of Intact Proteins." Presented at the 38th ASMS Conference on Mass Spectrometry and Allied Topics, Tucson, Arizona.

Loo, J. A., C. G. Edmonds, H. R. Udseth, and R. D. Smith. 1990. "Dissociation of Multiply Charged Protein Ions from Electrospray Ionization in the ESI-MS Interface." Presented at the 38th ASMS Conference on Mass Spectrometry and Allied Topics, Tucson, Arizona.

Miller, J. H. 1990. "Role of Energy and Charge Transfer in DNA Damage by Densely Ionizing Radiation." Presented at the NATO Advance Research Workshop, Early Effects of Radiation on DNA, San Miniato, Italy. PNL-SA-18017A, Pacific Northwest Laboratory, Richland, Washington.

Miller, J. H. 1990. "Modeling Energy Transport and DNA Damage in Heterogeneous Macromolecular Solutions." Presented at the DOE Radiological and Chemical Physics Contractors Meeting, Berkeley, California. PNL-SA-18312A, Pacific Northwest Laboratory, Richland, Washington.

Miller, J. H. 1990. "DNA Supercoiling Radiation Sensitivity, and Radiation Modifiers." Presented at the Southern California Radiation Biology Group Annual Meetings, Los Angeles, California. PNL-SA-18569A, Pacific Northwest Laboratory, Richland, Washington.

Morgan, T. L. 1990. "Effects of Radiation Damage and Repair on the Spectrum of Molecular Alterations in the DNA of Radiation-Induced Mammalian Cell Mutants." Presented at the DOE Radiological and Chemical Physics Contractors Meeting, Berkeley, California. PNL-SA-18310A, Pacific Northwest Laboratory, Richland, Washington.

Nelson, J. M., and L. A. Braby. 1990. "Survival of Irradiated Cells in the Absence of Potentially Lethal Damage Repair." Presented at the Cell Kinetics Society, St. Louis, Missouri. [Abstract Published: *Cell Tissue Kinet.* 23(4):364.] PNL-SA-17995A, Pacific Northwest Laboratory, Richland, Washington.

Nelson, J. M., and L. A. Braby. 1990. "Relative Effectiveness of Damage-Removal Processes After Low Doses of Radiation." Presented at the Cell Kinetics Society, St. Louis, Missouri. [Abstract Published: *Cell Tissue Kinet.* 23(4):346.] PNL-SA-18006A, Pacific Northwest Laboratory, Richland, Washington.

Nelson, J. M., and L. A. Braby. 1990. "Repair Capacity in Stationary Plateau-Phase CHO Cells." Presented at the 38th Annual Radiation Research Society, New Orleans, Louisiana. PNL-SA-17639A, Pacific Northwest Laboratory, Richland, Washington.

Nelson, J. M., and L. A. Braby. 1990. "Cellular Radiation Biophysics." Presented at the DOE Radiological and Chemical Physics Contractors Meeting, Berkeley, California. PNL-SA-18309A, Pacific Northwest Laboratory, Richland, Washington.

Ogorzalek-Loo, R. R., J. A. Loo, H. R. Udseth, and R. D. Smith. 1990. "Factors Influencing the Ionization and Desolvation Processes of Electrospray Ionization Mass Spectrometry." Presented at the 38th ASMS Conference on Mass Spectrometry and Allied Topics, Tucson, Arizona.

Reinhold, C. O., D. R. Schultz, R. E. Olson, and L. H. Toburen. 1990. "Ejected-Electron Spectra in Collisions of C^+ Ions with He." Presented at the Division of Atomic Molecular and Optical Physics of the American Physical Society, Monterey, California. PNL-SA-18169A, Pacific Northwest Laboratory, Richland, Washington.

Rottmann, M., R. Bruch, R. D. DuBois, and L. H. Toburen. 1990. "Total Charge Transfer Cross Sections for 100-1500 keV Multiply Charged Carbon, Nitrogen, and Oxygen Ions in Collisions with Gaseous He, Ne, and H_2 Targets." Submitted to the Eleventh International Conference on the Application of Accelerators in Research and Industry, Denton, Texas. PNL-SA-18453A, Pacific Northwest Laboratory, Richland, Washington.

Silverstein, T. P., and L. A. Braby. "Membrane Proteins Sensitive Sonicated Lipid Vesicles to Radiation Damage." Presented at the Biophysics Society, Baltimore, Maryland. PNL-SA-17587A, Pacific Northwest Laboratory, Richland, Washington.

Smith, R. D. 1990. "Combined Capillary Electrophoresis and Electrospray Ionization Mass Spectrometry." Presented at Spectroscopy Across the Spectra, Hertford, United Kingdom.

Smith, R. D., J. A. Loo, C. G. Edmonds, C. J. Barinaga, and H. R. Udseth. 1990. "Electrospray Ionization and Tandem Mass Spectrometry of Large Molecules." Presented at the 1990 ACS Symposium, Washington, D.C.

Smith, R. D., J. A. Loo, C. G. Edmonds, and H. R. Udseth. 1990. "Electrospray Ionization/Mass Spectrometry." Presented at the 43rd Annual Summer Symposium on Analytical Chemistry, Oak Ridge, Tennessee.

Smith, R. D., H. R. Udseth, and C. G. Edmonds. 1990. "Capillary Electrophoresis and Capillary Electrophoresis-Mass Spectrometry." Presented at the Pittsburgh Conference, New York.

Smith, R. D., H. R. Udseth, C. G. Edmonds, C. J. Barinaga, and J. A. Loo. 1990. "Combinations of Chromatography and Electrophoresis with Mass Spectrometry." Presented at the 14th International Symposium on Column LC, Boston, Massachusetts.

Smith, R. D., H. R. Udseth, C. G. Edmonds, and J. A. Loo. 1990. "Challenges for the Electrospray Ionization and Tandem Mass Spectrometry of Very Large Molecules." Presented at 38th ASMS Conference on Mass Spectrometry and Allied Topics, Tucson, Arizona.

Smith, R. D., H. R. Udseth, C. G. Edmonds, and J. A. Loo. 1990. "Combined Capillary Electrophoresis-Mass Spectrometry of Proteins." Presented at the Second International Symposium on High Performance Capillary Electrophoresis, San Francisco, California.

Smith, R. D., H. R. Udseth, C. G. Edmonds, and J. A. Loo. 1990. Electrospray Ionization-Mass Spectrometry of Proteins." Presented at the Second International Symposium on Applied Mass Spectrometry in the Health Fields, Barcelona, Spain.

Toburen, L. H. 1990. "The Role of Collision Physics in Radiobiology." Presented seminar at the University of Missouri-Rolla, Rolla, Missouri. PNL-SA-17863A, Pacific Northwest Laboratory, Richland, Washington.

Toburen, L. H. 1990. "Atomic and Molecular Physics in Gas Phase." (Invited paper.) Presented at the Physical and Chemical Mechanisms in Molecular Radiation Biology, Woods Hole, Massachusetts. PNL-SA-18193A, Pacific Northwest Laboratory, Richland, Washington.

Toburen, L. H. 1990. "Physics of Energy Deposition by High-LET Ions." Presented at the DOE Radiological and Chemical Physics Contractors Meeting, Berkeley, California. PNL-SA-18311A, Pacific Northwest Laboratory, Richland, Washington.

Toburen, L. H., and W. E. Wilson. 1990. "Biological Effects of Inner-Shell Ionization." (Invited talk.) Presented at the X-90 15th International Conference on X-Ray and Inner-Shell Processes. PNL-SA-18193A, Pacific Northwest Laboratory, Richland, Washington.

Udseth, H. R., C. J. Barinaga, and R. D. Smith. 1990. "Developments in Combined Capillary Electrophoresis-ESI-MS. Presented at the 38th ASMS Conference on Mass Spectrometry and Allied Topics, Tucson, Arizona.

Udseth, H. R., C. J. Barinaga, and R. D. Smith. 1990. "New Developments in Capillary Electrophoresis-Mass Spectrometry." Presented at the Second International Symposium on Applied Mass Spectrometry in the Health Fields, Barcelona, Spain.

Wilson, W. E., and L. A. Braby. 1990. "Charged Particle Track Simulation and Systematics of Energy Deposition in Microscopic Volumes." Presented at the DOE Radiological and Chemical Physics Contractors Meeting, Berkeley, California. PNL-SA-18308A, Pacific Northwest Laboratory, Richland, Washington.

Wilson, W. E., and H. G. Paretzke. 1990. "Microscopic Dosimetry of Proton Tracks: Touchers." Presented at the 38th Annual Radiation Research Society, New Orleans, Louisiana. PNL-SA-17620A, Pacific Northwest Laboratory, Richland, Washington.

Ye, M., J. M. Nelson, J. H. Miller, E. W. Fleck, and C. E. Swenberg. 1990. "Superhelicity Increases the Sensitivity of Plasmid DNA to Strand-Break Induction by X-Rays." Presented at the 38th Annual Radiation Research Society, New Orleans, Louisiana. PNL-SA-17624A, Pacific Northwest Laboratory, Richland, Washington.

Author Index

Author Index

Distribution

Distribution

DOMESTIC

W. R. Albers
EH-12, GTN
Department of Energy
Washington, DC 20545

D. Anderson
ENVIROTEST
1108 NE 200th Street
Seattle, WA 98155-1136

Assistant Secretary
Environment, Safety & Health
EH-1, FORS
Department of Energy
Washington, DC 20585

F. Badgley
13749 NE 41st Street
Seattle, WA 98125

R. E. Baker
8904 Roundleaf Way
Gaithersburg, MD 20879-1630

R. W. Barber
EH-131, GTN
Department of Energy
Washington, DC 20545

A. D. Barker
Battelle Columbus Laboratories
505 King Avenue
Columbus, OH 43201

N. F. Barr
ER-72, GTN
Department of Energy
Washington, DC 20545

J. R. Beall
ER-72, GTN
Department of Energy
Washington, DC 20545

W. R. Bibb
Energy Programs and Support Division
Department of Energy
P.O. Box 2001
Oak Ridge, TN 38731

L. C. Brazley, Jr.
NE-22, GTN
Department of Energy
Washington, DC 20545

D. J. Brenner
Radiological Research Lab
College of Physicians and Surgeons
Columbia University
630 W. 168th Street
New York, NY 10032

G. Burley
Office of Radiation Programs, ANR-458
Environmental Protection Agency
Washington, DC 20460

W. W. Burr, Chairman
Medical & Health Sciences Division
Oak Ridge Associated Universities
P.O. Box 117
Oak Ridge, TN 37830

L. K. Bustad
College of Veterinary Medicine
Washington State University
Pullman, WA 99164-7010

R. J. Catlin, President
Robert J. Catlin Corporation
701 Welch Road, Suite 1119
Palo Alto, CA 94304

A. Chatterjee
Lawrence Berkeley Laboratory
MS 29-100
1 Cyclotron Road
Berkeley, CA 94720

N. Cohen
New York University Medical Center
P.O. Box 817
Tuxedo, NY 10987

Council on Environmental Quality
722 Jackson Place, NW
Washington, DC 20503

Department of Energy
Environment & Health Division
P.O. Box 5400
Albuquerque, NM 87115

Department of Energy
Director, Health Protection Division
P.O. Box 5400
Albuquerque, NM 87115

G. DePlanque, Director
Department of Energy-EMEL
375 Hudson Street
New York, NY 10014

DOE Office of Scientific and Technical Information (12)

G. D. Duda
ER-72, GTN
Department of Energy
Washington, DC 20545

A. P. Duhamel
ER-74, GTN
Department of Energy
Washington, DC 20545

W. H. Ellett
BRER--National Research Council, MH-370
2101 Constitution Avenue, NW
Washington, DC 20418

S. J. Farmer
17217 77th Avenue W.
Edmonds, WA 98020

B. H. Fimiani
Battelle, Pacific Northwest Laboratories
Washington Operations
370 L'Enfant Promenade, Suite 900
901 D Street, SW
Washington, DC 20024

W. R. Garrett
Oak Ridge National Laboratory
P.O. Box 2008
Oak Ridge, TN 37831

T. F. Gesell
Idaho Operations Office
Department of Energy
785 DOE Place
Idaho Falls, ID 83402-4149

R. D. Gilmore, President
Environmental Health Sciences, Inc.
Nine Lake Bellevue Building
Suite 104
Bellevue, WA 98005

G. Goldstein
ER-74, GTN
Department of Energy
Washington, DC 20545

G. H. Groenewold
Energy and Mineral Research Center
University of North Dakota
Box 8123, University Station
Grand Forks, ND 58202

E. J. Hall
Radiological Research Laboratory
Columbia University
630 West 168th Street
New York, NY 10032

J. W. Healy
51 Grand Canyon Drive
White Rock, NM 87544

R. O. Hunter, Jr.
ER-1, FORS
Department of Energy
1000 Independence Avenue, SW
Washington, DC 20585

F. Hutchinson
Department of Molecular Biophysics & Biochemistry
Yale University
260 Whitney Avenue
P.O. Box 6666
New Haven, CT 06511

M. Inokuti
Argonne National Laboratory
9700 South Cass Avenue
Argonne, IL 60439

H. Ishikawa, General Manager
Nuclear Safety Research Association
P.O. Box 1307
Falls Church, VA 22041

A. W. Johnson
Vice President for Academic Affairs
San Diego State University
San Diego, CA 92182

J. F. Johnson
Kenworth Truck Co.
P.O. Box 1000
Kirkland, WA 98083

L. J. Johnson
Idaho National Engineering Lab
IRC MS 2203
P.O. Box 1625
Idaho Falls, ID 83415

G. Y. Jordy, Director
ER-30, GTN
Department of Energy
Washington, DC 20545

B. J. Kelman
P. O. Box 3015
Menlo Park, CA 94025

G. A. Kolstad
ER-15, GTN
Department of Energy
Washington, DC 20545

R. T. Kratzke
NP-40
Department of Energy
Germantown, MD 20545

Librarian
Brookhaven National Laboratory
Research Library, Reference
Upton, Long Island, NY 11973

Librarian
Colorado State University
Documents Department--The Libraries
Ft. Collins, CO 80523

Librarian
Electric Power Research Institute
3412 Hillview Avenue
P.O. Box 10412
Palo Alto, CA 94303

Librarian
Health Sciences Library, SB-55
University of Washington
Seattle, WA 98195

Librarian
Los Alamos National Laboratory
Report Library, MS P364
P.O. Box 1663
Los Alamos, NM 87545

Librarian
Oregon Regional Primate Research Center
505 NW 185th Avenue
Beaverton, OR 97006

Librarian
Washington State University
Pullman, WA 99164-6510

Library
Serials Department (#80-170187)
University of Chicago
1100 East 57th Street
Chicago, IL 60637

J. N. Maddox
ER-73, GTN
Department of Energy
Washington, DC 20545

J. R. Maher
ER-65, GTN
Department of Energy
Washington, DC 20545

C. R. Mandelbaum
ER-32, GTN
Department of Energy
Washington, DC 20545

S. Marks
c/o U.S. Marine Corp. Air Station
ABCC/RERF
FPO
Seattle, WA 98764-5000

H. M. McCammon
ER-75, GTN
Department of Energy
Washington, DC 20545

C. B. Meinhold
Radiological Sciences Division
Bldg. 703M
Brookhaven National Laboratory
Upton, Long Lsland, NY 11973

M. L. Mendelsohn
Biomedical and Environmental Research Program
Lawrence Livermore National Laboratory, L-452
University of California
P.O. Box 5507
Livermore, CA 94550

C. Miller
P.O. Box 180
Watermill, NY 11976

N. S. Nelson
Office of Radiation Programs, ANR-461
Environmental Protection Agency
401 M Street, SW
Washington, DC 20460

W. R. Ney, Executive Director
National Council on Radiation Protection and Measurements
7910 Woodmont Avenue
Suite 1016
Washington, DC 20014

Nuclear Regulatory Commission
Advisory Committee on Reactor Safeguards
Washington, DC 20555

M. J. O'Brien
Radiation Safety Office, GS-05
University of Washington
Seattle, WA 98195

R. H. Poirier
Battelle Memorial Institute
505 King Avenue
Columbus, OH 43201-2693

R. G. Rader
ER-33, GTN
Department of Energy
Washington, DC 20545

D. P. Rall, Director
National Institutes of Environmental Health Sciences
P.O. Box 12233
Research Triangle Park, NC 27709

L. A. Rancitelli
Battelle Memorial Institute
505 King Avenue
Columbus, OH 43201-2693

J. Rasey
Division of Radiation Oncology
University of Washington Medical School
Seattle, WA 98195

C. R. Richmond
Oak Ridge National Laboratory
4500N, MS-62523
P.O. Box 2008
Oak Ridge, TN 37831-6253

J. S. Robertson
ER-73, GTN
Department of Energy
Washington, DC 20545

S. L. Rose
ER-73, GTN
Department of Energy
Washington, DC 20545

R. D. Rosen, Tech. Librarian
Environmental Measurements Laboratory
Department of Energy
376 Hudson Street
New York, NY 10014

L. Sagan
Electric Power Research Institute
3412 Hillview Avenue
P.O. Box 10412
Palo Alto, CA 94304

R. A. Scarano
Mill Licensing Section
Nuclear Regulatory Commission
Washington, DC 20545

M. Schulman
ER-70, GTN
Department of Energy
Washington, DC 20545

R. Shikiar
Battelle - Seattle
4000 NE 41st Street
Seattle, WA 98105

P. H. Silverman
Lawrence Berkeley Laboratory
Bldg. 50A/5104
Berkeley, CA 94720

W. K. Sinclair, President
National Council on Radiation Protection
7910 Woodmont Avenue
Suite 1016
Bethesda, MD 20814

D. H. Slade
ER-74, GTN
Department of Energy
Washington, DC 20545

J. N. Stannard
University of California
17441 Plaza Animado #132
San Diego, CA 92128

E. T. Still
Kerr-McGee Corporation
P.O. Box 25861
Oklahoma City, OK 73125

J. Stroman
Library
Department of Energy/NIPER
P.O. Box 2128
Bartlesville, OK 74005

Technical Information Service
Savannah River Laboratory
Room 773A
E. I. duPont de Nemours & Company
Aiken, SC 29801

R. G. Thomas
ER-72, GTN
Department of Energy
Washington, DC 20545

P. W. Todd
Center for Chemical Engineering
National Bureau of Standards (773.10)
325 Broadway
Boulder, CO 80303

E. J. Vallario
15228 Red Clover Drive
Rockville, MD 20853

M. N. Varma
ER-74
Department of Energy
Washington, DC 20545

C. R. Vest
Battelle, Pacific Northwest Laboratory
Washington Operations
370 L'Enfant Promenade, Suite 900
901 D Street, SW
Washington, DC 20024

G. J. Vodapivc
DOE - Schenectady Naval Reactors Office
P.O. Box 1069
Schenectady, NY 12301

G. L. Voelz
Los Alamos National Laboratory
MS-K404
P.O. Box 1663
Los Alamos, NM 87545

B. W. Wachholz
Radiation Effects Branch
National Cancer Institute
EPN, Room 530
8000 Rockville Pike
Bethesda, MD 20892

R. A. Walters
Assistant to the Associate Director
Los Alamos National Laboratory
MS-A114
P.O. Box 1663
Los Alamos, NM 87545

W. W. Weyzen
Electric Power Research Institute
3412 Hillview Avenue
P.O. Box 10412
Palo Alto, CA 94303

W. E. Wilson, Associate Director
Nuclear Radiation Center
Washington State University
Pullman, WA 99164

F. J. Wobber
Department of Energy
14 Goshen Court
Gaithersburg, MD 20879-4403

R. W. Wood
PTRD, OHER
ER-74, GTN
Department of Energy
Washington, DC 20545

D. Woodall, Manager
Physics Group
EG&G Idaho, INEL
P.O. Box 1625
Idaho Falls, ID 83415

Zhu Zhixian
Laboratory for Energy-Related Health Research
University of California
Davis, CA 95616

FOREIGN

G. E. Adams, Director
Medical Research Council
Radiobiology Unit
Harwell, Didcot
Oxon OX11 ORD
ENGLAND

D. C. Aumann
Institut für Physikalische Chemie
Universität Bonn
Abt. Nuklearchemie
Wegelerstrasse 12
5300 Bonn 1
FEDERAL REPUBLIC OF GERMANY

M. R. Balakrishnan, Head
Library & Information Services
Bhabda Atomic Research Centre
Bombay - 400 085
INDIA

G. W. Barendsen
Laboratory for Radiobiology
AMC, FO 212
Meibergdreef 9
1105 AZ Amsterdam
THE NETHERLANDS

A. M. Beau, Librarian
Département de Protection Sanitaire
Commissariat á l'Énergie Atomique
BP No. 6
F-92265 Fontenay-aux-Roses
FRANCE

G. Bengtsson, Director-General
Statens Stralskyddsinstitut
Box 60204
S-104 01 Stockholm
SWEDEN

D. J. Beninson
Gerencía de Protección Radiológica y Seguridad
Comisión Nacional de Energía Atómica
Avenida del Libertador 8250
2° Piso Of. 2330
1429 Buenos Aires
ARGENTINA

J. Booz
KFA Jülich Institut für Medezin
Kernsforschungsanlage Jülich
Postfach 1913
D-5170 Jülich
FEDERAL REPUBLIC OF GERMANY

M. J. Bulman, Librarian
Medical Research Council
Radiobiology Unit
Harwell, Didcot
Oxon OX11 ORD
ENGLAND

Cao Shu-Yuan, Deputy Head
Laboratory of Radiation Medicine
North China Institute of Radiation Protection
P.O. Box 120
Tai-yuan, Shan-Xi
THE PEOPLE'S REPUBLIC OF CHINA

M. Carpentier
Commission of the European Communities
200 rue de la Loi
J-70 6/16
B-1049 Brussels
BELGIUM

Chen Xing-An
Laboratory of Industrial Hygiene
Ministry of Public Health
2 Xinkang Street
Deshengmenwai, Beijing
THE PEOPLE'S REPUBLIC OF CHINA

R. Clarke
National Radiological Protection Board
Harwell, Didcot
Oxon OX11 ORQ
ENGLAND

Commission of the European Communities
DG XII - Library SDM8 R1
200 rue de la Loi
B-1049 Brussels
BELGIUM

Deng Zhicheng
North China Institute of Radiation Protection
Tai-yuan, Shan-Xi
THE PEOPLE'S REPUBLIC OF CHINA

Director
Commissariat á l'Énergie Atomique
Centre d'Etudes Nucléaires
Fontenay-aux-Roses (Seine)
FRANCE

Director
Commonwealth Scientific and Industrial Research Organization
Aspendal, Victoria
AUSTRALIA

Director
Laboratorio di Radiobiologia Animale
Centro di Studi Nucleari Della Casaccia
Comitate Nazionale per l'Energia Nucleare
Casella Postale 2400
I-00100 Roma
ITALY

D. Djuric
Institute of Occupational and Radiological Health
11000 Beograd
Deligradoka 29
YUGOSLAVIA

L. Feinendegen, Director
Institut für Medezin
Kernsforschungsanlage Jülich
Postfach 1913
D-5170 Jülich
FEDERAL REPUBLIC OF GERMANY

A. Geertsema
Sasol Technology (Pty), Ltd.
P.O. Box 1
Sasolburg 9570
REPUBLIC OF SOUTH AFRICA

G. B. Gerber
Radiobiology Department
Commission of the European Communities
200 rue de la Loi
B-1049 Brussels
BELGIUM

J. A. B. Gibson
Radiation Dosimetry Department
AEA Environment & Energy
Harwell Laboratory
Didcot
Oxon OX11 ORA
ENGLAND

D. Goodhead
Medical Research Council
Radiobiology Unit
Harwell, Didcot
Oxon OX11 ORD
ENGLAND

A. R. Gopal-Ayengar
73-Mysore Colony
Mahul Road, Chembur
Bombay-400 074
INDIA

G. F. Gualdrini
ENEA
8 Viale Ercolani
I-40138 Bologna
ITALY

J. L. Head
Department of Nuclear Science & Technology
Royal Naval College Greenwich
London SE109NN
ENGLAND

T. Jaakkola
University of Helsinki
Department of Radiochemistry
Unioninkatu 35, 00170
Helsinki 17
FINLAND

Jiang Shengjie, Standing Vice President
Chinese Nuclear Society
P.O. Box 2125
Beijing
THE PEOPLE'S REPUBLIC OF CHINA

K. E. Lennart Johansson
Radiofysiska Inst.
Regionsjukhuset
S-901-82 Umeå
SWEDEN

A. M. Kellerer
Institut für Medezin Strahlenkunde
Universität Würzburg
Versbacher Strasse 5
D-8700 Würzburg
FEDERAL REPUBLIC OF GERMANY

H.-J. Klimisch
BASF Aktiengesellschaft
Abteilung Toxikologie, Z470
D-6700 Ludwigshafen
FEDERAL REPUBLIC OF GERMANY

A. Kövér
Nuclear Ressearch Institute of Hungary
Hungarian Academy of Science
P.O. Box 51
H-4001 Debrecen
HUNGARY

G. H. Kraft
c/o GSI Postbox 110541
Planck Str.
D-6100 Darmstadt
FEDERAL REPUBLIC OF GERMANY

T. Kumatori
National Institute of Radiological Sciences
9-1, Anagawa-4-chome
Chiba-shi 260
JAPAN

H. P. Leenmouts
National Institute of Public Health & Environmental Hygiene
P.O. Box 1
NL-3720 BA Bilthoven
THE NETHERLANDS

Li De-Ping
Professor and Director of North China Institute of Radiation Protection, NMI
Tai-yuan, Shan-Xi
THE PEOPLE'S REPUBLIC OF CHINA

Librarian
Centre d'Etudes
Nucléaires de Saclay
P.O. Box 2, Saclay
Fig-sur-Yvette (S&O)
FRANCE

Librarian
CSIRO
314 Albert Street
P.O. Box 89
East Melbourne, Victoria
AUSTRALIA

Librarian
HCS/EHE
World Health Organization
CH-1211 Geneva 27
SWITZERLAND

Librarian
Kernforschungzentrum Karlsruhe
Institut für Strahlenbiologie
Postfach 3640
D-75 Karlsruhe 1
FEDERAL REPUBLIC OF GERMANY

Librarian
Max-Planck-Institut für Biophysics
Forstkasstrasse
D-6000 Frankfurt/Main
FEDERAL REPUBLIC OF GERMANY

Librarian
Ministry of Agriculture, Fisheries & Food
Fisheries Laboratory
Lowestoft, Suffolk NR33 OHT
ENGLAND

Librarian
National Institute of Radiological Sciences
9-1, Anagawa-4-chome
Chiba-shi 260
JAPAN

Librarian
Supervising Scientist for the Alligator Rivers Region
Level 23, Bondi Junction Plaza
P.O. Box 387
Bondi Junction NSW 2022
AUSTRALIA

Library
Atomic Energy Commission of Canada, Ltd.
Whiteshell Nuclear Research Establishment
Pinawa, Manitoba ROE 1L0
CANADA

Library
Department of Meteorology
University of Stockholm
Arrhenius Laboratory
S-10691 Stockholm
SWEDEN

Library
Risø National Laboratory
DK-4000 Roskilde
DENMARK

Ma Fubang, Director
Chief Engineer
Institute of Atomic Energy
P.O. Box 275
Beijing
THE PEOPLE'S REPUBLIC OF CHINA

A. M. Marko
9 Huron Street
Deep River, Ontario KOJ 1PO
CANADA

H. Matsudaira, Director-General
National Institute of Radiological Sciences
9-1, Anagawa-4-chome
Chiba-shi 260
JAPAN

R.G.C. McElroy
Atomic Energy Commission of Canada, Ltd.
Dosimetric Research Branch
Chalk River, Ontario K0J 1J0
CANADA

J. C. Nénot, Deputy Director
Département de Protection
Centre d' Etudes Nucléaires
BP No. 6
F-92260 Fontenay-aux-Roses
FRANCE

R. V. Osborne
Atomic Energy of Canada Ltd.
Chalk River Nuclear Laboratories
Chalk River, Ontario KOJ1JO
CANADA

H. G. Paretzke
GSF Institut für Strahlenschutz
Ingolstadter Landstrasse 1
D-8042 Neuherberg
FEDERAL REPUBLIC OF GERMANY

O. Pavlovski
Institute of Biophysics
Ministry of Public Health
Givopisnaya 46
Moscow D-182
USSR

V. Prodi
Department of Physics
University of Bologna
Via Irnerio 46
I-40126 Bologna
ITALY

Reports Librarian
Harwell Laboratory, Bldg. 465
UKAEA
Harwell, Didcot
Oxon OX11 ORB
ENGLAND

P. J. A. Rombout
Inhalation Toxicology Department
National Institute of Public Health and Environmental Protection
P.O. Box 1
NL-3720 BA Bilthoven
THE NETHERLANDS

M. Rzekiecki
Commissariat à l'Énergie Atomique
Centre d'Etudes
Nucleaires de Cadarache
BP No. 13-St. Paul
Les Durance
FRANCE

H. Smith
International Commission on Radiological Protection
P.O. Box 35
Didcot
Oxon OX11 ORJ
ENGLAND

J. W. Stather
National Radiological Protection Board
Building 383
Chilton, Didcot
Oxon OX11 ORQ
ENGLAND

Sun Shi-quan, Head
Radiation-Medicine Department
North China Institute of Radiation Protection, MNI
P.O. Box 120
Tai-yuan, Shan-Xi
THE PEOPLE'S REPUBLIC OF CHINA

J. W. Thiessen
Radiation Effects Research Foundation
5-2 Hijiyama Park
Minami-Ku
Hiroshima 732
JAPAN

D. Van As
Atomic Energy Corporation
P.O. Box 582
Pretoria 0001
REPUBLIC OF SOUTH AFRICA

Vienna International Centre Library
Gifts and Exchange
P.O. Box 100
A-1400 Vienna
AUSTRIA

M. Waligorski
Institute of Nuclear Physics
Radzikowskiego 152
31-342 Urakow
POLAND

Wang Hengde
North China Institute of Radiation Protection
P.O. Box 120
Tai-yuan, Shan-Xi
THE PEOPLE'S REPUBLIC OF CHINA

Wang Renzhi
Institute of Radiation Medicine
11# Tai Ping Road
Beijing
THE PEOPLE'S REPUBLIC OF CHINA

Wang Ruifa, Associate Director
Laboratory of Industrial Hygiene
Ministry of Public Health
2 Xinkang Street
P.O. Box 8018
Deshengmenwai, Beijing
100088
THE PEOPLE'S REPUBLIC OF CHINA

Wei Lü-Xin
Laboratory of Industrial Hygiene
Ministry of Public Health
2 Xinkang Street
Deshengmenwai, Beijing
100088
THE PEOPLE'S REPUBLIC OF CHINA

B. C. Winkler, Director Licensing
Raad Op Atomic
Atoomkrag Energy Board
Privaatsk X 256
Pretoria 0001
REPUBLIC OF SOUTH AFRICA

Wu De-Chang
Institute of Radiation Medicine
27# Tai Ping Road
Beijing
THE PEOPLE'S REPUBLIC OF CHINA

ONSITE

DOE Richland Operations Office (3)

P. W. Kruger, A5-90
E. C. Norman, A5-51
R. D. Freeburg, A5-55

Tri-Cities University Center

J. Cooper, Librarian, H2-52

Hanford Environmental Health (2)

L. J. Maas, B6-61
M. J. Swint, H1-02

Westinghouse Hanford Co.

D. E. Simpson, B3-51

Pacific Northwest Laboratory
(92)

W. J. Apley, BWO
S. T. Autrey, K2-21
R. W. Baalman (5), K1-50
W. J. Bair (15), K1-50
N. E. Ballou, P7-07
R. M. Bean, P8-08
L. A. Braby, P8-47
B. A. Bushaw, K3-58
B. D. Cannon, K3-58
F. Carr, Jr., K5-23
T. D. Chikalla, P7-75
T. T. Claudson, B1-40
D. W. Dragnich , K1-46
R. D. DuBois, P8-47
C. G. Edmonds, P8-19
C. E. Elderkin, K6-03
J. W. Falco, K6-78
D. R. Fisher, K3-53
J. S. Fruchter, K6-81
G. K. Gerke, P7-25
M. E. Geusic, K2-57
W. A. Glass, K4-13
R. H. Gray, K1-30
R. Harty, K3-57
L. A. Holmes, K1-29
J. R. Houston, A3-60
A. C. James, K3-51
J. R. Johnson, K3-53
M. L. Knotek, K1-48
W. W. Laity, K2-15
E. A. Lepel, P8-08
J. A. Mahaffey, P7-82
M. E. Mericka, K4-10
N. F. Metting, P8-47
J. H. Miller, P8-47
T. L. Morgan, P8-47
J. T. Munley, K3-57
J. M. Nelson, P8-47
J. F. Park, P7-50
K. A. Parnell, P7-18
R. W. Perkins, P7-35
W. D. Reece, K3-70
G. F. Schiefelbein, K2-03
L. C. Schmid, K1-34
B. D. Shipp, K1-73
R. D. Smith, P8-08
D. L. Springer, P7-50
G. M. Stokes, K1-74
J. A. Stottlemyre, K6-78
T. S. Tenforde (2), K1-50
B. L. Thomas, P7-72
L. H. Toburen, P8-47
R. J. Traub, K3-57
H. R. Udseth, P8-19
B. E. Vaughan, K1-66
T. J. Whitaker, K2-21
R. E. Wildung, P7-54
W. R. Wiley, K1-46
J. R. Williams, K1-86
L. D. Williams, K1-41
W. E. Wilson, P8-47
N. A. Wogman, P7-35
C. W. Wright, P8-08
J. D. Zimbrick, P7-50
Health Physics Department Library
Life Sciences Library (2)
Publishing Coordination
Technical Report Files (5)